

PEPT Visualisation of Continuous Twin Screw Granulation

By

Tim Chan Seem

A thesis submitted to

The University of Birmingham

for the degree of

DOCTOR OF PHILOSOPHY

School of Chemical Engineering

The University of Birmingham

November 2018

UNIVERSITY OF
BIRMINGHAM

University of Birmingham Research Archive

e-theses repository

This unpublished thesis/dissertation is copyright of the author and/or third parties. The intellectual property rights of the author or third parties in respect of this work are as defined by The Copyright Designs and Patents Act 1988 or as modified by any successor legislation.

Any use made of information contained in this thesis/dissertation must be in accordance with that legislation and must be properly acknowledged. Further distribution or reproduction in any format is prohibited without the permission of the copyright holder.

Abstract

Wet granulation is one of the key processes in the manufacture of pharmaceutical tablets.

Traditionally this has been carried out as a batch process, however the need to improve the manufacturability, flexibility and control of products has seen a move toward continuous processing.

Of the existing technologies Twin Screw Granulation has emerged as one of the most promising candidates for continuous wet granulation. Implementation of a new technology in a QbD manner requires robust process understanding and there is a need for characterisation of the fundamentals of this new process. This thesis seeks to bridge this gap by building process understanding of the equipment and mechanisms of granulation. A robust and complete review of the current literature is included in order to compile current knowledge and highlight gaps. This includes a review of the different components of twin screw granulators, particularly the role of the available screw elements and how these form granules. The current work to explore the mixing and residence time is presented as this represents one of the key areas of consideration when moving from a batch to continuous process. Liquid to solid ratio is crucial in the formation of granules in wet granulation and is discussed in detail, including the demonstrated wider applicable range compared to high shear granulation and the attempts at quantification through granulation regime maps. The interaction between screw speed and material feed rate is examined with particular focus on the resultant fill level during granulation. This review highlights gaps in the current research and proposes areas of interest worthy of further investigation, particularly around screw configuration and modelling of the granulation system.

Twin screw granulators are adapted from twin screw extruders and used to process materials of very different physical properties with different target results. The differences in material properties and equipment operation lead to differences in flow within the granulator. These differences in flow and the impact on granulation are explored. The starve fed nature of the granulator leads to preferential loading of one screw in conveying zones. It is believed this results in poor mixing during nucleation

and results in the measured uneven distribution of liquid within final granules. Considerable improvement in liquid distribution can be made by increasing the overall fill level within the granulator. This highlights the importance of fill level during scale up in ensuring good mixing of during granulation and minimising variance in product. The formation mechanism of 60°F kneading blocks is proposed to be primarily breakage of agglomerates formed during nucleation and the need to correlate screw configuration with granule formation is highlighted.

The role of temperature during granulation is explored and in particular highlights the significantly lower mechanical power requirements to granulate at elevated temperature. The physical properties of the formulation materials are explored in detail and it is proposed that the change in solubility with temperature causes the lower power requirement. The impact of temperature highlights the need for good temperature control within granulation systems. It is demonstrated that heat generated through mechanical work can lead to considerable time for the system to reach steady state. The changes in the resultant granule properties with temperature are described demonstrating that variability in temperature can have considerable impact over granule consistency.

Flow of material, residence time distribution and mixing are explored in detail through PEPT. Particular emphasis is made to understand the behaviour of screw configuration. It is demonstrated for the first time how torque and residence time increase proportionally with kneading block length. Increasing homogeneity in the sizes in the granule population suggest a predictable relationship between kneading block length and the degree of mixing. The impact of the angle of kneading block is explored and forwarding geometries are shown to have much higher conveying capacities than neutral. Direct comparison of the residence time distributions of 60°F and 90° kneading blocks are made and highlight the comparatively low levels of axial mixing in 60°F blocks. The arrangement of screw configuration is shown to impact the flow of material in the granulator and the properties of granules formed. Results suggest that positioning a mixing zone close to the nucleation site is

advantageous in producing more uniform granules. Changes in fill level along the axial length of the granulator are measured through PEPT showing consecutively longer residence time and show the potential to link granule properties to mixing zone intensity as part of process design. The impact of kneading element width is explored and highlights how wide elements produce very dense, similar in size granules for the same length of kneading block. As a result it is proposed that exploration of novel geometries tailored to granulation would be valuable.

A novel proof of concept for determining distribution of water throughout the intragranular structure through X-ray Micro-Tomography is presented. The potential to scale the technique to the intergranular level and to quantify the degree of distribution is discussed.

Acknowledgements

I would like to acknowledge the funding from AstraZeneca and the support of my industrial supervisors, Drs. Gavin K. Reynolds, Zhenyu Huang, Ian Gabbott and Marcel de Matas without whom this project would not have been possible.

My thanks goes to Dr. James Bowen for all the training and support in Science City, as well as always being open to bounce creative ideas off. To Dr. Thomas Leadbeater and Prof. David Parker for the endless supplies of PEPT tracers I demanded. To my colleagues at the University, especially Charlotte Iosson and John Ramsay who made Room 118 such a great place to be. To my friends old and new, in particular David Pope and Karin Diaconu who dragged me out to enjoy life both in and outside of Birmingham. To my family and to my parents, Kathleen and Chow Poo for their continued love and support throughout my life.

My heartfelt thanks goes to my supervisors Dr. Andy Ingram and Prof. Neil A. Rowson for their support and guidance throughout my PhD. Especially to Andy for all the time and support in helping me develop as a researcher and of course for being a fantastic supervisor.

And finally to the University of Birmingham, for giving me such a wonderful experience.

CHAPTER 1 - INTRODUCTION	1
1.1 BACKGROUND	1
1.2 CONTINUOUS PROCESSING	5
CHAPTER 2 – TWIN SCREW GRANULATION – A LITERATURE REVIEW	7
2.1 INTRODUCTION	7
2.2 COMPONENTS	12
2.2.1 CONVEYING ELEMENTS	16
2.2.2 KNEADING BLOCKS	19
2.2.3 COMB MIXER ELEMENTS	23
2.3. MIXING AND RESIDENCE TIME	27
2.4 LIQUID TO SOLID RATIO	34
2.4.1 BINDER VISCOSITY	39
2.4.2 GRANULATION REGIME MAPS	42
2.4.3 BINDER ADDITION METHOD	46
2.5 FILL LEVEL, SCREW SPEED AND FEED RATE INTERACTION	48
2.5.1 SCREW SPEED	49
2.5.2 MATERIAL FEED RATE	50
2.6 CONCLUSIONS	53
CHAPTER 3 – ASYMMETRIC DISTRIBUTION IN TWIN SCREW GRANULATION	56
3.1 INTRODUCTION	56
3.2 EXPERIMENTAL METHOD	59
3.2.1 PREPARATION OF POWDER FORMULATION	59
3.2.2 GRANULATION PROCESS	59
3.2.3 DETERMINATION OF TRANSVERSE DISTRIBUTION IN CONVEYING ZONES AS A FUNCTION OF FILL	59
3.2.4 SIZE SELECTIVE SEGREGATION	60
3.2.5 POSITRON EMISSION PARTICLE TRACKING (PEPT)	60
3.2.6 LIQUID DISTRIBUTION	61
3.3 RESULTS	64
3.3.1 ASYMMETRIC MATERIAL DISTRIBUTION IN CONVEYING ZONES	64
3.3.2 SIZE SELECTIVE SEGREGATION IN CONVEYING ZONES	70
3.3.3 FILL LEVEL AND LIQUID DISTRIBUTION	72
3.4 DISCUSSION	77
3.4.1 ASYMMETRIC TRANSVERSE DISTRIBUTION	77
3.4.2 SIZE SEGREGATION IN CONVEYING ZONES	78
3.4.3 FILL LEVEL AND LIQUID DISTRIBUTION	79
3.5 CONCLUSIONS	82
CHAPTER 4 – THE GRANULATION PROCESS AND TEMPERATURE SENSITIVITY	83

4.1	ABSTRACT	83
4.2	INTRODUCTION	83
4.2	MATERIAL AND METHODS	85
4.2.1	GRANULE FORMULATION	85
4.2.2	GRANULATION EXPERIMENTS	85
4.2.3	GRANULE SIZE ANALYSIS	86
4.2.4	RESIDENCE TIME DISTRIBUTION	86
4.2.5	RHEOLOGY	87
4.2.6	DYNAMIC VAPOUR SORPTION	88
4.2.7	MECHANICAL TESTING	88
4.3	RESULTS AND DISCUSSION	90
4.3.1	GRANULATION AT TEMPERATURE	90
4.3.2	RTD AT DIFFERENT TEMPERATURE	97
4.3.3	HYDROXYPROPYL CELLULOSE RHEOLOGY	99
4.3.4	GRANULATION TEMPERATURE RESPONSE WITHOUT BINDER	101
4.3.5	LACTOSE RHEOLOGY	103
4.3.6	DYNAMIC VAPOUR SORPTION	105
4.3.7	MECHANICAL TESTING	106
4.4	CONCLUSIONS	111
<u>CHAPTER 5 – SCREW CONFIGURATION AND DEGREE OF MIXING</u>		113
5.1	INTRODUCTION	112
5.2	MATERIALS AND METHODS	113
5.2.1	GRANULE FORMULATION	113
5.2.2	16 MM SCALE GRANULATION EXPERIMENTS	113
5.2.3	GRANULE ANALYSIS	114
5.2.4	PEPT	115
5.3	RESULTS AND DISCUSSION	118
5.3.1	EFFECT OF KNEADING BLOCK LENGTH	118
5.3.2	KNEADING BLOCK ANGLE	128
5.3.3	ARRANGEMENT OF SCREW CONFIGURATION	132
5.4	CONCLUSIONS	151
<u>CHAPTER 6 – QUANTIFYING DISTRIBUTION</u>		153
6.1	QUANTIFYING DISTRIBUTION THROUGH X-RAY MICRO-TOMOGRAPHY	153
<u>CHAPTER 7 – CONCLUSIONS AND FUTURE WORK</u>		160
<u>REFERENCES</u>		168

Table of Figures

Figure 1.1 – Flowchart of tablet manufacturing routes for secondary pharmaceutical oral solid dosage products	2
Figure 2.1 - Components of a typical Twin Screw Granulation module.....	12
Figure 2.2 – Typical Screw Profile of a bilobal screw geometry.....	14
Figure 2.3 Pair of intermeshed conveying elements (a) Isometric view to show self-wiping geometry (b) End view to show screw profile	16
Figure 2.4 - 60° Forwarding kneading block (a) Isometric view and (b) End view to show shared profile with conveying elements.....	19
Figure 2.5 - Pair of Comb mixer elements (a) Isometric and (b) End view.....	23
Figure 2.6 Optical micrographs demonstrating particle shape for specimens found on the 850 µm sieve for screws with the following element at location 180 mm from the screw tip: (a) 30 mm conveying, (b) 60° kneading block, (c) forwarding comb mixer, (d) series of two forwarding comb mixers, (e) 60° kneading block followed by forward comb mixing element, and (f) reverse comb mixer. Conditions: 7.5% (w/w) binder and 30% channel fill. Included scale bar represents 1 mm.	25
Figure 2.7 Residence time distribution curves at different powder feed rates.	28
Figure 2.8 Residence time distribution with increasing amounts of HPC at different liquid to solid ratios.	28
Figure 2.9 Occupancy along granulator with (a) 30°; (b) 60° and (c) 90° mixing zones (c = conveying, k = kneading)	32
Figure 2.10(a) Rough elongated granules produced at L/S of 0.25. (b) Rounder, smoother granules produced at L/S of 0.4.	38
Figure 2.11 Granule growth regime map for twin screw granulation with kneading elements.	44
Figure 2.12 Granule regime map for TSG using conveying screws.	45
Figure 3.1 - Transverse material distribution of dry ungranulated formulation conveyed at a range of feed rates a) 100 rpm screw speed, b) 400 rpm screw speed.	64
Figure 3.2 - Example image of the HAAKE TSE showing the distribution of material during granulation. Looking down the barrel rotation is counter-clockwise.....	65
Figure 3.3 - a) Overhead view of the GEA Niro TSG showing each detection of the PEPT tracer in 100 passes through the granulator at 10 g/min and 150 rpm b) End on view showing the position of the tracer in the conveying sections of the TSG, rotation is counter clockwise and flow in direction of the reader c) Single pass of a tracer through the TSG with screw configuration [4x 0.25D K// 4x 1.5D C// 6x 0.25D K// 1x1.5D C] to illustrate conveying load asymmetry, axial flow is away from the reader and rotation is clockwise.	66
Figure 3.4 Front on schematic representing the transverse fill profile which establishes across the entire length of conveying zones and the transfer of material between screws. Axial flow is toward the reader.	69
Figure 3.5 Size distribution and normalised liquid content of granules produced at 2 kg/h – 0.15 L/S – 400 rpm.	73
Figure 3.6 Size and liquid distributions of granules formed with a 1D 60°F kneading block at low and high overall fill level a) 1 kg/h – 0.18 L/S – 200 rpm, b) 4 kg/h – 0.18 L/S – 200 rpm. Density distribution is a numerical count frequency of granule size relative to the breadth of size class. L/S ratio is normalised against the overall average L/S ratio of the granule population.	74
Figure 3.7 Optical micrographs of granules formed at low (top) and high (bottom) overall fill a) & c) 710 – 1000 µm, b) & d) 1000 – 1400 µm.	75
Figure 4.1 – Granulator steady state torque at different coolant temperature set points.....	90
Figure 4.2 – Particle size distributions of granules made at 0, 20 and 80°C at a) 2 kg/h feed rate and b) 3 kg/h feed rate.....	91
Figure 4.3 – Position of the thermocouples in the HAAKE twin screw granulator	92
Figure 4.4 – Change in torque and temperature due to heat generated through granulation with a coolant temperature set point of -15°C.	93
Figure 4.5 – Residence time distributions obtained using an impulse response test with the granulator operating at 2 kg/h feed rate, 0.3 L/S and 200 rpm at 20°C and 80°C set point temperature.....	98
Figure 4.6 – Temperature sweep of a 4% HPC (aq) solution between 5°C and 80°C at 10 reciprocal seconds constant shear rate.	100

Figure 4.7 – Steady state granulator torque at coolant set point temperatures of 0, 20 and 80°C of a formulation consisting of 80% lactose and 20% MCC. Granulation liquid was water only, with no additional binder. Process parameters were 3 kg/h material feed rate, 0.45 L/S ratio and 200 rpm screw speed.....	101
Figure 4.8 – Particle size distributions of granules formed at coolant set point temperatures of 0, 20 and 80°C of a formulation consisting of 80% lactose and 20% MCC. Process parameters were 3 kg/h material feed rate, 0.45 L/S ratio and 200 rpm screw speed.....	102
Figure 4.9 – Flow curve of a saturated 25% lactose solution (aq) showing Newtonian rheology.....	103
Figure 4.10 – Viscosity of a saturated 25% lactose solution (aq) across a temperature sweep between 5 and 80°C at constant shear rate of 10 reciprocal seconds.	104
Figure 4.11 – Water vapour sorption and desorption isotherms at 25°C for a) Lactose, b) Microcrystalline Cellulose and c) Hydroxypropyl Cellulose	106
Figure 4.12 – Stress strain curves obtained through spherical compaction at 20°C and 80°C of a) 20% L/S wetted formulation mixture and b) 20% L/S wetted lactose.....	107
Figure 4.13 – Solubility of lactose in water. Recreated from Fox et al, Dairy Chemistry and Biochemistry, 2015 [54].....	110
Figure 5.1 – Steady state granulation torque values for increasing lengths of kneading block. Process parameters were 2 kg/h material feed rate, 0.2 L/S and 200 rpm screw speed.	118
Figure 5.2 – Mean residence times determined across the kneading block for 90° and 60°F screw configurations through PEPT analysis of the GEA 19 mm TSG. Process parameters were 2 kg/h material feed rate, 0.2 L/S and 200 rpm screw speed.	120
Figure 5.3 – Average time per element in the kneading blocks of 90° and 60°F screw configurations obtained through PEPT analysis of the GEA 19 mm TSG.....	121
Figure 5.4 – Particle size distributions of granules produced using increasing lengths of 90° kneading blocks with the Haake TSG. Note that the length of kneading block increases through A-B-C-D.....	122
Figure 5.5 – Bulk densities of granules produced with increasing lengths of 90° kneading blocks using the Haake TSG. Error bars represent the extremes of measurements made in triplicate	124
Figure 5.6 – Barrel temperatures at time of sampling and bulk densities obtained for granules produced using 90° kneading blocks with the Haake TSG.	126
Figure 5.7 – Granule size distributions made with increasing lengths of 30°F kneading blocks	128
Figure 5.8 – Granule size distributions made with increasing lengths of 60°F kneading blocks	129
Figure 5.9 – Local residence time per 0.25D element along the axial screw length of the GEA TSG with two 1D kneading blocks obtained through PEPT analysis, showing the difference in residence time between 60°F and 90° elements. Red and blue dots represent individual residence times per pass of the tracer for the 60°F and 90° screw configurations respectively. The mean local residence times are shown by lines. Note the grey hatched area represents the position of the kneading blocks. Process parameters were 2 kg/h material feed rate, 0.2 L/S and 200 rpm screw speed.....	130
Figure 5.10 – Residence time distributions obtained through PEPT analysis of the GEA TSG. a) & b) with 60°F screw configurations, c) and d) with 90° screw configurations.	131
Figure 5.11 – Steady state torque values for a 90° 1D kneading block with increasing lengths of conveying section between liquid injection port and kneading block. The liquid injection port is located at 9D and these represent 1-13D lengths of conveying section before the kneading block. Obtained on the Haake TSG running at 2 kg/h material feed rate, 200 rpm screw speed and 0.2 L/S ratio. Note D refers to the screw diameter of 16 mm	133
Figure 5.12 – Particle size distributions of granules made with increasing lengths of upstream conveying elements (CE). Manufactured on the Haake twin screw extruder equipped with a 90° 1D kneading block, running at 2 kg/h material feed rate, 200 rpm screw speed and 0.2 L/S. Each conveying element is 1D (16 mm) in length, the total screw length is 25D.....	134
Figure 5.13 – Granulator torque, screw speed and feeder screw speed alternating between 200 rpm and 100 rpm screw speed to show granulation steady state torque at the different speeds. Material feed rate is constant at 2 kg/h, 0.2 L/S ratio and the screw configuration incorporated a 1D 90° kneading block (17x1D C// 4x0.25D K 90°// 7x1D C).....	136
Figure 5.14 – Local residence times per 0.25D element along the axial length of the GEA twin screw granulator obtained through PEPT analysis. The screw configuration consisted of three kneading blocks each 0.5D in length, separated by 1.5D conveying sections (4x0.25D K 30°F// 2x1.5D C// 2x0.25D K 90°// 1x1.5D C// 2x0.25D K 90°// 1x1.5D C// 2x0.25D K 90°// 1x1.5D C). Red dots represent the individual residence times per pass of the tracer and the average overall residence time by the solid black line. Grey hatched areas represent the positions of the kneading blocks.....	138

Figure 5.15 – Comparison of local residence times across sequential mixing zones for 60°F and 90° kneading blocks. Obtained through PEPT analysis of the GEA TSG at 2 kg/h, 0.2 L/S and 200 rpm. Black lines are the mean local residence time, representative of the local fill level, grey hatched areas show the position of the kneading blocks.	139
Figure 5.16 – Residence time distribution curves for screw configurations consisting of 8 kneading elements total comparing the distributions when kneading elements are arranged as a single kneading block to two separate 4KE kneading blocks at a) – 60°F offset angle and b) – 90° offset angle	140
Figure 5.17 – Comparison of two 1.5D 30°F kneading blocks on the Haake TSG. a) – 6x 0.25D elements and b) – 3x 0.5D elements (arranged as pairs of 0.25D elements).....	142
Figure 5.18 – Resultant particle size distributions of granules made using the Haake TSG at 2 kg/h material feed rate, 0.2 L/S and 200 rpm screw speed. Mixing zones consisted of a single 1.5D kneading block arranged at a 30°F angle with a) six 0.25D kneading elements (1x0.5D C// 19x1D C// 6x0.25D K 30°F// 4x1D C) and b) three 0.5D kneading elements (1x0.5D C// 19x1D C// 3x0.5D K 30°F// 4x1D C).	143
Figure 5.19 – Steady state torque values generated on the Haake TSG using different widths of kneading elements a) with a 1.5D kneading block and b) with a 2D kneading block	144
Figure 5.20 – Local residence times and representative fill level across screw configurations consisting of 30°F 1.5D kneading blocks obtained through PEPT analysis of the GEA TSG at 1.8 kg/h material feed rate, 0.2 L/S and 200 rpm. a) using standard 0.25D kneading elements b) using 0.5D kneading elements.....	145
Figure 5.21 – Comparative granule size distributions made with narrow 0.25D kneading elements and wide 0.5D elements on the 16 mm Haake granulator and 19 mm GEA granulator. Granulation was performed at 2 kg/h material feed rate, 0.2 L/S and 400 rpm screw speed.	147
Figure 5.22 – Cumulative pore size distributions obtained through mercury intrusion porosimetry comparing granules made using a 1.5D kneading block with wide to narrow kneading elements a) – at 16 mm scale and b) – at 19 mm scale.....	149
Figure 6.1 – Raw X-ray image of a 1 mm granule.....	154
Figure 6.2 – Granule containing iron tracer particles showing 4 stages of rotation. Iron particles are the dark black areas in the image	155
Figure 6.3 – 3D volume reconstructed from the X-ray images of an iron tracer dosed granule, the iron particles have been coloured red for identification.....	156
Figure 6.4 – Reconstructed 3D volume of a granule made using Potassium Iodide labelled water as tracer solution, areas of low attenuation are coloured in green, areas of high attenuation are coloured blue. Clockwise from top left, the entire reconstructed volume, half the volume sliced through the centre of the granule, and a 2D slice through the centre of the granule	158

***Chapter 1* - Introduction**

1.1 Background

Wet granulation is a manufacturing step commonly used in the manufacture of tablets within the pharmaceutical industry. Tablets are the most common form of oral solid dose (OSD). The goal of pharmaceutical OSD is to deliver an accurate dose of Active Pharmaceutical Ingredient (API) to a patient. Tablets are a preferred dosage form due to their stability and ease of administration to a patient.

A typical API dose will be in the region of micrograms but a suitable size of tablet to ease handling and patient administration is approximately 500 mg. For this reason tablets are typically a mixture of API and additional excipients. Common pharmaceutical excipients are sugars such as lactose or mannitol or compounds such as microcrystalline cellulose. These excipients do not exhibit any pharmacological activity but are present to produce a tablet of sufficient size and provide critical tablet quality attributes, such as tablet strength and dissolution time. The tablet formulation, the mixture of API and excipients must be carefully selected to deliver tablet requirements i.e. stability and bioavailability. The functional performance of this formulation is then determined through the tablet manufacturing process.

APIs can be relatively complex molecules. As such they are frequently poorly flowing and poorly soluble. Crystallised APIs may exhibit acicular habit, where the needle like shape of individual particles makes flow difficult. To overcome low solubility APIs may be micronised, where the particle size is significantly reduced to approximately 1 – 5 μm . The increased surface area improves the solubility and thus bioavailability of the API but at the expense of flowability, with fine powders adding process complexity. Because APIs can be poorly flowing and have low solubility the excipients in the formulation must compensate to allow tablet production and delivery of the API dose to the functional location.

The simplest method of tablet production is Direct Compression (DC) of a blended formulation. In development of a new drug manufacturing process this would be preferred as a first intent but is not always feasible. The formulation may not display the compressibility properties to form tablets of sufficient strength. Alternatively compression may result in highly dense compacts, which while strong have too low dissolution rates to effectively deliver the API dose. When direct compression of a formulation is not feasible an alternative manufacturing route must be considered. Wet granulation is a technique which can be used in order to improve the tableability of a formulation.

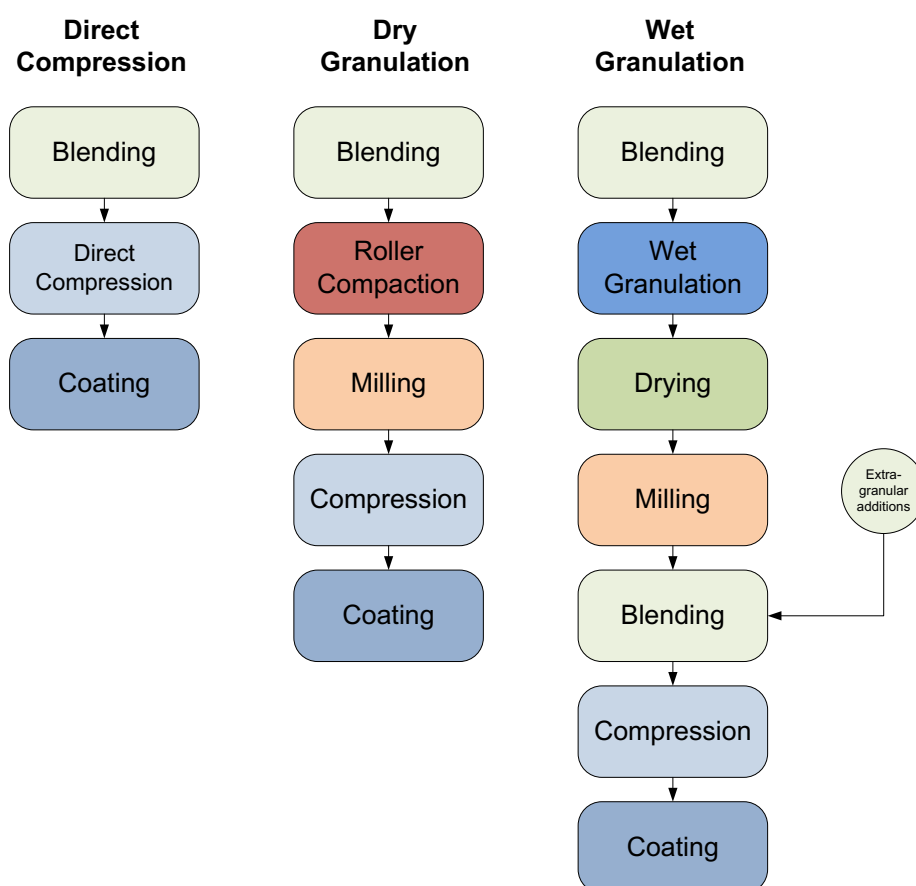


Figure 1.1 – Flowchart of tablet manufacturing routes for secondary pharmaceutical oral solid dosage products

Granulation is a tool which can be used to improve the physical properties of pharmaceutical formulations, making them better suited for tableting. Granulation adds process complexity by increasing the number of manufacturing steps in tablet manufacture, but is sometimes required in order to produce tablets of sufficient quality. Figure 1.1 shows a general flowchart comparing the

manufacturing steps in direct compression to wet and dry granulation. DC is a relatively simple process, additional granulation steps increase the process complexity but add a greater degree of product control. First intent is to use the simplest process possible as each manufacturing stage carries risk of batch failure. However due to the complex properties of pharmaceutical powders direct compression is often not feasible for meeting target tablet properties such as strength or dissolution rate. Granulation stages are often required in order to meet target quality specifications.

Granulation provides many benefits in controlling the physical properties of materials. Formulations may be mixtures of micronised drugs ($\sim 5 \mu\text{m}$) and much larger excipient particles ($\sim 100 \mu\text{m}$), this difference in size gives a risk of segregation during material handling. The risk here is segregation of a blend leading to an incorrect dose in the final tablet. Granulation eliminates this risk by fixing API together with excipients in a stable granular matrix. By producing a population of ideally uniformly sized granules granulation preserves the homogeneity of the mixed blend.

Powders can be poorly flowing making them difficult to transport and handle. This is linked to multiple factors, particle size, shape, surface chemistry etc. Granulation can be used to form free flowing aggregates of powder particles in order to ease handling, processing and transport.

Increasing particle size through granulation reduces the surface area to volume ratio of particles, making them less subject to cohesive surface forces such as Van der Waals and more influenced by gravitational forces. Improving the flowability through granulation is sometimes necessary in order to avoid handling problems such as rat-holing. Granulation reduces the dustiness of powders, this is important in reducing the risk of dust explosions during handling and may be necessary from a safety position. Reducing the dustiness of powders means less material is aerosolised and presents less of a risk of inhalation.

One of the major benefits of granulation in pharmaceutical tablet manufacturing is improving the compressibility of formulations and allowing viable tablets to be made. Poorly compressed tablets may exhibit capping or lamination, where the structural integrity of the tablet is compromised.

Blends of fluffy pharmaceutical powders may not deaerate effectively during compression, leading to trapped pockets of air and weak points in the tablet structure [1]. High shear granulation results in relatively dense granules, where the low porosity aids deaeration during compression.

Compression of granulated material here results in tablets of higher strength as stronger bonds form. Strong tablets are required to survive packaging, shipping and handling to ensure they do not break before reaching the patient. Tablets are designed to deliver a dose based on their dissolution rate, thus broken tablets will affect the delivered dose to a patient.

As granulation improves the compressibility of pharmaceutical blends it allows for a greater range of compaction force to be used during tableting. This provides a degree of control over the tablet density and dissolution rate. On top of this the properties of granules themselves affect dissolution rate. A tablet consisting of granules blended with a disintegrant will rapidly break apart in vivo and absorption of drug is then a function of the dissolution rate of granules, likely dependent on their size and density. Thus granulation can be used to modify or control the dissolution rate of tablets. This may be a somewhat empirical process, as the density of granules increases their dissolution rate will decrease, however densifying granules to the point where their compressibility is poor will result in weak tablets. Low strength tablets may then break more rapidly and dissolve faster than intended. Nevertheless granulation provides a control over dissolution rate, as this is a tablet property to ensure drug dosing granulation is an important tool in tablet design.

Because granulation can be used to process difficult to handle materials into agglomerates it is an effective way of forming sustained release tablets. Polymeric binders such as hydroxypropyl methylcellulose (HPMC) can be incorporated into the granule structure during granulation. On contact with water during dissolution the binder will swell and form gel layers due to the high affinity for water, this preserves the tablet structure and reduces the overall dissolution rate [2].

Thus granulation is often a crucial stage in tablet manufacture, both in allowing the processing of materials to form tablets and in reaching tablet critical quality attributes.

1.2 Continuous processing

Pharma is a unique industry where the production batch sizes must be fixed to match registered production processes. This is a step in ensuring patient safety by undertaking manufacture only through a well understood and tested process. From a business viewpoint this has the disadvantage that batch sizes must comply with the registered process and cannot be reduced in line with customer demand. This fixed process approach has other disadvantages in that it does not allow for continuous improvement. When problems arise in compression changes in granulation cannot be made without a significant piece of process validation work.

With the publication of the FDA's guidelines to pharmaceutical manufacture in 2004 [3] there has been a shift in attitude toward increasing efficiency. One of the results being a shift in direction from fixed batch processes towards continuous manufacturing. One of the key concepts of this is Quality by Design (QbD). Which uses robust process understanding to adapt to variation and ensure consistent final product quality. This integrates well with continuous processes and the design space for manufacturing. Process Analytical Technology (PAT) is used as a tool here to measure process response as part of the feedback loop for process control. The design space allows for a range of process parameter settings to adapt the process to measured variation. This is reliant on good process understanding. The development of a manufacture route of a pharmaceutical product usually involves initial small scale experimentation with often limited, expensive quantities of API. Following this a series of scale up exercises are required to achieve an effective manufacturing scale, each with a risk of product loss associated with them. Because continuous manufacture does not have a fixed batch size, development equipment and manufacturing equipment can be the same and simply run long enough to reach required manufacturing volumes. This eases the complexity of product transfers between R&D and manufacturing sites and removes the risks associated with scale up.

While the drive exists for continuous manufacturing technologies, the challenges in implementing these have been one of the barriers in their adoption. Adapting continuous equipment to the complex material properties of pharmaceutical formulations is challenging and there exist logistical difficulties in ensuring continuous product quality. Granulation is one of the more complex steps in tablet making in secondary pharmaceutical manufacture. Only relatively recently have suitable processes been developed to meet the associated challenges. Twin screw granulation is one of the more popular technologies to emerge. Given the strict regulation of pharmaceutical manufacture robust process understanding is required before widespread adoption is feasible. This body of work examines and characterises the process in order to build this basis of process understanding.

The aim of this thesis is to use Positron Emission Particle Tracking to visualise the flow of material within the actively running twin screw granulation process. A key goal is to characterise the differences in flow caused by the arrangement of screw configuration. By examining the flow of material and comparing it to the properties of granules of granules formed inferences can be made on granule formation mechanisms. Understanding how granules are formed provides a tool for designing a process to give granules with desired attributes, such as size, shape, compressibility and porosity. This helps in industry where processes can be implemented and controlled in a QbD manner and granulation can be designed intelligently rather than empirically.

Chapter 2 – Twin Screw
Granulation – a Literature
Review

2.1 Introduction

Granulation is a size enlargement process where particles are brought together to form larger permanent agglomerates. Granulation improves the physical properties of a material making it easier for handling and downstream processing. In pharmacy granules are typically used as an intermediary before compaction into tablets, the most common type of oral solid dosage. Mixing can be a desirable feature of granulation processes, particularly when homogenous distribution of precise low fractions of active ingredient are required.

Wet granulation is the most commonly used method of granulation. Wet granulation processes such as high shear granulation or fluidised bed granulation involve the addition of a solvent or binder solution to a powder bed to cause agglomeration. Traditionally the pharmaceutical industry has employed batch granulation techniques and has faced many obstacles to adopting continuous production. Perceived issues include cost, product quality, matching the low volume and flexibility in formulations required in some processes and the concerns of regulatory authorities regarding the inability to monitor “batch” quality.

Multiple factors have led to a shift in attitude in pharmaceutical manufacturing towards continuous processing. With the introduction of the concepts of Quality by Design (QbD) and Process Analytical Technology (PAT) in the Pharmaceutical industry by the FDA [3] in 2003 there has been a re-evaluation of current manufacturing techniques. The opportunity to improve process efficiency through continuous processing is now being seriously considered by the pharmaceutical manufacturing industry.

With the developing interest in continuous granulation the advantages over conventional batch granulation methods have become apparent:

- Continuous granulation is more suited to high volume production of material as the production of a similar volume using batch-wise production requires either multiple or very large granulators increasing space and energy demands;
- Similarly continuous granulation is more amenable to variation in production volume. Final product volumes are determined by the running time of the process and are not limited by batch sizes. This is particularly relevant in the production of small volumes, where under filled batch granulators can result in unpredictable poor quality granules;
- Continuous processes require less product development time as they are more adaptable to control strategies outlined by PAT;
- Continuous granulation processes can handle a higher throughput of material compared to traditional batch granulation processes while requiring a smaller equipment footprint [4].

Twin screw extrusion (TSE) is a continuous process widely used in the food, polymer and chemical processing industries for compounding and extruding. Over the last decade or so the use of twin screw extruders for granulation has attracted considerable and serious interest in the pharmaceutical industry. Manufacturers (Leistritz Extrusionstechnik GmbH - NANO 16 [5], Thermo Fisher Scientific – Pharma 16 TSG[6]) now offer extruders marketed as capable for granulation. The ConsiGma™ system from GEA Pharma Systems [7] incorporates the first proprietary use of twin screw granulation (TSG) as a continuous granulation module. ConsiGma™ is a complete continuous package comprising some or all of blending, TSG, drying (semi-continuous), milling and tableting.

Granulation in a twin screw extruder was first reported by Gamlen and Eardley in 1986 [8] in the production of paracetamol extrudates. Followed by Lindberg et al [9] who used a similar extruder in the production of an effervescent granulation [9] and produced a series of papers in 1987-1988 on the determination of residence time [10] and the effect of process variables on granule properties and equilibrium conditions [9, 11].

A Patent for twin screw granulation was awarded to Ghebre-Sellasie et al [12] in 2002 for the use of a twin screw granulator in a single pass continuous pharmaceutical granulation process. Since then the level of interest and depth of research into TSG has greatly increased. Research work has been undertaken including;

- Work into understanding the geometry of the screws and equipment;
 - Screw configuration
 - Note that granulator dimensions are commonly described relative to the screw diameter (D). Typical screw diameters range from 11 – 25 mm
 - Screw configurations are typically a long conveying section leading into a single mixing zone occupying approximately 4% of the axial length
 - Conveying elements – pitch and length
 - Elements are normally 1D in length and arranged in sections that occupy the majority of the length of the screws
 - Normally 1D in pitch but 0.5D to 2D have been explored
 - Kneading elements – thickness and angle
 - Individual elements are almost always 0.25D in width
 - Elements are arranged in a block. The angle between elements determines their conveying capacity. 30°, 60° and 90° are most commonly used
 - Cross sectional area
 - Length to Diameter (L/D) ratio
 - L/D ratio has been proposed as a dimensionless factor for scale up between granulators [13]
- Operation variables;
 - Liquid to Solid (L/S) ratio
 - Formulation dependent – 0.1 – 0.5
 - Material properties – Excipient and binder formulation

- Screw speed
 - 100 – 800 rpm
- Material feed rates
 - Typical feed rates of:
 - <1 – 5 kg/h at small scale ($D \leq 16$ mm)
 - Up to 25 kg/h at production scale ($D \approx 25$ mm)
- Process outcomes and product quality;
 - Mixing and Residence Time Distribution (RTD)
 - Residence times are generally less than 10 seconds
 - Granule Particle Size Distribution
 - Variable depending on process. Granulation will see particle size change from 50 – 100 μm or <10 μm primary particles to agglomerates 200 – 1600 μm
 - Torque
 - Granule porosity/density
 - Final tablet properties

Given both the need for viable continuous processing and the developing interest in twin screw granulation this chapter seeks to review and present currently available research work in an effort to further process understanding and development.

The principle of operation of operation in twin screw granulation is to use mechanical energy from the rotation of screws to mix powder and liquid binder in order to form powder agglomerates. The pitched flight of the screws results in axial flow of material under rotation. Intermeshing regions the screws provide the mixing and compaction to form agglomerates. Twin screw granulation is a continuous process and thus operates at steady state during normal operation. A steady state process is one where process variables are constant and there is no accumulation of mass or energy

in the system. In twin screw granulation this would be a constant feed of material into the granulator and equal flow of material out. Similarly energy transferred from the screws is consumed in the formation and breakage of granules. A process generating heat for example would increase in temperature over time and is therefore not at steady state. Should the rate of heat loss become equal to the rate of heat generated, assuming all other process variables are constant, the system would be considered to be at steady state. Naturally there will be variance thermodynamically in process variables in the running process, however under steady state these average out to constant. An appropriate time frame would be the residence time of the granulator (in the region of 10 seconds).

2.2 Components

A twin screw granulator consists of two intermeshed screws enclosed in a barrel. As such there is small variety between granulators and differences are typically limited to geometric constraints i.e. length, screw diameter and specific screw element geometry. Co-rotating twin screw extruders are more popular in industry and so far only co-rotating twin screw granulators have been investigated. The effectiveness of counter-rotating screws on granulation has not been explored. Twin screw granulators work by conveying material along their screw length while imparting the mechanical energy required for liquid distribution and granulation in mixing zones. As the screws are intermeshing they are self-cleaning with the flight of one screw scraping clear the surface of the other in rotation.

There exists a large number of twin screw granulators with varying size and geometry. Granulators in use have varied from initial experiments carried out on modified twin screw extruders [13, 14], to purpose built continuous tableting systems in GEA Pharma Systems ConsiGma™ continuous granulation module [7]. As the dimensions and processing capacity of granulators can vary greatly granulators are most commonly defined by the ratio of screw Length to Diameter (L/D). However granulation does not scale up linearly based around similar L/D ratios and instead requires optimisation based on the geometry of the granulator [13].

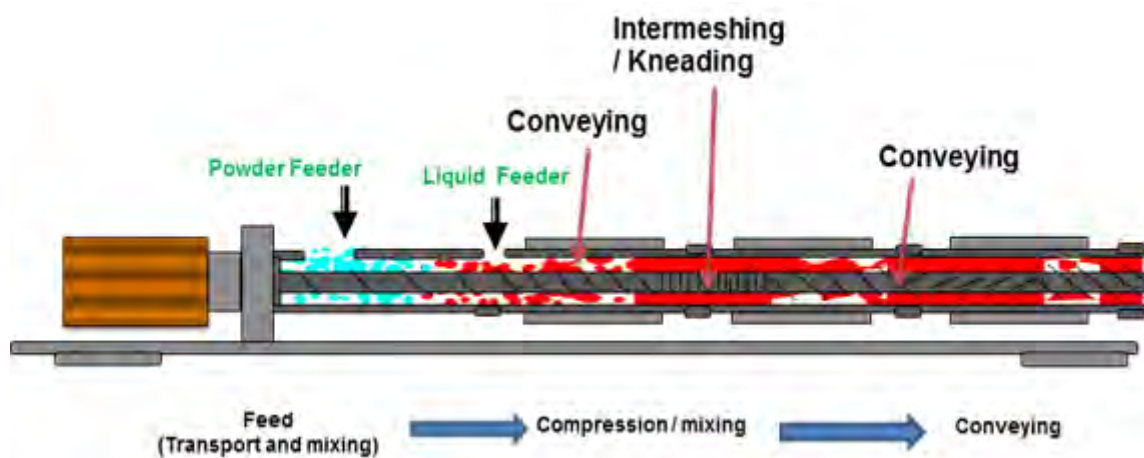


Figure 2.1 - Components of a typical Twin Screw Granulation module

Figure 2.1 shows the typical components of a twin screw granulator. A variety of feeders exist to feed powder into the barrel inlet such as screw feeders, gravity feeders and vibratory feeders. One of the challenges associated with feeding is the delivery of consistent feed of material which can be particularly difficult when dealing with materials with poor handling properties. Cartwright et al [15] have examined feeding of a poorly flowing API using a variety of loss in weight feeders. To consistently feed the API to the granulator, the original rigid walled hopper twin screw feeder had to be replaced with one of flexible wall design to prevent powder bridging. Additionally the various designs of screws available to the twin screw feeder were evaluated; feeding at the desired range was only possible with one design of screw (core and spiral) at a severely reduced maximum feed capacity. The other screw designs would lead to compaction of the API material and eventually cause the feeder to jam. Three different flexible wall single screw gravimetric feeders were compared to the twin screw feeder, it was concluded that for the application the Brabender FW40 gave the best performance due to its mechanical design and broad weight capability of the load cell [15]. It should not be forgotten that tablets are multicomponent formulations. The decision must be made whether to premix ingredients and feed with a single feeder (and run the risk of segregation/demixing) or to have multiple feeders. The latter presents a physical challenge of installation as well as the need to provide feeders of a wide range of delivery accuracy. The benefit would be to eliminate a step within a processing line however it also increases the mixing burden of the TSG. Despite some work covering co-feeding relatively small proportions of API [15, 16] this has not been covered in the literature and is worthy of investigation.

Material in the granulator typically experiences a rise in product temperature due to friction between the material and barrel and the extensive work caused by kneading elements. Temperature controlled jackets allow for precise control of product temperature through cooling or heating, in the case of hot melt granulation [17-20] temperature profiles along the length of the barrel are also possible with appropriate design of the jacket.

The screws used in twin screw granulators are typically modular and are built up of matching pairs of individual elements on the screw root. There are broadly three types of screw elements used in granulation Conveying elements, Kneading blocks and Comb mixer elements.

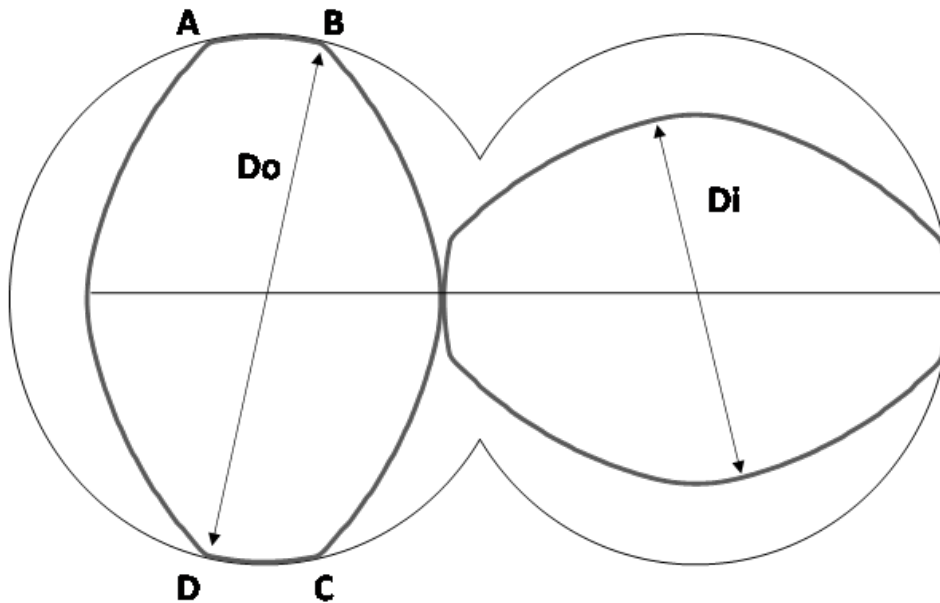


Figure 2.2– Typical Screw Profile of a bilobal screw geometry

The profile of two screw elements is shown in Figure 2.2. All screw elements, with the exception of comb mixer elements, share the profile **ABCD** and hence all elements have the same cross sectional area. Conveying elements can be considered to be made of an infinite number of slices of profile **ABCD** offset at slight angle to each other to produce a continuous helical flight. Kneading elements clearly share the profile **ABCD** with defined thickness, typically at a minimum of $1/8 D$ or $1/4 D$, where D refers to the screw diameter. Screws with a double-flighted profile are typically used in twin screw granulation. Granulation with screws with single, triple or higher flighted profiles has not yet been reported.

As all elements (with the exception of comb mixer elements) share the same profile, the cross sectional area of the screws does not change along their length. The screw cross sectional area determines the free volume - the available volume within the barrel unoccupied by the screws. The cross-sectional area is dependent on the ratio of inner (D_i) to outer (D_o) diameter [21]. Consider the hypothetical case of two granulators of different free volume but otherwise identical geometry, operating at the same speed and throughput. The material passing through the extruder with the lower free volume might be expected to be squeezed and compacted more. Shear stress might also be higher as the average gap would be lower. Hence the ratio $D_i:D_o$ is an important design and operation consideration. This has received scant attention in the literature.

2.2.1 Conveying Elements

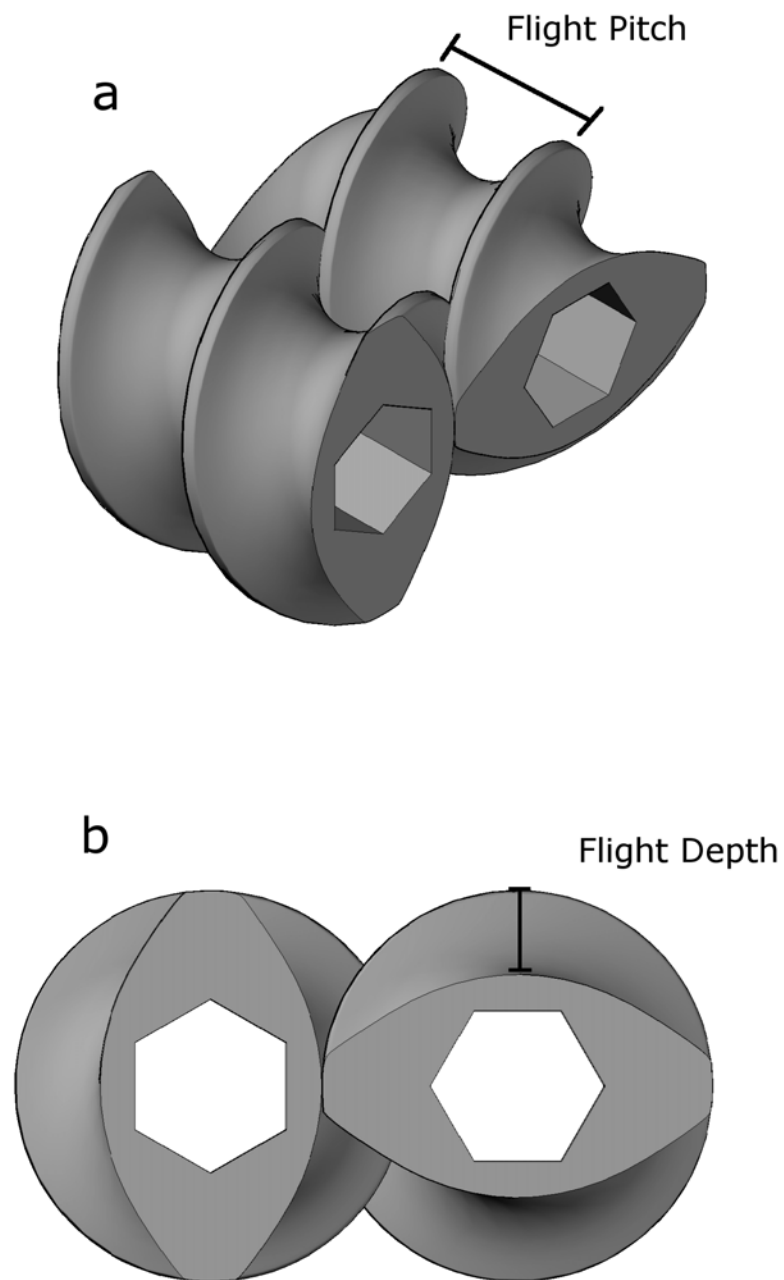


Figure 2.3 Pair of intermeshed conveying elements (a) Isometric view to show self-wiping geometry (b) End view to show screw profile

Conveying elements (see Figure 2.3) are designed to impart low mechanical energy and act to transport material between mixing zones. As their main role is transportation of material they impart low shear force. Screws operate part filled, with fill level dependent on screw geometry, material feed rate and screw speed. The angle of pitch determines conveying capacity. For a given rotation speed, longer pitch elements will operate at lower fill level or accommodate higher throughput without over fill. It is not solely about transport between mixing zones however:

Djuric and Kleinebudde [22] found an increase in the proportion of fine and oversize granules with decreasing flight pitch. Short pitch conveying elements have more flight chambers with smaller volume in a given length. Material can potentially become unevenly distributed between these flight chambers and remain isolated from interaction with adjacent chambers. This promotes the formation of lumps and reduces agglomeration, giving high proportions of oversize agglomerates and fines. Granule porosity decreases slightly with increasing flight pitch and is attributed to increased densification in the barrel chamber. The cause of the increased densification was not explored and the result is unintuitive as the superior feeding properties of long pitch elements would imply a lower overall fill level and less compaction [22].

Thompson and sun [23] found the size distribution of granules produced using only conveying elements to be bimodal with a high proportion of fines. When the fill level was increased from 30% to 70% by reducing the screw speed, the size distribution of granules remained bimodal however a greater proportion of large granules were formed. The authors suggest that the greater channel fill insulates the granules from the high shear environment at the barrel wall, leading to less breakage. Additionally, higher fill leads to higher compressive forces leading to consolidation and granule growth. Although granules of sufficient quality for tableting could be produced using just conveying screws only at high barrel fill level, further optimisation would be required to reduce the high proportion of unwanted fines.

While granulation has been shown to be possible with conveying elements only [23, 24] further research would be required to establish that adequate mixing is achieved.

2.2.2 Kneading Blocks

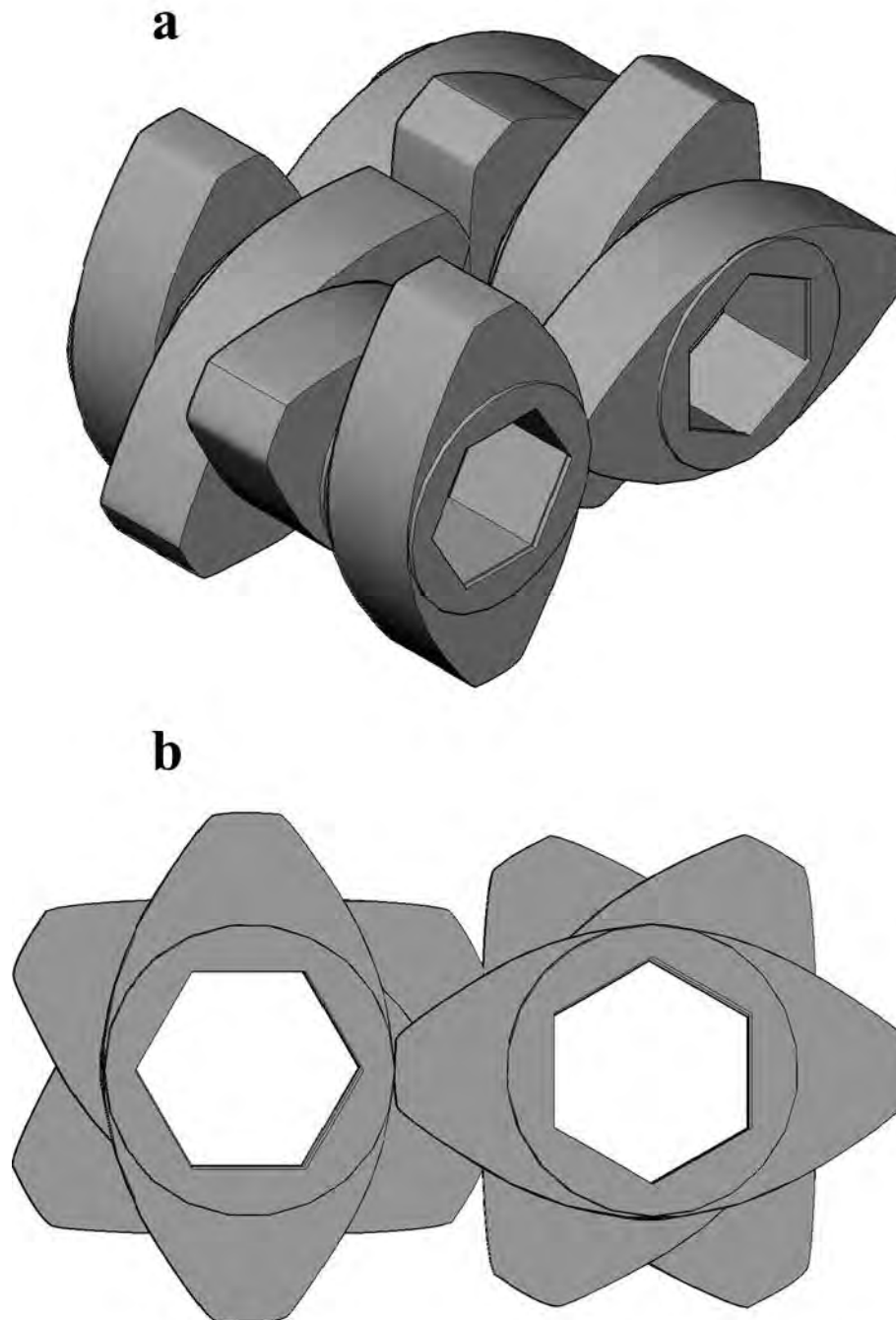


Figure 2.4 - 60° Forwarding kneading block (a) Isometric view and (b) End view to show shared profile with conveying elements

Figure 2.4 shows a typical kneading block used for granulation. Kneading blocks are made up of individual kneading discs and act as mixing zones in twin screw granulation. Kneading blocks impart high mechanical energy into the wetted mass of powder, producing high shear forces, compaction and distributive mixing. Pairs of kneading discs in kneading blocks provide a region of compaction in the intermeshing region of the screws. The compaction between discs causes densification and squeezes liquid to the outside of the granule allowing for growth through consolidation. The chopping and shearing motion of kneading block breaks apart large agglomerates and disperses liquid.

The kneading discs in a kneading block are typically offset at angles of 30°, 60° or 90°. Depending on the angle of offset kneading blocks can produce forwarding or reversing flow [21, 25]. Kneading blocks offset at 30° forwarding and 60° forwarding have some conveying capacity and will tend to push material forward along the screw. Reversing kneading blocks force material back against the direction of flow leading to areas of high pressure and compaction. Although strong granules can be formed the risk of blockages is high [22]. 90° blocks have no inherent conveying capacity and are dependent on “pressure” driven flow [23].

Vercruyssen et al [26] found the angle of kneading elements to have no significant effect on particle size distribution under the conditions investigated. However the number of kneading elements contributes significantly to the properties of granules [22, 26]. An increase in the number of kneading elements leads to a reduction in the proportion of fines (defined as granules <150 µm) formed and an increase in the proportion of oversize agglomerates (>1400 µm). A correlation between the number of kneading elements and torque generated was found. Higher numbers of kneading elements lead to granules with higher density and longer dissolution times. The number of kneading elements significantly affects the heat generated in the barrel. Within the study, higher barrel temperatures were found to lead to less friable granules. This was thought to be due to the increased solubility of the lactose, theophylline mixture resulting in more solid bridges formed after

recrystallisation. An analysis of start-up time was undertaken and it was found that more kneading elements leads to a longer time to equilibrium (steady state torque and temperature). The time taken to equilibrium was suggested to be the period within which gradual layering of material on the barrel wall in mixing zones completes. It was suggested that material loss during start up could thus be minimised through a feedback control system within the temperature control jacket in order to compensate for heat generated through friction in mixing zones.

Thompson and Sun [23] found that the angle of kneading elements only affect granule properties when the fill level is high. At low fill only small changes in granule properties were observed for kneading discs offset at different angles. Thus the intermeshing region between kneading discs is the important factor in determining granule morphology. Long compressed granules with a ribbon like shape were formed in the intermeshing region, suggesting the thickness of the kneading discs in a kneading block controls the size of granules.

Van Melkebeke et al [16] found that the inclusion of a conveying element after a kneading block led to a reduction in oversize agglomerates, but otherwise no effect on granule properties. The porosity of granules produced with a single kneading block were similar for 30°, 60° forwarding and 90° offset angles however the median pore diameter from the 90° configuration was significantly lower. The neutral conveying characteristics at 90° led to higher material pressures and compaction. Tablets were formed by compression and while all granules had similar compressibility tablet strength decreased slightly at higher offset angle. However all tablets displayed similar disintegration times.

Periodic surging of material has been observed by Shah [27] and Thompson and Sun [23]. Surging could be eliminated through modification of the screw configuration and was a result of the specific equipment setup. Periodic surging is not typical of twin screw granulation and was attributed to the high flow resistance of the kneading block. However surging is likely a result of the liquid inlet port location relative to the kneading block rather than kneading block characteristics. Shah [27] explored atypical configurations where liquid was injected directly before the kneading block rather than in a

relatively long conveying section. It is likely that the long residence time in the kneading block led to an overly wetted zone due to the constant liquid feed, resulting in sticky flow resistant material. A build-up of material in the conveying zone leading up to the kneading block would then be required to generate the throughput force required to dislodge the paste like pseudo-blockage, resulting in the periodic surging. Thompson and Sun [23] explored methods of liquid injection, the exact configuration is not described but was likely similar to that of Shah [27].

2.2.3 Comb mixer elements

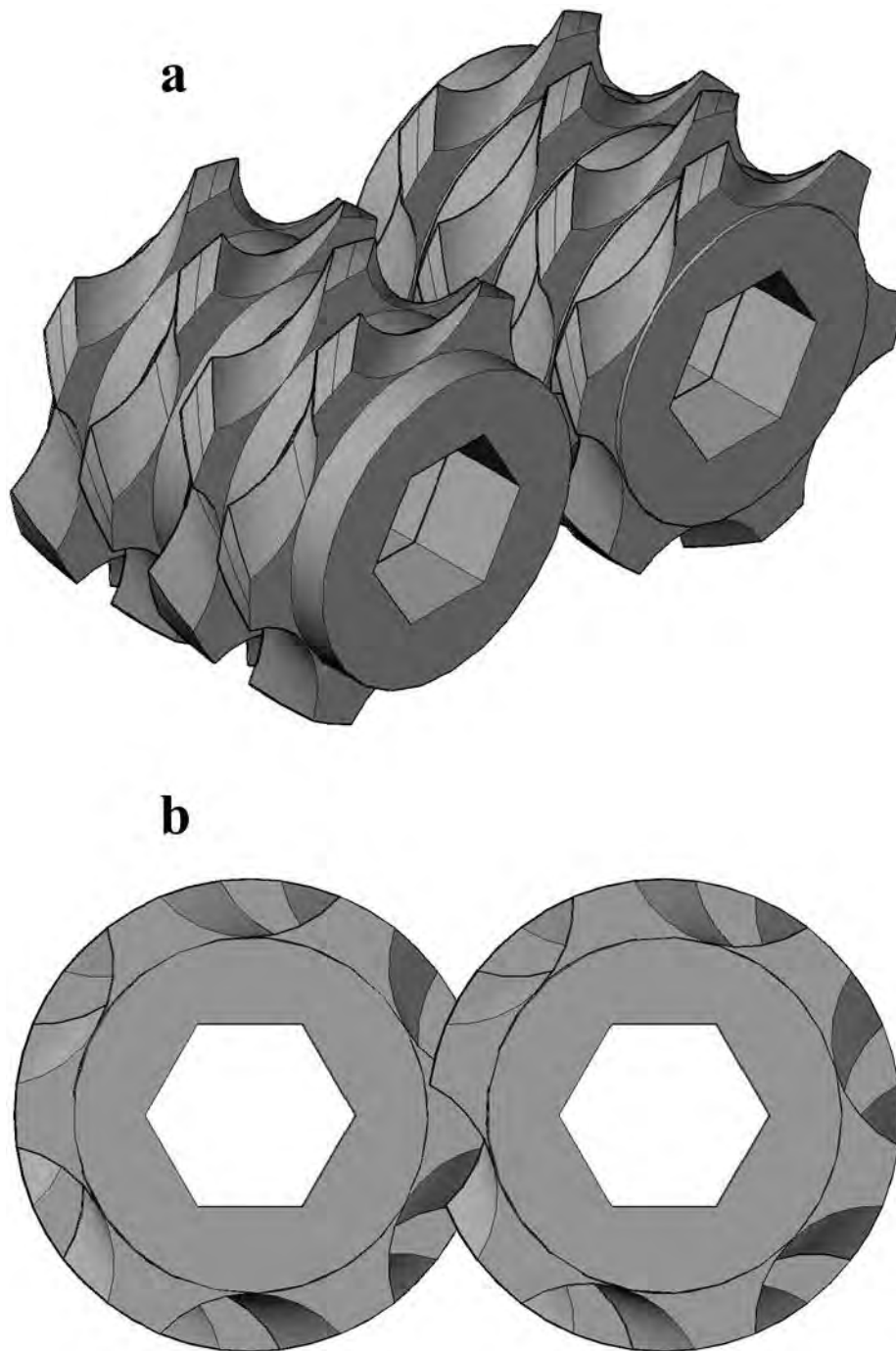


Figure 2.5 - Pair of Comb mixer elements (a) Isometric and (b) End view

Comb mixer elements shown in Figure 2.5 are a type of distributive mixing element typically used in extrusion processes. Comb mixers are composed of rings arranged perpendicular to the direction of

flow containing angular cuts in the ring wall to allow for the passage of material through the element. Comb mixers act to distribute and recombine flow streams in the extruder in a low shear environment providing good mixing of material. The angle of cut in the ring wall determines the direction of flow generated by the comb mixer element, comb mixers can generate forwarding or reversing flow either aiding or opposing downstream flow. As flow through comb mixer elements is dependent on material pressure flow they generally operate fully filled [23].

Thompson and Sun [23] investigated the effect of the Leistritz GLC-type comb mixer element. Their results showed that reversing mixer elements would lead to high pressure zones in the mixing section leading to extensive agglomeration of material and the formation of a large proportion of oversize agglomerates even at low fill level. At high fill level the high pressure zone caused by the mixing element would lead to blockage of the granulator. Forwarding mixer elements behave similarly to kneading elements, producing granules with a bimodal size distribution with increasing particle size with increasing fill level. Placing two comb mixers in series removed the effect of fill level on granule size distribution as the compaction and fracture of particles was mitigated between the two elements, leading to a uniform particle size distribution [23].

Comb mixer elements produce granules of greater density than conveying elements but lower density than kneading blocks. With high density granules being the least friable [22].

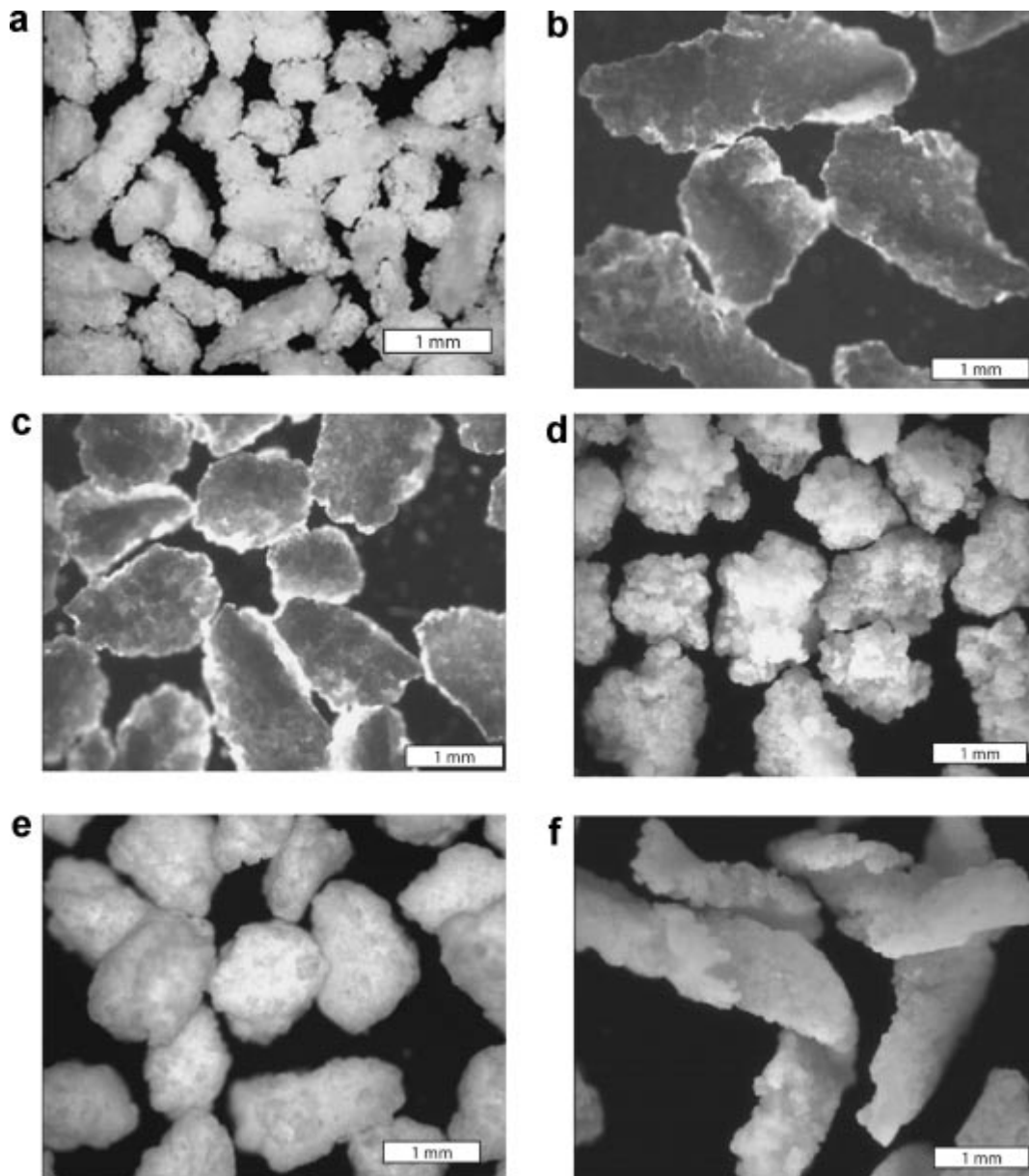


Figure 2.6 Optical micrographs demonstrating particle shape for specimens found on the 850 μm sieve for screws with the following element at location 180 mm from the screw tip: (a) 30 mm conveying, (b) 60° kneading block, (c) forwarding comb mixer, (d) series of two forwarding comb mixers, (e) 60° kneading block followed by forward comb mixing element, and (f) reverse comb mixer. Conditions: 7.5% (w/w) binder and 30% channel fill. Included scale bar represents 1 mm.

(Thompson, M. R. and J. Sun (2010) **Wet granulation in a twin-screw extruder: Implications of screw design** Journal of Pharmaceutical Sciences 99(4): 2090-2103.)

In Figure 2.6 Thompson and Sun [23] demonstrate the wide range of granule shapes that could be produced in the same size range with various screw elements by twin screw granulation. From their findings they suggest that the particle shape could be tailored allowing a user another dimension of control unavailable in batch granulation techniques such as high shear mixing and fluidized bed granulation.

The shape of granule formed was dependent on the type of screw element used and was dominant over changes in formulation or binder concentration. It was suggested that the differences in granule shape observed in the study would persist for any comparable material system.

2.3. Mixing and Residence time

Characterisation of the residence time distribution is an important step in design, improvement and scale-up of twin screw systems [28, 29]. Typically higher mean residence times lead to better distributive mixing during extrusion, however the complex rheological mixtures used in granulation increase design complexity. Understanding of residence time distribution is a powerful tool in process design in producing high quality product while meeting design criteria. RTD represents the degree of axial mixing, where good mixing is important in smoothing out any variation in feed. RTD can either be measured by a stimulus response test [18, 30-34] or direct measurement such as through particle tracking [35].

In a series of papers on the mechanics of twin screw granulation Dhenge et al [30-32] investigated the effect of process parameters on residence time. RTD was determined using an impulse response technique where a dye was added as a tracer. Given the short mean residence times measured (10-20 seconds) it should be noted the sampling interval was fairly broad at 10 seconds.

Mean residence time decreases with increasing screw speed due to the increased conveying capacity of the screws. Residence time was shown to decrease with increasing material feed rate. Dhenge et al [30] came up with the concept of “throughput force” to describe efficiency of transport. Low feed rates lead to small material throughput force and what was described as increased “back mixing” due to the smaller degree of forwarding flow, giving broader residence time distribution curves Figure 2.7 [30]. Both an increase in liquid to solid ratio and binder viscosity leads to an increase in mean residence time and a broadening of residence time distribution curves. Both liquid to solid ratio and binder viscosity change the rheology of the mixture in the granulator, increasing either factor causes the wetted powder to become stickier and more resistant to flow, shown in Figure 2.8 [31].

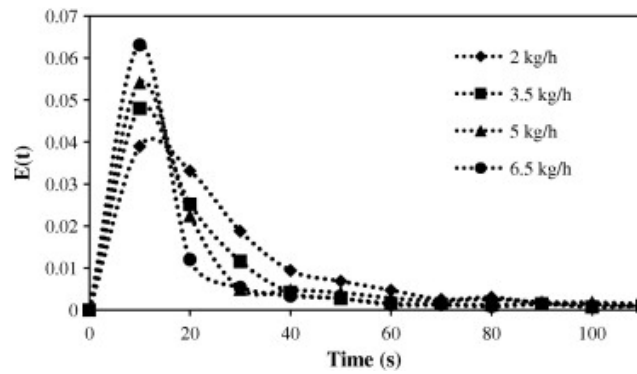


Figure 2.7 Residence time distribution curves at different powder feed rates.

(Ranjit M. Dhenge, James J. Cartwright, David G. Doughty, Michael J. Hounslow, Agba D. Salman, **Twin screw wet granulation: Effect of powder feed rate**, *Advanced Powder Technology*, Volume 22, Issue 2, March 2011, Pages 162–166)

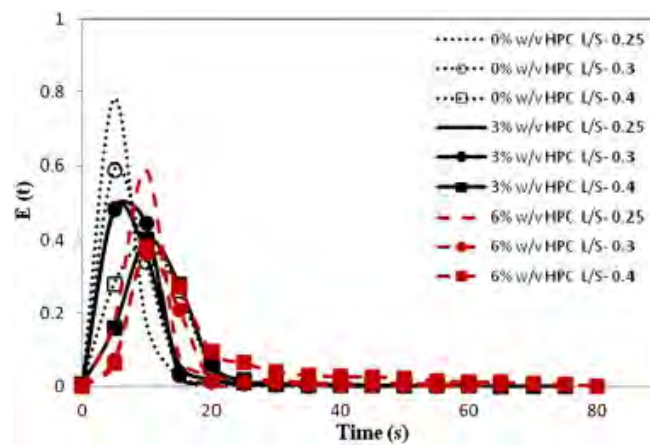


Figure 2.8 Residence time distribution with increasing amounts of HPC at different liquid to solid ratios.

(Ranjit M. Dhenge, James J. Cartwright, Michael J. Hounslow, Agba D. Salman, **Twin screw wet granulation: Effects of properties of granulation liquid**, *Powder Technology*, Volume 229, October 2012, Pages 126–136)

Note that $E(t)$ is the Residence Time Distribution function, defined as:

$$E(t) = \frac{C(t)}{\int_0^{\infty} C(t) dt} \quad (2-1)$$

Where $C(t)$ is the concentration of tracer leaving the system at time t . The residence time distribution is a probability distribution of the fraction of material entering a system at $t = 0$ to

leave at time t and thus describes the extent of axial mixing in a system is. With a broad RTD implying good axial mixing compared to a narrow.

Lee et al [35] used PEPT (Positron Emission Particle Tracking) to determine residence time in the granulator and RTD across individual screw elements. Due to the nature of PEPT residence time distribution was determined at low material flow rate and screw speed. Residence time was observed to decrease with increasing screw speed. Increasing the material feed rate also decreases the overall residence time as shown by Dhenge et al [30], due to the greater amount of material in the granulator producing more conveying capacity. Increasing the kneading disc offset angle increased the residence time due to the reduced conveying capacity at higher angles. At higher material feed rates and screw speeds the difference in residence time between 30° and 60° kneading blocks becomes less significant. It was suggested the higher material throughput allowed for more bypassing of the 60° blocks [35].

The extent of mixing of different screw configurations was compared by Lee et al [35] through normalisation of the residence time distribution. Near identical normalised RTD curves and Peclet numbers were found for screws with 30°, 60° and 90° kneading blocks. It was concluded that the extent of axial mixing is similar regardless of screw speed, powder feed rate and screw configuration [35]. This contradicts the results of Kumar et al [34] who found considerable variation in axial mixing and may be a feature specific to the low screw speeds and feed rates necessary for PEPT. Thus this is worthy of further investigation.

Using a method developed by Vercruyssen et al [36], Kumar et al [34] carried out an extensive study on RTD and mixing within TSG. RTD was determined by near infra-red (NIR) chemical imaging of granules discharged onto a moving conveyor belt. RTD curves were determined and three factors quantified; the mean residence time (t_m), the Peclet number (Pe) and the normalised variance (σ_θ^2) a description of the breadth of the RTD curve which represents the extent of axial mixing. t_m is determined from the mean tracer concentration between time $t + dt$ and calculated as:

$$t_m = \frac{\int_0^{\infty} t \cdot E(t) dt}{\int_0^{\infty} E(t) dt} \quad (2-2)$$

Peclet numbers are derived numerically from the following equation:

$$\frac{\sigma^2}{t_m^2} = \frac{2}{Pe} - \frac{2}{Pe^2} (1 - e^{-Pe}) \quad (2-3)$$

Where σ^2 is the variance which measures the broadness of the distribution of the RTD curve. Peclet numbers describe the ratio of the rate of axial transport by convection to the rate of axial transport by diffusion or dispersion, where higher numbers show more axial mixing.

The normalised variance term (σ_θ^2) was thus defined as the left hand side of equation (2-3) (σ^2/t_m^2), which represents the broadness of the residence time distribution normalised around the mean residence time and allows for direct comparison of RTD curves. The variance is calculated using the following equation:

$$\sigma^2 = \frac{\int_0^{\infty} (t - t_m)^2 \cdot e(t) dt}{\int_0^{\infty} e(t) dt} \quad (2-4)$$

In this study screw speed, material feed rate, number of kneading elements and element offset angle were the parameters explored. Multivariate analysis was undertaken to determine the factors of greatest impact. Screw speed has the largest effect on t_m , higher speeds give shorter residence times. Screw speed has the greatest interaction with material feed rate which alone had relatively small effect on RTD. Screw speed and material feed rate were equated as the factors most important in generating "throughput force", a crucial factor in determining RTD and mixing behaviour. Both screw speed and material feed rate cause a reduction in t_m at higher values, however neither scales linearly, with a greater effect from transition from low to middle conveying capacities than middle to high. Higher screw speeds lead to improved axial mixing, indicated by a rise in σ_θ^2 . This is most prevalent under low fill conditions with reduced material feed rate and few kneading elements.

Under high fill conditions increasing screw speed will reduce mean residence time without improving

axial dispersion as flow becomes plug like. At low screw speeds Pe rises sharply with feed rate, number of kneading elements and element angle indicating a transition to plug flow when there is low throughput force.

The offset angle of kneading discs only affects RTD when high numbers of kneading discs are used. The number of kneading discs has a considerable effect on RTD. As expected mean residence rises with increasing number of elements, however the relationship is not linear: the effect diminishes with increasing number [18, 34]. Increase in the flow impediment through higher number of elements or more pronounced offset angle leads to longer mean residence times and by implication longer mixing times. However with high flow impediment variance is lower and Peclet numbers increase, indicating less axial mixing and more plug like flow. Thus to ensure good axial mixing it was concluded that throughput force must be correspondingly raised through screw speed [34]. While the RTD study of Kumar is in depth and extensive, further understanding of the relationship of flow impediment and throughput force is required, particularly in understanding the mechanisms of mixing elements. No data on granule properties was presented thus it is difficult to correlate changes in granule quality and mixing mechanisms with changes in axial dispersion.

An advantage of PEPT over other techniques is that it allows for analysis of residence time within individual screw elements as well as the entire screw length. Lee et al [35] determined that kneading blocks have a longer residence time than conveying zones and broader RTD curves, indicating the dispersive mixing of material passing through them. Analysis across individual elements also allows for calculation of the fill level in mixing and conveying zones, based on the steady state material throughput and the average residence time, as shown in Figure 2.9. Fill levels are shown to be proportional to the material input rate and inversely proportional to the screw speed. Fill levels across the kneading block are low for 30° and 60° offset angles indicating that the flow of material is mainly due to their inherent conveying capability. Fill levels across 90° blocks never reach 100%

occupancy and a fill gradient is established decreasing from the first kneading disc suggesting pressure driven flow of material.

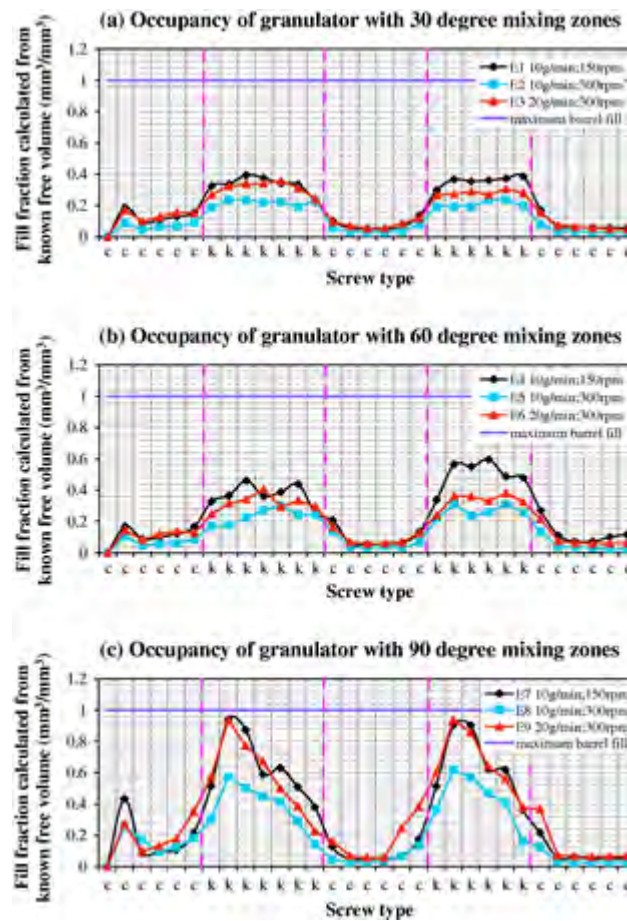


Figure 2.9 Occupancy along granulator with (a) 30°; (b) 60° and (c) 90° mixing zones (c = conveying, k = kneading)

(Kai T. Lee, Andy Ingram, Neil A. Rowson, **Twin screw wet granulation: The study of a continuous twin screw granulator using Positron Emission Particle Tracking (PEPT) technique**, European Journal of Pharmaceutics and Biopharmaceutics, Volume 81, Issue 3, August 2012, Pages 666–673)

Van Melkebeke et al [16] analysed the mixing efficiency in twin screw granulation through co-feeding of tracers. In separate experiments low volumes of tracer were fed as a separate dry stream (2.5% w/w) and within the granulation liquid (0.05% w/w). Analysis of granules showed tracer distribution was excellent for both feed methods with homogeneous tracer distribution across all granule sizes. Tracer distribution was also independent of time with small variance over one hour. As

such it was determined that twin screw granulation displays good mixing efficiency independent of tracer addition method, screw configuration, granulation time and granule size. The conclusions for liquid tracer distribution contradict somewhat the results of El Hagrasy & Litster [37] who found the screw configuration to have considerable control over liquid distribution across the granule size range.

2.4 Liquid to Solid Ratio

Liquid to solid ratio is an important factor in twin screw granulation. TSG is advantageous in that the minimum liquid to solid ratio to consistently granulate a formulation is lower than in other conventional wet granulation techniques such as high shear mixing and fluidised bed granulation [13, 14, 38, 39]. TSG is also more tolerant of high liquid to solid ratios and the point at which over-wetting occurs is higher than in high shear granulation [39]. Thus the operating range for TSG is broader providing a higher degree of process control. Minimum liquid levels are required for granulation to take place [13, 14, 40, 41], similarly an upper limit exists beyond which powder becomes over wetted and forms a paste [13, 14, 23, 40, 41].

Twin screw granulation has some advantages over high shear mixing in its capability to granulate difficult to process active pharmaceutical ingredients. Keleb et al [38] were able to produce granules of pure paracetamol using water as a granulation liquid through twin screw extrusion granulation but were unable to do so by high shear mixing. Similarly through the use of a modified twin screw extruder Shah [27] was able to produce granules with high drug dosage at API to excipient ratios that would result in a tacky mess through high shear granulation.

The size distribution of granules produced by TSG is characteristically broad and bimodal at low liquid to solid ratios becoming narrow and monomodal at high liquid to solid ratio. However it is important to note that the monomodally distributed granules at high liquid to solid ratios are too large to be directly used for tableting [30, 33, 39].

Multiple authors [4, 18, 33] found the average size of granules to increase with increasing liquid to solid ratio. Dhenge et al [4] suggest this is due to the higher liquid amount leading to greater liquid distribution and providing more surface wetting of granules. Contrary to this, in a separate paper Dhenge et al [32] found the average size of granules to decrease with increasing liquid to solid ratio however this was due to the shape of granules being produced. Low liquid to solid ratios would result in elongated granules which skew the size distribution. Granules produced at low liquid to

solid ratios generally consist of a mixture of fines and large oversize agglomerates, increasing liquid to solid ratio gives both a reduction in both fines and oversize agglomerates [32]. However El Hagrasy et al [33] observed that some oversize lumps remained regardless of liquid to solid ratio, from which they inferred that kneading blocks partially break down lumps formed by liquid addition but do not cause complete liquid dispersion.

El Hagrasy et al [33] analysed the effect of changing liquid to solid ratio on formulations consisting of three different grades of lactose. Size distributions displayed the bimodal to monomodal shift at high liquid to solid ratio regardless of the grade of lactose. Despite one grade of lactose investigated, Supertab 30GR, having a narrow monomodal size distribution, the size distribution of granules at low L/S ratios were bimodal, similar to the other grades of lactose (Pharmatose 200 M and Lactose Impalpable).

El Hagrasy et al [33] believe the method of binder addition contributes to bimodality, analogous to spray versus drop-wise binder addition in high shear mixing. The current most commonly used method of liquid addition is by direct injection through liquid inlet ports, resulting in concentrated wetted areas, as with drop wise addition in high shear mixing. The granulator provides insufficient mechanical dispersion to give homogenous liquid distribution, resulting in large wetted agglomerates and small dry fines [33].

In a recent paper El Hagrasy and Litster [37] examined granule formation in the kneading elements of a twin screw granulator and developed concepts for the dominant rate processes. Liquid distribution was analysed and found to be unevenly distributed within the granule population, skewed toward the top end. Liquid distribution became more uniform in screw configurations that provided more densification and similarly with increasing kneading block length. As such for mixing zones with three kneading elements the liquid distribution could be ordered from best to worst as follows: 30°R > 60°R > 90° > 30°F > 60°F. Interestingly the 60°F setup, which is generally the most commonly used in current granulation work, displayed the worst liquid distribution, with

characteristics closest to conveying elements [37]. Contrary to this Yu et al [42] found a notably higher improvement in liquid distribution homogeneity with increasing number of 60°F kneading elements than that observed by El Hagrasy and Litster [37]. This was attributed to the differences in liquid injection method. The granulator used by Yu et al [42] featured dual inlet ports set in parallel on top of either screw, the authors believe this setup results in a more uniform distribution during nucleation, making the granulator less reliant on mechanical dispersion. A similar result was obtained by Vercruyse et al [36] with the variance in moisture content reducing with when a larger number of elements was used.

El Hagrasy and Litster [37] suggested granulation rate processes in kneading sections according to the three dimensional shape characterisation of granules. Analysis of the morphology of the granules allowed for inference of the mechanisms behind formation. Two main rate processes by which the granule shape, size and liquid distribution are determined were suggested. The two main rate processes are: firstly: Breakage and Layering and secondly: Shear-elongation and Breakage followed by Layering. Breakage and layering occurs in neutral and forwarding kneading blocks (90° and 30°F), barring 60°F kneading blocks which display characteristics closer to conveying elements. Reversing geometries (30°R and 60°R) exhibit Shear-elongation combined with breakage and layering.

A point to note is that 60 granules for each configuration were chosen for shape analysis, all from the 2-2.8mm size range, corresponding to the second mode in the bimodal size distribution. As such the differences in shape between these and smaller granules was not considered. Presumably the shape of granules within this size range is considered comparable to granules of all sizes, which may not necessarily be a fair assumption.

Primary agglomerates are formed by drop nucleation at the point of liquid addition, resulting in large, low strength, intensely wetted agglomerates. In configurations where breakage and layering is the main rate controlling process these primary agglomerates are broken apart by the "chopping"

motion from intersection of the kneading elements. This results in smaller rounded granules with exposed wetted edges. These newly formed wetted edges then allow for growth through layering as dry primary powder particles adhere to the surface.

In reversing configurations the kneading block operates fully filled and generates force against the direction of forwarding flow. Material passes through the kneading block as it becomes smeared out between the block and barrel wall, forced through by build up of material within the conveying section upstream of the kneading block. This is similar to flow through reversing geometries in extrusion processes. Shear-elongation occurs as the material becomes smeared against the barrel wall, causing densification and driving liquid to the outside of the granule structure. The thinning in structure during shear-elongation results in an easily broken "ribbon" that splits into thin, dense "flake-like" granules. The wetted surface of these flake-like granules formed in shear-elongation allows for secondary growth through a layering stage [37]. While it was shown that 30° reversing kneading blocks result in monomodal granules with the most uniform liquid distribution, it is important to note that other properties may mean these granules are impractical for downstream use. Their flake-like will result in difficulties with handling and particle flow. Furthermore the high densification that granules undergo during shear-elongation may result in granules with poor dissolution times, as well as low strength, friable tablets due to the low granule compressibility leading to poorly interlocked particles during tableting.

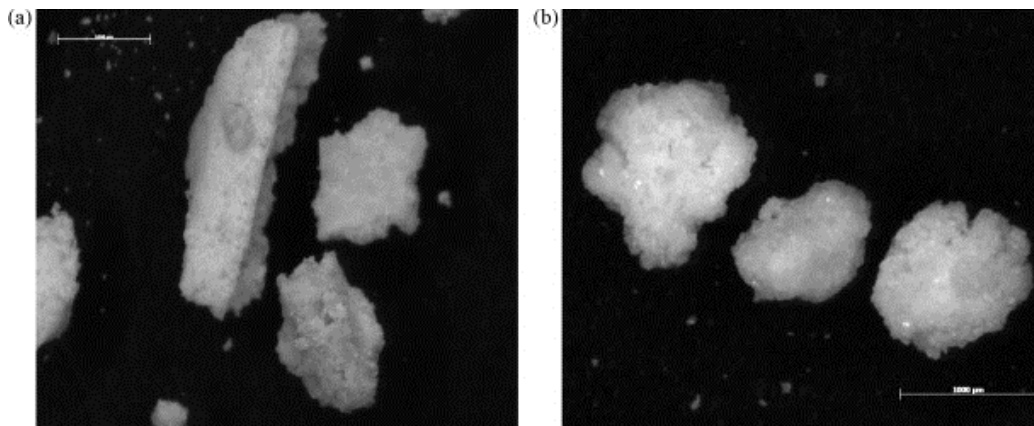


Figure 2.10(a) Rough elongated granules produced at L/S of 0.25. (b) Rounder, smoother granules produced at L/S of 0.4.

(Ranjit M. Dhenge, Richard S. Fyles, James J. Cartwright, David G. Doughty, Michael J. Hounslow, Agba D. Salman, **Twin screw wet granulation: Granule properties**, Chemical Engineering Journal, Volume 164, Issues 2–3, 1 November 2010, Pages 322–329)

Many authors have examined the effect liquid to solid ratio has on the shape of granules produced by twin screw granulation. The aspect ratio of granules decreases with increasing liquid to solid ratio as particles become more rounded [24, 32, 43]. Figure 2.10 shows granules produced at low and high liquid to solid ratios. At low liquid to solid ratios granules produced by twin screw granulation are long and elongated with rough surfaces. High L/S granules become more spherical with smooth surfaces due to surface wetting and increased granule deformability [32]. In the granulation of pure microcrystalline cellulose with water, Lee et al [39] produced granules with similar aspect ratios through both twin screw granulation and high shear mixing. However granules produced by twin screw granulation were found to have a much lower sphericity than high shear mixer granules. Scanning electron micrographs attribute this to the much rougher surfaces of granules produced by twin screw granulation. The porosity of granules decreases with increasing liquid to solid ratio [31, 33], due to the greater wetting of the powder bed producing more deformable granules that are more easily compacted. With the addition of liquid, wetted material becomes cohesive and resistant to flow. So granulator torque initially increases with rising liquid to solid ratio, until a critical liquid to

solid ratio is reached beyond which the liquid acts as lubricant reducing friction and flow resistance [31].

Note that the term sphericity is defined as the ratio of the perimeter of an equivalent circle to the true perimeter of a particle. This is a parameter obtained via particle image analysis defined as:

$$S = \frac{2\sqrt{\pi A}}{P_{real}} \quad (2-5)$$

Where S is sphericity, A the 2-dimensional surface area of the particle captured by image analysis and P_{real} the true perimeter of the particle. A more correct term would than sphericity would be circularity as this is only a measure of how round a particle is in 2 dimensions and not 3 as the name would imply.

2.4.1 Binder viscosity

In TSG an increase in viscosity of binder liquid (i.e. binder concentration) reduces the amount of liquid required to produce granules with a monomodal size distribution [31]. Dhenge et al [31] found the average size of granules to be proportional to the binder viscosity and a similar result was found by Keleb et al [13]. An increase in PVP concentration led to an increase in the mean granule size due to the superior binding properties of PVP over pure water. It is possible to produce granules within higher size classes at lower water concentrations with the addition of PVP [14, 38].

When using screw configurations with conveying elements only the relationship between average granule size and binder viscosity is reversed. Dhenge et al [24] attributed this to the low shear environment caused by conveying screws leading to a dependence on drop penetration time for liquid dispersion. High viscosity binder solutions penetrate the bed slowly leading to poor liquid distribution and a high proportion of fines.

The relationship between binder viscosity and granule size is formulation dependent and will require process optimisation based around material. Yu et al [42] demonstrated that although d_{50} increases

for hydrophilic formulations at higher binder concentration, when formulations contain substantial hydrophobic materials d_{50} is lower following the addition of binder than with pure water. This was explained by the preferential take up of liquid by hydrophilic components during nucleation resulting in more ungranulated hydrophobic fines. The presence of binder in the hydrophilic agglomerates increases their strength making them more resistant to breakage and redistribution of liquid. Further increases in binder viscosity result in higher d_{50} values as the increased strength of the hydrophilic agglomerates allow them to retain size and skew the size distribution [42].

Binder viscosity displays a small influence over the shape of granules, with more rounded granules formed at higher binder viscosity. Thompson and Sun [23] suggest that the effect of binder concentration on shape factor only occurs with conveying screw elements.

The porosity of granules decreases with increasing binder viscosity as stronger liquid bonds are formed under compaction and consolidation, leading to denser particles. Similarly the strength of granules increases with increasing binder viscosity due to the overall 'stickiness' of the material increasing, leading to a greater number of viscous bonds being formed during particle interaction [4, 31, 42].

Viscous binders change the rheology of the powder mixture. Dhenge et al [31] describe how viscous binders cause "thickening" leading to an increase in the cohesiveness and frictional resistance of the material to flow. This increases the energy required to rotate the screws which is observed as an increase in motor torque. The mean residence time increases due to the increased cohesiveness and resistance to flow. This increase in residence time in the granulator means intensified compaction and consolidation of granules. This explains the raise in granule strength and decrease in porosity observed in granules. Similarly aspect ratios are closer to unity as elongated granules are broken and compressed to more uniform shape [31].

Dhenge et al found [31] the surface tension of binders to have no notable effect on the residence time of the granulator or motor torque. However it should be noted that the concentrations of surfactants used in this study were low and surface tensions were similar. Surface tension produces no discernible changes in granule size, shape and morphology. This is due to viscous forces being far more dominant over surface forces, meaning that variation in surface tension has little effect on the mixture rheology [31].

2.4.2 Granulation Regime maps

Existing regime maps for batch wet granulation such as that for drum and high shear granulation developed by Iveson and Litster [44] are robust and play an important role in process development. Understanding the granulation rate processes is essential for regime map development. Twin screw granulation differs from batch granulation in that it is a continuous, ideally steady state process. Granulation regimes occur simultaneously and are physically separated from each other, with nucleation, growth and breakage processes occurring one after the other along the length of the screws. As such granulation becomes unique for each screw configuration and the application of a general regime map may not be feasible [45]. Furthermore despite insightful studies [37, 43] granulation rate processes of screw elements are still not well understood. This is frequently reflected in the lack of systematic arrangement in screw configurations, elements are approached as a series of “black boxes” or the screw unit as a single “black box”.

Nevertheless authors have made efforts to develop regime maps for twin screw granulation. Tu et al [45] developed regime maps based on variation in screw speed (and thus fill level) and L/S ratio; such regime maps are highly geometry, formulation and screw configuration dependent. This was demonstrated by re-feeding the granules in a series of passes through the granulator to imitate multiple mixing sections in a longer screw length. Multiple passes consolidated granules to a more homogenous state resulting in an increasingly uniform size distribution. However behaviour was different in a long single mixing section which was more prone to blockages, highlighting the interdependency of conveying and mixing elements. By non-dimensionalisation of the screw speed in terms of Froude number (Fr) an attempt was made to compare granules produced at similar values of Fr to that of previous work on high shear granulation. Froude number was identified as not a viable factor for comparison as screw speeds required for TSG were an order of magnitude higher than those investigated [45]. Froude number is the ratio of rotational to gravitational forces and measures where particles may overcome gravity during mixing, Froude number is calculated as:

$$Fr = \omega \sqrt{\frac{r}{g}} \quad (2-6)$$

Where ω is impellor rotation frequency in a stirrer system, r the impellor radius and g the gravitational force.

Similar to the regime map for drum and high shear granulation developed by Iveson and Litster [42][44], Dhenge et al [24, 31] have developed two regime maps for twin screw granulation. A granulation regime map for screws including kneading elements [31] and for screws with conveying elements only [24]. Dhenge et al [31] suggest that as twin screw granulation is an open ended process growth mechanisms are not time dependent, therefore granulation is less dependent on rate processes and more dependent on the binding capability of the liquid. The binding capability of the liquid is determined by the liquid to solid ratio and the binder viscosity. The free volume in twin screw granulation is smaller than in high shear or fluidised bed granulation and the stresses acting on material are believed to be higher. As the stresses on the material are more important in determining rate mechanisms and granule properties the value of Stokes deformation used in Litster and Iveson's [44] regime map has been replaced by the deformation value (β) equal to the ratio of the stresses acting on powder or granules (σ) to the strength of granules (τ) [26]. The stresses (σ) acting on material are represented by the value of torque (T) divided by the volume of material in the barrel (V). The strength of granules was determined using Adams' model [46] following a uniaxial compression test of dried granules, which as stated should be ideally replaced by the wet granule strength [31]. This is a weakness of the regime maps and work is required to measure the wet granule strength.

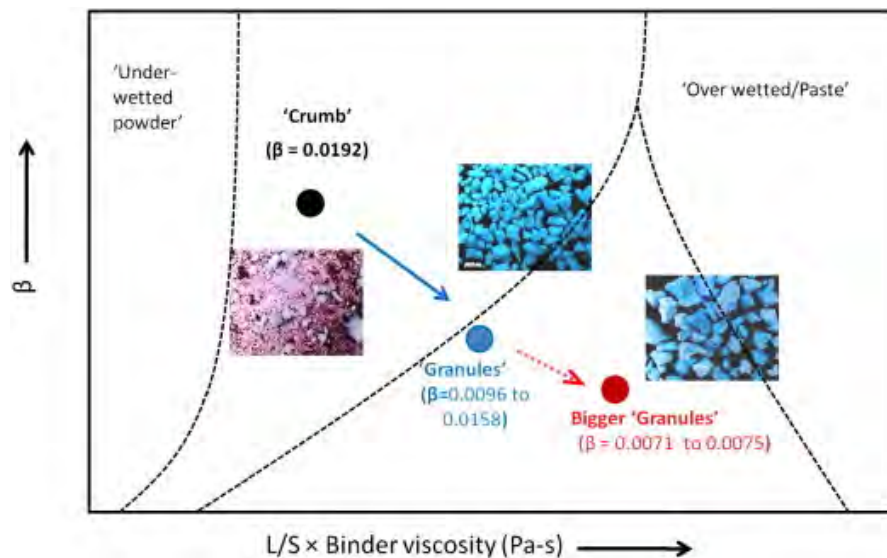


Figure 2.11 Granule growth regime map for twin screw granulation with kneading elements.

(Ranjit M. Dhenge, James J. Cartwright, Michael J. Hounslow, Agba D. Salman, **Twin screw wet granulation: Effects of properties of granulation liquid**, Powder Technology, Volume 229, October 2012, Pages 126–136)

Figure 2.11 shows the granulation regime map for screws with kneading elements. There are four different regions in the regime map; "under-wetted (dry)", "crumb", "granules" and "over wetted or paste". The "under-wetted" region consists of un-granulated or poorly granulated powder, the boundary between the "under-wetted" and crumb region is determined by the liquid to solid ratio and binder viscosity. Small increases in liquid to solid ratio or binder viscosity will shift the material into the "crumb" region consisting of small or poorly granulated granules. Addition of higher amounts of liquid will lead to the "granule" region where consolidated, strong and stable granules are formed. Higher liquid to solid ratios or binder viscosities will result in "over-wetted material or paste". High deformation values at intermediate L/S & binder values can shift the system from the "granule" to the "crumb" regime; at high deformation values the system is weaker and granules are unable to support their structure under the stresses they are undergoing. The boundaries of the granule regime map are highly system dependent and will move according to the process parameters used such as screw configuration, material properties and operating conditions.

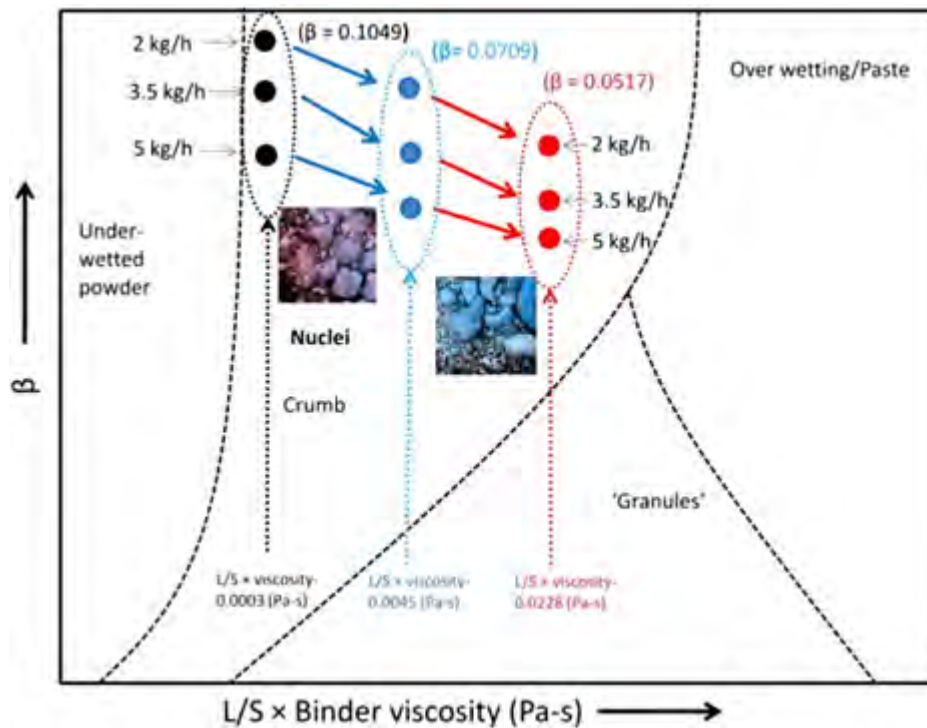


Figure 2.12 Granule regime map for TSG using conveying screws.

(Ranjit M. Dhenge, Kimiaki Washino, James J. Cartwright, Michael J. Hounslow, Agba D. Salman, **Twin screw granulation using conveying screws: Effects of viscosity of granulation liquids and flow of powders**, Powder Technology, Available online 29 May 2012)

The regime map for conveying screw in Figure 2.12 is similar to that for screws with kneading elements, however it differs in the formation of nuclei in the crumb region. “Nuclei” refers to the wetted mass formed after liquid addition under the liquid injection port in the granulator. These are relatively well wetted but poorly formed, loose agglomerates. They remain fully formed when using conveying screws due to the low shear forces imparted on to the material and are easily broken down by kneading blocks.

2.4.3 Binder addition method

El Hagrasy et al [33] compared the results of adding dry binder (in the solid phase) to wet binder (in the liquid phase) on granulation. Formulations were a mixture of lactose and microcrystalline cellulose with HPMC as a binder. Granulation was carried out at a liquid to solid ratio of 0.3 and the effect of adding binder in the solid or liquid phase was compared. Three methods of binder addition were used: first with the HPMC binder mixed with the excipients fully in the solid phase, secondly in a 1:1 ratio in the solid phase and solubilised in the liquid phase, and finally with all the binder fully solubilised in the liquid phase. The size distributions for all conditions and grades of lactose were similar, however it was found that the greater the proportion of binder in the liquid phase, the lower the amount of fines and narrower the size distribution. This was attributed to the short residence in the granulator meaning the dry binder has insufficient time to solubilise and become fully distributed. The use of a wet binder allows for greater binder distribution, giving a smaller proportion of fines [33]. A similar result was observed by Vercruyssen et al [26] who concluded binder was more effective when added in the liquid phase.

Typically granulation liquid is fed into the barrel through a single injection port. Shah [27] explored a range of locations for single and dual injection ports. How these were arranged relative to the screw configurations used is a little ambiguous. A single liquid injection port led to surging of material and “torque excursions” possibly due to over-wetting of material as described earlier. Optimisation of liquid injection was explored via dual ports. The set-up which resulted in minimum torque featured two ports both located in the feed conveying zone, the first port positioned at the point of powder feed inlet and the second immediately before the first pair of mixing elements. This also eliminated surging of material [27]. Vercruyssen et al [36] determined the moisture content of granules as they were discharged through NIR chemical imaging. A periodic fluctuation in the granule moisture content corresponded to pulsation of the peristaltic pump delivering liquid. By running two pumps out of phase the fluctuation in moisture content was eliminated however the standard deviation in moisture content was only marginally improved. As the size distributions of granules were bimodal

under these conditions according to the results of El Hagrasy and Litster [37], the variance in liquid distribution may be a result of the non-uniform liquid distribution of liquid across the size range exhibited in granules formed by 60°F kneading blocks. Contrary to the results of Shah [27] the use of dual injection ports led to no improvement in liquid homogeneity. The liquid injection port is the same as that of Yu et al [42] where each port consists of two nozzles mounted in parallel, one above each screw. Yu et al [42] believe this setup leads to superior liquid distribution during nucleation and may be the reason why Vercruyse et al [36] observed no differences with the addition of a secondary port.

The droplet size is important in high shear granulation. To explore the comparative effect in TSG Vercruyse et al [36] used nozzles of varying diameter to inject liquid assuming that the liquid would enter the granulator in discrete droplets proportional in size to the nozzle diameter. No effect on liquid homogeneity or particle size distribution was observed. However the assumption of droplet nucleation may not be valid, given the layering of material observed on barrel walls [26] liquid may be delivered into a region of saturated paste rather than forming separate droplets. Thus wetting during nucleation may be more reliant on liquid feed pulsation than theoretical droplet size.

Thompson et al [41, 47] investigated the use of foam granulation in a twin screw extruder as a method of reducing surging and improving process stability. To achieve this a foamed binder was fed into the extruder through a side stuffer. The shear strength of the foam allows it to flow separately alongside the powder material and the slow drainage time into the powder bed gives a large wetted contact area, which allows for more homogenous growth of granules. The foam forms a boundary slip layer between the barrel wall and powder material during penetration, reducing the frictional forces and heat generated.

2.5 Fill level, Screw Speed and Feed rate interaction

The barrel fill level in granulation depends on three factors: the screw and barrel geometry, the screw speed and the material feed rate. High screw speed lowers fill level, high feed rate raises it, thus operating fill level is determined by these factors. The fill level is an essential factor in determining granule properties. High fill levels result in high compaction and densification, low fill levels can result in insulation of material from interaction. Fill level affects the residence time in dictating the throughput force for material to flow through mixing zones and affects mixing mechanisms [34]. Thus fill level is an essential consideration during scale up as behaviour may be totally different despite similar screw speeds and feed rates.

The free volume in the barrel is determined by the screw geometry and is therefore a fixed property, during operation the fill level can therefore be controlled by the screw speed and material feed rate. Granulator geometry has variation between different vendors including the clearance between the barrel wall and screws. These differences in clearance are believed to have impact on the granulation process and product quality. For example the residence time and thickness of the slip layer of material which forms against the barrel wall [34, 35] which has repercussions for the “Shear elongation and breakage” rate process proposed by El Hagrasy et al [37]. Thus despite similar operating conditions operators may see variation in granule quality from different granulators.

Therefore knowledge of the fill level relative to operating conditions is important in interpreting the final properties of granules, however quantifiable determination of fill level is noticeably absent within papers, potentially due to the complexity in calculating free volume and determination of residence time. Additionally the axial variation of fill level as shown by Lee et al [35] increases complexity.

Fill level is an important factor which should be considered in comparison of different granulators.

An additional property overlooked is Specific Mechanical Energy (SME), the energy input per unit mass, essentially power consumption divided by mass rate. SME would allow for direct comparison

between different granulators and provide understanding into how granule properties relate to the energy input. Furthermore, SME has importance in an industrial context in determining running costs of equipment.

2.5.1 Screw speed

Screw speed has been reported to have a minor influence over the properties of granules formed by twin screw granulation [13, 32, 48]. This appears to contradict the fact that screw speed is a critical factor in determining the barrel fill level, which is crucial in determining granule properties. It may be that, as reported within typical operation limits screw speed has small effect over granule properties, however toward the upper and lower limits of barrel fill the properties of granules become more dependent on fill level. High screw speeds lead to short residence times in the granulator and the conveying capacity is greater [32]. At a constant feed rate, low screw speeds result in high torque values due to the greater mass load of material filling the granulator. High screw speeds give a reduction in torque as the increased conveying capacity of the screws results in a lower barrel fill level and a lower mass load [23]. Tan et al [49] suggest that at low screw speeds frictional resistance between material and the internal granulator surfaces plays a role in increasing the energy demand in addition to mass load. At high screw speed frictional resistance is considered less important.

Low screw speeds result in high fill levels in the granulator barrel, leading to material compaction where blockages can form at high mass loads. High screw speeds result in low barrel fill levels, where the screw channels may become starved of powder resulting in low compaction and particle interaction. As variation in fill level can result in considerable differences in binder distribution and granule properties screw speed is an important factor to be considered during scale up of twin screw granulation [50].

Dhenge [32] found a small reduction in the size of granules with increasing screw speed, the longer residence times at low screw speeds allow for greater growth of granules. The combination of higher shear and lower fill at high screw speed leads to poorly compacted, rough surface, elongated granules. Conversely granules produced at low screw speeds undergo greater compaction resulting in smooth surfaces and more spherical shape.

Similar results were found by Thompson et al [41] who suggest that the lower screw speed leads to an upstream pressure at the kneading block leading to greater compaction of material. Furthermore granules experience fewer "chopping" events as they flow through the kneading block, leading to less breakage. This is supported by the work of Kumar et al [34] who demonstrated that flow becomes more plug like at low screw speed. Thompson et al [41] found an increase in granule fracture strength with screw speed. Screw speed was inversely correlated with granule size, small granules produced at high screw speeds displayed higher fracture strengths than large granules produced at low screw speeds. However this may be the result of the size strength relationship of granules, a full evaluation should compare the strength of granules in comparable size classes in order to determine this.

Lee et al [39] observe that the influence of screw speed on average particle size only occurs at higher liquid to solid ratios. Variation in screw speed gave no change in average granule size at low liquid to solid ratio however at high ratios an increase in screw speed led to a decrease in average granule size. However screw speed produced no significant effect on granule porosity or strength.

2.5.2 Material Feed Rate

Many authors observe that the strength of granules is dependent on the fill level. The higher the feed rate, the more powder in the barrel and the denser and stronger the granules formed [23, 30, 32, 48, 50]. Motor torque at steady state increases with increasing material feed rate [26, 30].

Dhenge et al [30] took torque values to be an indication of the degree of compaction of the material in the granulator, as the porosity of granules decreased with increasing material feed rate, shown by

X-ray tomography. The greater compaction of granules at higher feed rates leads to stronger granules with longer dissolution times [48, 50].

Surface velocity of powder above conveying screws was determined by Dhenge et al [24] through Particle Image Velocimetry (PIV). The surface velocity of powder was higher at lower feed rates. Dhenge et al [24] suggest that the higher fill level at pronounced feed rates leaves less space for individual particle movement due to the close packing of particles. Powder moves in the form of compacts as opposed to individual particles. The higher fill level results in greater frictional forces between the powder and barrel wall, giving lower surface velocity. At low fill levels particles are able to move freely and experience less frictional resistance and therefore surface velocities are higher [24]. This is confirmed by Kumar et al [34] who observed poorer axial dispersion under higher feed rates.

Contrary to the results of Dhenge et al [24, 32], Djuric et al [48, 50] found the median size of granules to increase with increasing material input rate. The difference in results can be explained by the different screw configurations used in the studies. Djuric [48] compared two granulators with the same screw configuration but different size. Both had a single long kneading block. Dhenge et al [32] used the same number of kneading elements relative to screw length but arranged as two separate kneading blocks. The single long kneading block leads to enhanced compaction and consolidation meaning growth rates outweigh breakage rates. This provides evidence for the as yet unquantified fill dependency of granulation mechanisms and their variation with screw configuration.

The two granulators compared by Djuric et al [48] had similar screw configurations but different free volumes. A Leistritz extruder with a screw diameter of 27 mm and an APV Baker extruder with a screw diameter of 19 mm. Increasing the feed rate gave a considerable increase in median granule size in the granulator with smaller free chamber volume and only a small increase in median granule

size in the granulator with a larger free chamber volume. Showing the importance for fill level consideration in scale up as well as material feed rate, screw speed and geometry.

Vercruysse et al [26] found no significant effect on the size distribution of granules with varying material feed rate. Although varying the feed rate gave different degrees of barrel filling and torque values there were no significant differences in size distribution. Fill levels were not quantified but may have been below levels that result in significant changes in degree of compaction similar to Thompson and Sun [23] who found the angle of kneading elements to only affect size distribution when the fill level is high, at 70% in their work.

2.6 Conclusions

Twin screw granulation is a technique rapidly growing in popularity for pharmaceutical processes. While research on TSG has advanced considerably within the past two decades there still exists considerable need and potential for developing process understanding and optimisation. The process is still frequently taken with a black box approach and granulation mechanisms must be better understood. Whilst insightful work has helped develop understanding into the mechanisms of mixing elements [34, 37], the complex interaction between conveying and mixing zones and the dependency on process and formulation properties remains poorly comprehended.

Design of screw configuration remains very empirical, the traditional configuration is a long conveying section feeding into one or two mixing sections however it remains unknown if this is the optimum configuration. Adaption of screw configuration has been shown to have the potential for control of granule size and shape [23]. By developing understanding of the granulation mechanisms of screw elements and their interaction with each other a systematic approach can be taken by an operator to optimise the process in a true quality by design approach.

A challenge which exists in building understanding is knowing what factors to measure and how to measure them. Interpreting the granulation mechanisms is inherently difficult due to the complexity in visualising the active process. Techniques such as NIR chemical imaging employed by Kumar et al [34], PEPT employed by Lee et al [35] and 3D shape characterisation employed by El Hagrasy and Litster [37] are powerful tools in understanding flow and mixing properties. While traditional methods of granule quality measurement are essential due to the continuous nature of TSG there is a need to develop methods of in-line quality measurement. Fonteyne et al [51] have made progress in this area through the application of in-line sizing and NIR and Raman spectroscopy for continuous measurement of solid state distribution.

Currently work is being carried out on a variety of different granulators of varying geometry with often apparently contradictory observations. Because of this there exists a need to develop a

quantifiable measurement to allow for comparison between different granulators. Fill level is a dimensionless quantity that can allow comparison but is incomplete in that residence time and energy input are not considered. Development of a quantifiable measurement will ease both scale up and process characterisation. Attempts to achieve this have been made through the development of regime maps [24, 31, 45] but these remain extremely equipment and formulation specific.

Despite the progress made in understanding TSG there is still difficulty in producing high quality granules. The characteristic bimodal granule size distribution adds complexity to downstream processing, similarly monomodal distribution granules formed at high L/S are consistently too large for tableting without milling. Fines are often in abundance and factors leading to reduction in fines often result in higher proportions of oversize agglomerates [26, 36]. There exists a large scope for process optimisation to increase the yield and the need to develop the understanding to achieve this.

Formulation varies widely within the different bodies of work on TSG and will have strong influence over granulation mechanisms, granule physical properties and suitability for tableting. While it has been demonstrated that TSG is effective in granulating high drug load formulations [17, 20, 27, 40] and traditionally difficult to process materials [15] most papers are limited to easily processed common pharmaceutical excipients. Work has gone into understanding the process response to variation in formulation properties [42] but extensive optimisation will still be required for new process lines, particularly due to the unique flow properties associated with many APIs. Because of the variation found in model formulations there exists a need for a thorough exploration into process formulation dependence such that conclusions drawn from a wide variety of sources can be consolidated.

Finally modelling of twin screw granulation is an area conspicuously under-represented from research work, with only two instances of recently published work [25, 52]. Development of robust models is an essential requirement for process understanding and scale up.

Nevertheless twin screw granulation remains an attractive method of continuous wet granulation.

The wide scope and success of research work shows the potential of this emerging granulation process.

Chapter 3 - Asymmetric
Distribution in Twin Screw
Granulation

3.1 Introduction

Granulation consists of multiple granulation rate processes, in a batch granulation process these processes change over time and a process must be developed to find an end point which results in granules of desired properties. Continuous granulation differs from this in that rate processes occur uniformly, each “plug” of material passing through the granulator undergoing the same rate processes with similar residence times. Granulation time is not a control factor in continuous granulation thus rate processes, i.e. growth and breakage must be controlled through other process parameters. Changes to which will be shown by the change in residence times. To gain this degree of control over the granulation process it is first required to build understanding of the granulation rate processes which are occurring.

The rate processes in a batch high shear wet granulation process can be thought of in three broadly sequential stages in time, first nucleation during liquid addition, second growth in wet massing and third breakage as mixing continues. In a similar vein continuous wet twin screw granulation can be thought of as following three stages, nucleation at liquid addition, growth during mixing and breakage with further mixing. The crucial difference is that these stages are separated by distance rather than time, with a plug of material undergoing each process sequentially as the material changes travelling through the granulator. This analogy is somewhat simplistic as in any real granulation process multiple rate processes will be occurring concurrently, but serves to describe the dominant rate processes and differences between batch and continuous granulation.

As the rate processes do not change with time in a continuous process it is important to consider what effect process parameters have. A twin screw granulator can operate at a range of different steady states across where for example, the ratio of liquid to solid is the same but the material feed rate is different.

This chapter seeks to explore the flow of material within the granulator and how this affects granulation rate processes, with a particular focus on nucleation. In the past two decades the depth

of research into TSG has increased considerably. Research has looked into the response to process parameters including: screw speed [13, 32, 48], material feed rate [21, 23, 30, 32] and liquid to solid ratio [13, 14, 38, 39]. Despite this the mechanisms of TSG are still not well understood, the modular nature of the screws and differences in granulator size and geometry makes drawing comparison between different granulators difficult. Visualisation of the flow inside the granulator is inherently difficult due to the requirement of running within an enclosed barrel. Granulation mechanisms must usually be inferred from final granule properties. Dhenge et al [4] examined the steps in granule growth by stopping an actively running process and extracting samples of granules from the different regions of the granulator. El Hagrasy & Litster [37] used three dimensional shape characterisation to develop concepts for the dominant granulation rate mechanisms in the mixing zones of a twin screw granulator. Kumar et al [34] employed near infra-red chemical imaging in order to determine residence time distribution (RTD) and infer the degree of axial mixing with changes in process parameters. Visualisation of the flow of material inside an actively running granulator was achieved by Lee et al [35] who employed PEPT (Positron Emission Particle Tracking) to determine RTD and fill level occupancy across individual screw elements.

Twin screw granulators have modular screws, allowing for transport and mixing elements to be arranged in numerous permutations. Screw elements can be classified as either transport or mixing elements. Conveying elements are transport elements which consist of helical flighted screws, these can be single or double flighted with double flighted elements being the most commonly used. There is some variety in mixing elements, with kneading elements and various designs of comb mixer elements between different manufacturers. Kneading elements are the most commonly used type of mixing element across the available literature. Bilobal kneading elements always mesh at 90° to their opposing element. Rotation of the screws causes material to be kneaded and compressed between the lobes of the elements. Kneading elements with a width of 0.25 times the screw diameter are most commonly used amongst granulator manufacturers and appear to be the default type of mixing element. It is not known if this ratio for kneading element width is optimum for

granulation. The profile of these elements differs between manufacturers leading to differences in screw clearances but there has not been a great deal of work into how these differences in screw clearances affect granulation. Kneading elements are arranged in sections known as kneading blocks. This results in a mixing zone on the granulator screw. The angle at which each element is arranged relative to the element downstream of it determines the conveying capacity of the kneading block. Typical angles are 30° , 60° and 90° but depending on the design of screw root many more angles can be used. The arrangement angle can result in either forwarding or reversing conveying capacity, where the tips of the bilobes form a screw flight either pushing material downstream or upstream against bulk flow. 90° elements are the exception to this and possess neutral conveying capacity. Flow through the kneading block is not determined exclusively by the arrangement angle however and is driven in large part by the force feeding of upstream conveying elements. This is why reversing angles can be used but overall forwarding flow maintained.

There remains a need to understand processes occurring within the granulator. This chapter examines fundamentals of material flow within conveying zones of the granulator and their dependence on fill level. Liquid distribution is examined and the importance of nucleation in determining granule properties is highlighted. Finally the conveying zone mixing efficiency is examined and typical granulation formation mechanisms suggested.

3.2 Experimental Method

3.2.1 Preparation of powder formulation

For granulation experiments a formulation consisting of 75% alpha lactose monohydrate (316/FAST-FLO®, Foremost Farms, USA), 20% Microcrystalline Cellulose (Avicel PH101, FMC BioPolymer, Ireland) and 5% Hydroxypropyl Cellulose (Klucel EXF, Ashland Inc, USA) was used. The formulation was blended in a Pascal lab mixer for 25 minutes to ensure homogenous mixing. Median particle size was determined to be ~125 µm through image size analysis (Sympatec QICPIC).

3.2.2 Granulation process

Granulation was performed using a lab scale co-rotating Twin Screw Extruder (TSE) (Haake, Thermo Scientific, Germany) with screw diameter of 16 mm and length to diameter ratio of 25:1. Granulation was performed based around screw configurations consisting of a single 60° Forwarding kneading block, assigned the notation [18x 1D C//4x 0.25D K 60°F//6x 1D C] where D represents the screw length expressed in number of diameters, C conveying elements and K kneading elements. Thus from the screw inlet the configuration consists of 18 conveying elements each 1 diameter in length, 4 kneading elements each 0.25 diameters in length offset at an angle of 60° in the forwarding direction and finally 6 conveying elements each 1 diameter in length. Powder was fed into the barrel at the base of the screws via a volumetric twin screw feeder (T20, K-Tron Soder). Granulation liquid (distilled water) was added through a single injection port positioned above the screws approximately 9 diameters length from the base and provided by an 8 roller peristaltic pump (REGLO Digital, Ismatec, Switzerland).

3.2.3 Determination of Transverse Distribution in Conveying Zones as a Function of Fill

In order to determine the mass load conveyed by each screw the Haake TSE was fitted with screws consisting of only conveying elements (25x 1D C). The dry formulation was fed through to the granulator and the fill level varied through material feed rate (1-7 kg/h) at set screw speed (100 and

400 rpm). A stainless steel sheet was positioned at the outlet aligned with the barrel centreline to physically separate the material as it was discharged from each screw into separate vessels. The mass of material collected in each container at steady state was measured. The distribution of material at the discharge is believed to be representative of the transverse distribution of material across the entire conveying section.

3.2.4 Size Selective Segregation

The extent of size segregation in conveying zones was examined by feeding a bimodal mixture of spherical MCC pellets through the long conveying section of the Haake extruder. The mixture consisted of a 50/50% (w/w) blend of 1000 μm and 100 μm pellets (Cellets 1000 & Cellets 100, Pharmatrans Sanaq AG, Switzerland). No granulation liquid was added to ensure the surface forces between particles and the screws was the same and segregation was as a result of differences in particle volume only. Material was separated at the discharge as described above and the size distribution determined by the mass fraction of material which could be passed through a 500 μm aperture sieve.

3.2.5 Positron Emission Particle Tracking (PEPT)

In their work on twin screw granulation at the University of Birmingham Lee et al [35] generated a wealth of data through PEPT on a specially modified twin screw granulator (GEA Niro, UK). This was taken advantage of and reprocessed in order to gain a picture of material flow in the conveying zones of the granulator. The experimental setup is described by Lee et al [35]. PEPT is a technique which allows for the tracking of a radioactive tracer particle in three dimensions within an actively running process. The tracers used in the experiments were 100 μm ion exchange resin particles labelled with Fluorine-18 through an ion exchange technique. ^{18}F was selected as the tracer radionuclide as it undergoes beta decay, has a short half-life and degrades to water. As the tracer undergoes beta decay it releases a positron which very quickly collides with a local electron and is annihilated to release two "back to back" 511 keV gamma rays. PEPT cameras detect the γ -rays and

the position of the tracer is determined from the intersection of multiple pairs. PEPT visualisation was performed on a specially modified twin screw granulator provided by GEA Niro, UK. The granulator barrel was machined down to a low thickness to minimise the attenuation of gamma rays and maximise tracer detection. The screws of the granulator were 19 mm in diameter with a length to diameter ratio of 10:1. For each experiment the tracer was fed through the granulator a minimum of 100 times in order to build a dataset representative of the flow of material.

The raw data generated by Lee et al [35] was reprocessed in order to examine flow of material in the conveying sections of the twin screw granulator. Note that no additional PEPT experimentation beyond that of Lee et al [35] was performed. The data presented here comes entirely from re-processing of this raw data to characterise a novel area.

The time spent by the tracer in the different regions of the granulator is representative of the distribution of material within the actively running process. In order to show how material is distributed between the two screws in conveying zones for each pass of the tracer through the granulator the time spent by the tracer on each screw was determined. The final value of transverse distribution was determined from the summation of time spent by the tracer in all passes.

Raw PEPT data was processed using the in house “track.exe” program developed by the University of Birmingham Physics department to translate the data into a matrix of cartesian coordinates with timestamp. Code was written in MATLAB in order to process this data to selectively examine the conveying sections and the radial distribution between them.

3.2.6 Liquid Distribution

The effect of fill level on nucleation and final liquid distribution was investigated in this study. Granules were produced using the Haake TSE, local fill level was controlled by including elements with longer residence times immediately upstream of the point of liquid injection. Long residence time elements have correspondingly high local material fill levels. Overall fill level was controlled

through material feed rate at set screw speed. The screw configurations used to achieve desired fill level distributions are shown in Table 1. Fill levels were not measured directly and 'high' and 'low' fill levels are qualitative relative descriptions. Granulation was performed at 400 rpm screw speed and 2 kg/h mass feed rate. Liquid distribution was first determined gravimetrically through loss on drying using the following method. Liquid was fed into the granulator at a liquid to solid ratio (L/S) of 0.15, after production of a minimum of 100 g of granules they were immediately transferred to a series of sieves (British Standard 5600 - 63 μm). Granules were sieved using a vibratory sieve shaker (Fritsch, Germany) at an amplitude of 2 mm for 10 minutes, samples of a minimum of 1 g were taken from each sieve and weighed. Granules were then oven dried at 100°C for 1 hour in order to measure the loss on drying. This method is flawed as it cannot account for changes in granule size during sieving or loss of liquid during this period. Granules undergo agitation during sieving which will result in growth and breakage of particles, thus the resultant material cannot be said to be truly representative. In addition the lactose monohydrate in the formulation will lose the hydrate during drying and this change in mass is not accounted for.

Acknowledging the fault in the above method an alternative was followed. Liquid distribution was secondly determined through tracer analysis following a procedure similar to el Hagrasy et al [37]. A 0.1% (w/v) Nigrosin dye solution was used as the granulation liquid. Granules were produced at an L/S ratio of 0.18 and oven dried at 100°C for 2 hours. Dried granules were sieved through the same series of 14 sieves. Samples representing less than 1% of the original sample mass were discarded. 2 g samples were taken from each sieve and dissolved in 10 ml of distilled water. Samples were sonicated for 1 hour to ensure complete dissolution of granules before being centrifuged at 4000 rpm for 10 minutes in order to separate insoluble excipients. Approximately 1.5 ml of the supernatant was drawn off each sample and the dye concentration determined from absorbance of light at 565 nm using a UV/Vis spectrophotometer (Aquarius 7500, Cecil, UK). 565 nm was selected as this is the wavelength at which the extinction coefficient of nigrosin is highest. The absorbance of light by a chemical species can be related to its concentration using the Beer-Lambert law where:

$$A = \log_{10} \left(\frac{I_0}{I} \right) = \varepsilon c L \quad (3-1)$$

Where A is the measured absorbance, I_0 the intensity of incident light at given wavelength, I the transmitted intensity, ε the extinction coefficient, c the concentration of the absorbing species and L the path length of light through the sample.

A series of nigrosin solutions were made up in water in order to build a calibration curve of known concentration against absorbance. Note that the path length of the spectrometer is fixed at 1 cm and thus absorbance is directly proportional to solution concentration. This calibration curve allowed for calculation of the concentration of nigrosin in granule samples and thus the water content.

Table 1 - Screw configurations explored in liquid distribution study.

Local Fill Level	Material Feed Rate (kg/h)	Screw Speed (rpm)	Screw Configuration
Unmodified	2	400	18x 1D C//4x 0.25D K 60°F//6x 1D C
Low	2	400	7x 1D C//3x 1D C (0.25D Pitch)//8x 1D C//4x 0.25D K 60°F//6x 1D C
Medium	2	400	7x1D C//4x 0.25D K 60°F//10x1D C//4x 0.25D K 60°F//6x 1D C
High	2	400	7x1D C//4x 0.25D K 90°//10x1D C//4x 0.25D K 60°F//6x 1D C
Overall Fill Level			
Low	1	200	18x 1D C//4x 0.25D K 60°F//6x 1D C
High	4	200	18x 1D C//4x 0.25D K 60°F//6x 1D C

3.3 Results

3.3.1 Asymmetric Material Distribution in Conveying Zones

The distribution of material in conveying zones is highly asymmetric, with one screw carrying the bulk of material. Figure 3.1 shows the distribution of material collected at the discharge of the granulator outfitted with conveying screws only. In order to differentiate between the two screws the well filled right screw has been termed the 'driving' screw as it carries the bulk of material forward while the poorly filled left screw has been termed the 'loading' screw as the main function is to load material onto the driving screw. The granulator operates in a starved fed fashion where material flow rate is determined by an upstream feeder. Increasing feed rate will lead to increasing fill level up to the point of complete fill at places in the barrel.

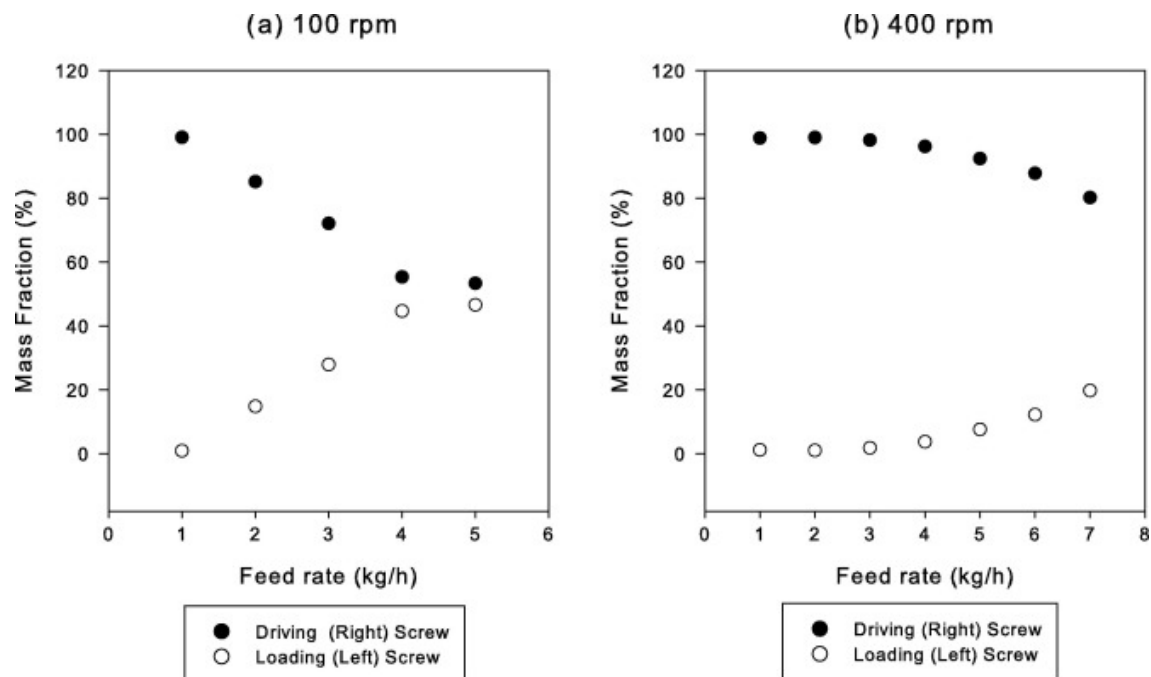


Figure 3.1 - Transverse material distribution of dry ungranulated formulation conveyed at a range of feed rates
a) 100 rpm screw speed, b) 400 rpm screw speed.

Figure 3.1b Shows that at low barrel fill level at low feed rates the transverse discharge of material is totally asymmetric with 100% of material discharged from the driving screw. The transverse distribution only approaches uniformity at the maximum conveying capacity of the granulator at

approximately 4.5 kg/h feed rate and a reduced 100 rpm screw speed in Figure 3.1a. The distribution of material at discharge is representative of the transverse distribution of material throughout the entire length of the conveying zone assuming uniform fill level along the barrel length.

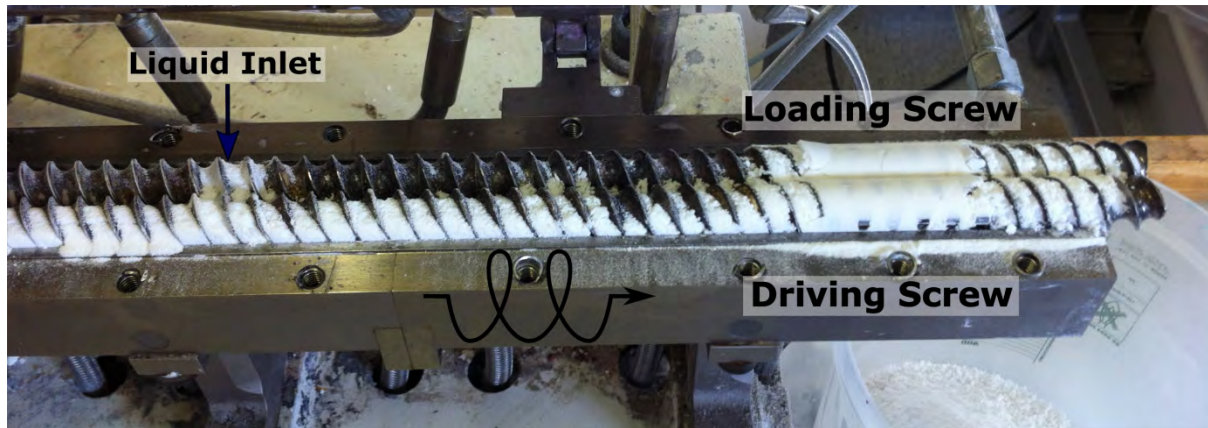


Figure 3.2 - Example image of the HAAKE TSE showing the distribution of material during granulation. Looking down the barrel rotation is counter-clockwise.

Figure 3.2 illustrates how conveying asymmetry can appear during granulation, note the well filled driving screw and poorly filled loading screw. Here the granulator had been brought from running to an emergency stop, so the loading of material is representative of the actual case during granulation. In this example the kneading block is operating highly filled and the fill level in the conveying section is comparably low. As the residence time of the kneading block is much longer than conveying sections it defines the feed rate the granulator is capable of operating at. Feed rates above this will lead to accumulation upstream and eventually blockages. As such, conveying sections in granulation systems are likely to typically operate partially filled.

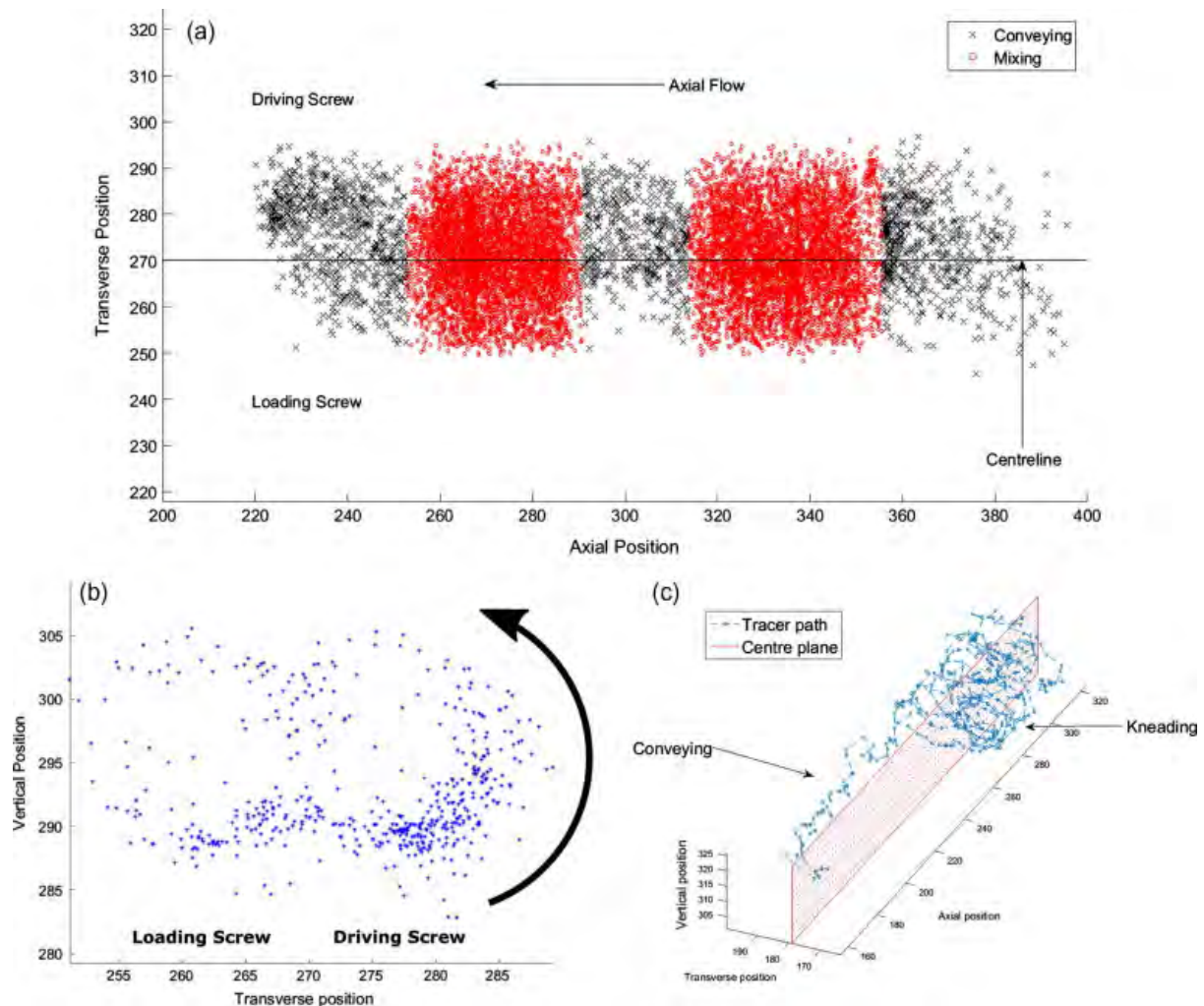


Figure 3.3 - a) Overhead view of the GEA Niro TSG showing each detection of the PEPT tracer in 100 passes through the granulator at 10 g/min and 150 rpm b) End on view showing the position of the tracer in the conveying sections of the TSG, rotation is counter clockwise and flow in direction of the reader c) Single pass of a tracer through the TSG with screw configuration [4x 0.25D K// 4x 1.5D C// 6x 0.25D K// 1x1.5D C] to illustrate conveying load asymmetry, axial flow is away from the reader and rotation is clockwise.

PEPT visualisation of the conveying zones of a twin screw granulator was undertaken in order to confirm the measured asymmetric transverse distribution. Figure 3.3a illustrates an overhead view of the GEA TSG with screw configuration [2x1.5D C//7 x 0.25D K 30°F//1x 1.5D C//6x 0.25D K 30°F//1 x 1.5D C] where each data point represents a detection of the tracer in approximately 100 passes through the granulator. The detection density is much higher in the mixing zones of the TSG indicative of the much longer residence time compared to conveying zones. Figure 3.3b shows the

vertical and transverse position of tracer detections within the conveying sections of the same geometry. The higher detection density to the bottom right of the image indicates the higher material loading of the driving screw. Figure 3.3c illustrates an example flow path of a tracer through the TSG with a single mixing zone showing the asymmetrical conveying flow path. The results of the PEPT study are shown in Table 2. The fraction of time spent by the tracer on the driving screw is greater than 50% for all the conditions investigated. Providing evidence toward the predicted flow asymmetry in conveying zones.

The original PEPT experimental setup had a broader investigative focus than applied in this study. Data was reprocessed to look exclusively at conveying zones in an effort to capture novel information. Due to this the useful measurement time is relatively small. In addition the flow of wet granular compared to dry powder material is likely to be different. As such the values generated through processing the PEPT data are not necessarily representative of all systems. In spite of this, as a tool for visualising the flow and distribution of material PEPT adds valuable evidence toward the measured and expected flow asymmetry.

While the time spent in conveying is so low, asymmetry here upstream of fluid addition could be very important. The difference in distribution of material is not as extreme as may be predicted from the outlet distribution of the Haake extruder in Figure 3.1 due to the higher overall fill level established by the mixing sections. Additionally the wet granular material is 'stickier' than the dry powder formulation fed through the Haake extruder, as such material is more likely to adhere to the screw surface under these conditions promoting the transfer from the driving to the loading screw. By adding liquid the 'rheology' of the material changes, wet granular material will have a higher wall friction angle aiding the transfer of momentum from the screw. This makes it more inclined to follow the rotation of the screw and be transferred to the loading screw. It is then interesting to note that despite this, differences in screw material loading can be observed through PEPT. When considering the transfer of material between screws with granulators from different manufacturers the

differences in screw clearances may have an important impact. Despite the differences in screw diameter the granulators in this study had similar screw-screw and screw-barrel clearances (~0.2 mm), thus any effect of clearances is expected to be similar. In systems where clearances are larger or smaller, particularly with respect to the particle size flow patterns may be different. Larger clearances may result in new flow paths, such as between the screws or extruded against the barrel wall which may affect the transfer of material between screws.

Table 2 - Sum of time spent by the PEPT tracer in each zone of the granulator.

Configuration	Total Time (min)		Time in conveying zones (s)		Percentage of Time - Driving Screw (%)
	Mixing	Conveying	Loading Screw	Driving Screw	
10g/min - 150rpm					
30°F KB	21:45	4:18	93.6	164.3	64
60°F KB	28:24	4:13	92.7	159.9	63
90° KB	25:40	3:24	47.4	157.1	77
10g/min - 300rpm					
30°F KB	12:42	2:18	59.6	78.5	57
60°F KB	17:27	1:42	34.2	67.8	66
90° KB	17:09	1:27	39.6	47.0	54
20g/min - 300rpm					
30°F KB	9:27	1:36	38.3	58.0	60
60°F KB	14:19	2:43	53.4	109.2	67
90° KB	20:22	1:48	51.5	56.4	52

The distribution between the driving and loading screw in the GEA and HAAKE granulators are not directly compared as there are too many variables between the two systems. Different formulations are used in different granulators and no scaling or matching of process parameters have been

performed. Therefore direct comparison would not be valid, however it is of interest to note the same observed effect in both systems. It is less pronounced on the GEA granulator and it is believed to be due in part to the wetted material being more cohesive and the experimental setup, the screw configuration and operational fill level. The lack of liquid binder in the HAAKE system being a key difference, which will result in very different powder rheology. It would be of interest in future work to carry out a PEPT measurement of conveying screws across varying fill levels only in order to study the effect in more detail.

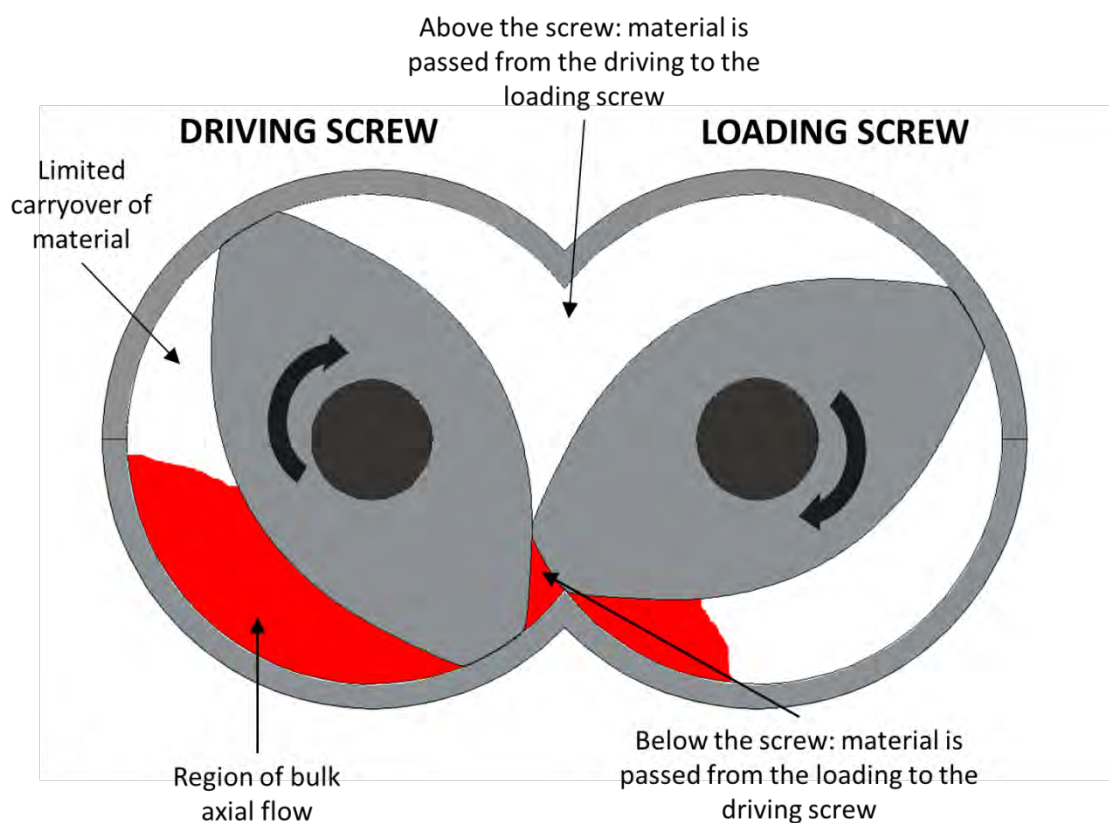


Figure 3.4 Front on schematic representing the transverse fill profile which establishes across the entire length of conveying zones and the transfer of material between screws. Axial flow is toward the reader.

The asymmetric distribution of material in conveying zones is a result of the screw geometry and the effect of gravity. Figure 3.4 illustrates the transverse distribution of material in conveying zones. In the partially filled environment of conveying zones the bulk material will tend to remain below the screws under gravity. Under rotation, the flight of both screws will push material axially toward the

barrel discharge and sideways in the direction of rotation. The screws are co-rotating meaning that material below the screws is conveyed in the same direction. This results in material being conveyed from the loading screw onto the driving screw and from the driving screw against the side wall of the granulator. As a result the rotation of the driving screw acts mainly to drive material axially forwards. For material to follow the rotation of the driving screw there has to be sufficient adhesion between the material in the limited volume of the flight channel and surface of the screw. Carryover of material to the top of the driving screw is thus dependent on the fill level in conveying zones, the force between material and screw surface, the stickiness and wall friction angle of material. Carryover of material will increase with fill level: under well filled conditions the radial flow pattern above the screws will be reverse of that below the screws, with the driving screw loading material onto the loading screw resulting in a "Figure of eight" flow. This is likely to only occur when the volume of material exceeds the free volume of the driving screw. Under low fill conditions material will remain isolated in the flight chambers of the driving screw undergoing plug like flow with minimal transverse mixing. In general the fill level in conveying zones will be low, to achieve high fill levels in conveying zones a high overall fill level is required which may result in blockages forming in mixing zones [45].

3.3.2 Size Selective Segregation in Conveying Zones

The crucial factor in flow asymmetry is the resistance to transfer of material from below the driving screw. The force acting on the material comes from the friction or transfer of momentum from the screw and resistance to flow from gravity acting on the material. Thus the higher the frictional force between a particle and the screw surface the greater the probability that it will be carried over. Carry over is selective to large particles due to their size relative to the screw clearance and the greater momentum imparted to them. Their greater volume results in compression against the barrel wall and increase in friction against the screw surface. Small fine particles can pass through the screw clearance and so do not get gripped between the screw and barrel wall and hence are not lifted with the rotation. Table 3 shows the distribution of a bimodal size mixture of MCC pellets fed

through the conveying section of the Haake extruder. Screw speed was constant at 200 rpm and mass feed rate increased to an arbitrary fill level where material discharge from the loading screw could be observed. The bulk of material is again conveyed by the driving screw. It can be seen that the material conveyed by the loading screw consists mainly of large particles (72% of material collected), illustrating the segregation effect and dependence on particle volume.

Table 3 - Distribution of a 50/50 wt% blend of 1000 and 100 μm MCC pellets discharged from either screw in a long conveying section at 200 rpm.

	Mass load Conveyed % (gram)	
	Driving Screw	Loading Screw
Total Material Conveyed (100 g)	78	22
Coarse Particles (1000 μm)	45 (35.1g)	72 (15.8g)
Fine Particles (100 μm)	55 (42.9g)	28 (6.2g)

Size segregation in conveying zones is a result of screw geometry. It occurs due to the higher probability of large volume particles to be carried over from the base to top of the driving screw. Material that is carried over following the rotation of the driving screw may additionally be segregated in transfer to the loading screws. Depending on the clearance between the screws fine particles may follow the rotation of the driving screw and fall through the gap between screws. Above the screws particles larger than the screw-screw clearance may become trapped between the flights of both screws and be conveyed forward with a rolling motion. The screw-screw clearance of the Haake extruder is 0.2 mm and thus larger than the size of the fine particles. This is likely to contribute to the segregation effect, forming a flow path which the coarse particles cannot take. However not all fine particles fall through this clearance, as implied by the fine material collected from the loading screw. The geometry of different extruders and their clearances varies between manufacturers. The clearance and relative particle sizes in any given system are likely to contribute to the degree of segregation.

3.3.3 Fill Level and Liquid Distribution

Figure 3.5 shows the size and normalised liquid distribution of granules produced by a single 60°F kneading block at low overall fill level. Liquid distribution for each size class was normalised against the average liquid content of the granule population. Liquid is non-uniformly distributed and skewed toward the top end of the granule size range. The bimodal size distribution is characteristic of twin screw granulation but it becomes sharply monomodal at high L/S ratio [32, 33, 39]. Despite being consistently monomodal in size distribution the granules produced at high L/S ratio are typically too large to be used directly for tableting, greater than 1400 µm in size. In addition liquid remains non-uniformly distributed at increasing L/S ratios. Granules produced at lower liquid to solid ratios are within a more useful size range, however the inherent heterogeneity indicated by the bimodal size distribution causes difficulties in downstream processing. The short 60°F mixing section in the screw configuration explored here is not adequate to ensure homogeneous liquid distribution. Table 4 shows the mass weighted coefficient of variance (CoV) in liquid distribution at various fill levels. CoV is a measure in the variance of liquid content between different particle size ranges averaged out over the mass of particles in that size range, and thus accounts for the different breadth of size classes. At higher local fill levels at the site of liquid injection the variance in liquid distribution is slightly reduced. Changes in size distribution are minimal and remain bimodal however the distribution of liquid becomes more uniform at high fill level as reflected by the values of CoV in Table 4. The data presented in Figure 3.5 was obtained using the method for loss in mass of wet granules and thus carries bias due to the handling of wet granules before measurement. The main mode in the size distribution is likely shifted to the right due to agglomeration of wet particles during sieving. The data presented in Table 4 and Figure 3.6 uses the improved nigrosin tracer method for obtaining liquid distribution and does not carry this bias.

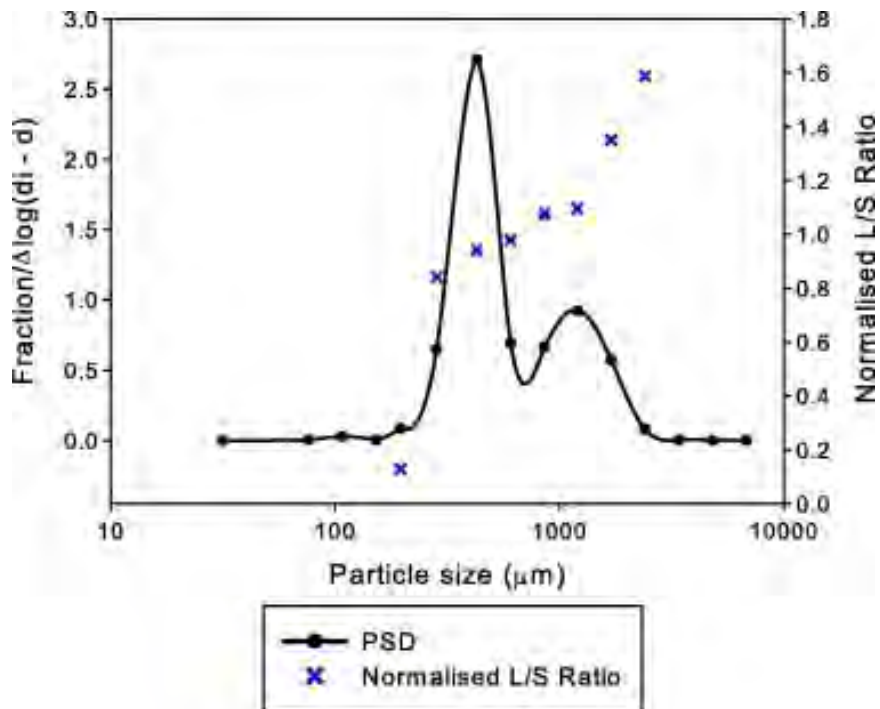


Figure 3.5 Size distribution and normalised liquid content of granules produced at 2 kg/h – 0.15 L/S – 400 rpm.

Table 4 - Coefficients of Variance in liquid distribution of granules produced at increasing local fill level at the site of liquid injection.

Local Fill Level	Liquid Distribution Coefficient of Variance (%)
Unmodified – No element	32.2
Low – 0.25D pitch conveying element	33.4
Medium – 1D 60° Kneading block	30.5
High – 1D 90° Kneading block	26.2

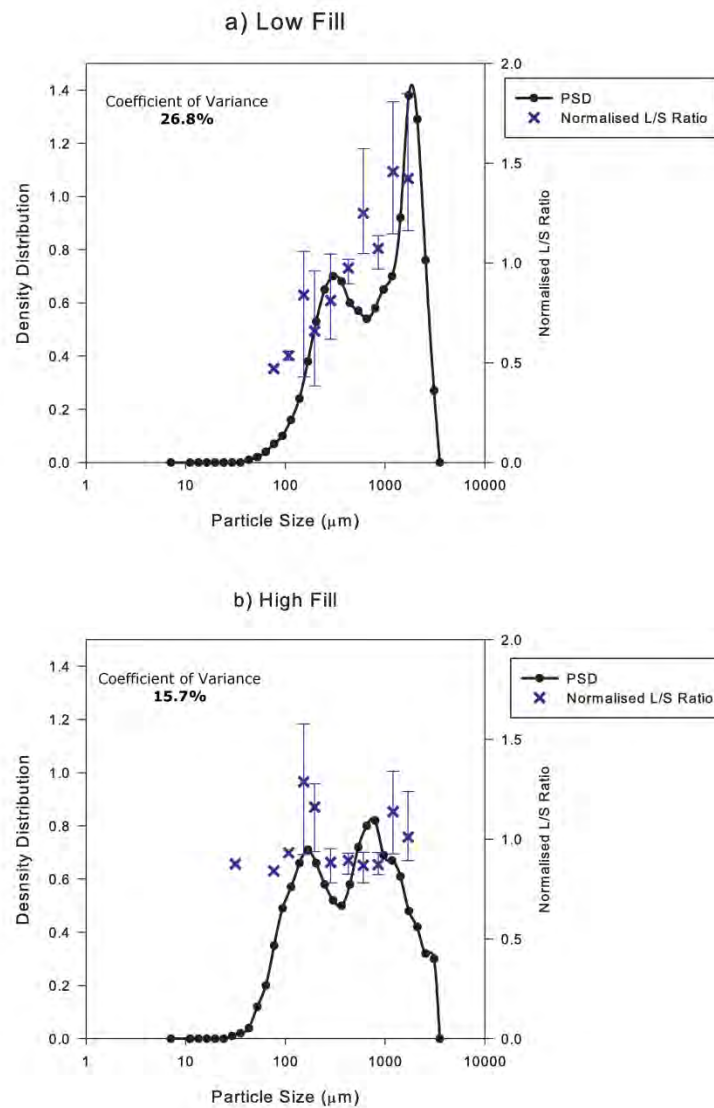


Figure 3.6 Size and liquid distributions of granules formed with a 1D 60°F kneading block at low and high overall fill level a) 1 kg/h – 0.18 L/S – 200 rpm, b) 4 kg/h – 0.18 L/S – 200 rpm. Density distribution is a numerical count frequency of granule size relative to the breadth of size class. L/S ratio is normalised against the overall average L/S ratio of the granule population.

The distribution of liquid at low and high overall fill level is shown in Figure 3.6. Liquid distribution is skewed at low fill level, however at high fill level is considerably more uniform across the entire range. Despite the improvement in liquid distribution at high fill the size distribution remains bimodal, with a greater proportion of fines. The low liquid variance would imply that despite the differences in size these granules are more similar in structure and properties. Thus high fill levels

promote more homogeneous liquid distribution. For these experiments liquid to solid ratio was measured in triplicate and calculated based on the content of nigrosin in dried granules, therefore there is no sampling bias from handling of wet granules with this method. The error bars represent the maximum and minimum measured values and the datapoint the middle. Particle sizes were obtained through QICPIC image size analysis. The frequency of granules in the size class is shown by the Density Distribution on the y-axis. This a number count distribution of individual particles weighted by the span of the measurement size class.

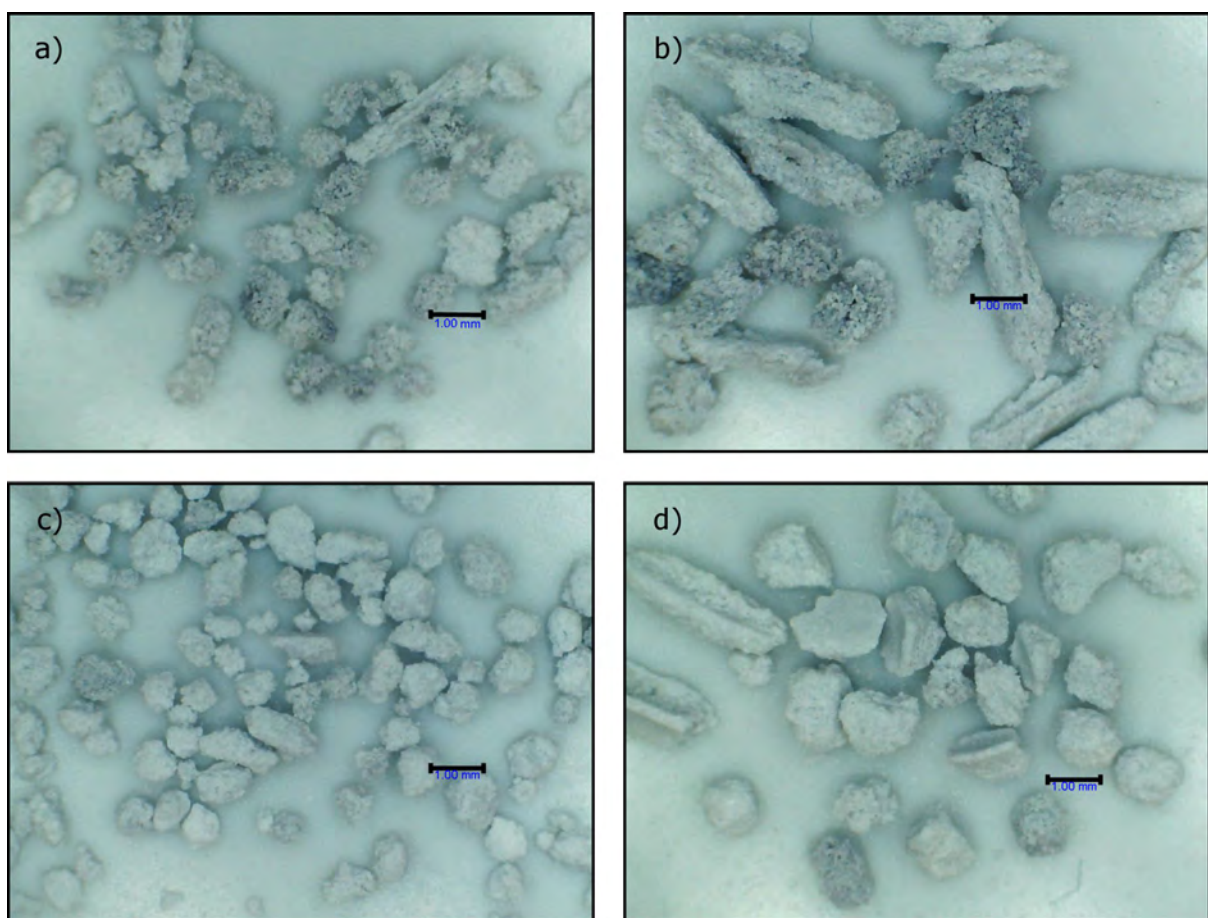


Figure 3.7 Optical micrographs of granules formed at low (top) and high (bottom) overall fill a) & c) 710 – 1000 μm , b) & d) 1000 – 1400 μm .

Granules formed at low and high fill level are shown in Figure 3.7, black surfaces contain the nigrosin dye and are indicative of wetted areas. Granules produced at high fill are more rounded and have smoother surfaces, implying higher compaction of material. Granules produced at low fill contain

elongated rectangular agglomerates and smaller granules can be seen to be fragments of these. It is believed these agglomerates are formed from the breakage of initial agglomerates formed during nucleation wetting. As granules are primarily fragments it can be inferred that the main role of the 60°F kneading block is breakage of these agglomerates. The rough surfaces of granules formed at low fill imply that the compaction in the kneading block is insufficient to cause significant densification and incorporation of fines. The low amount of mixing is not sufficient to ensure re-distribution of liquid. The surfaces of granules formed at high fill are lighter in colour showing the consolidation and incorporation of fines into the granule structure. It is believed that the higher fill level in the conveying zone promotes mixing of material and improves the distribution of liquid following nucleation.

3.4 Discussion

3.4.1 Asymmetric Transverse Distribution

Asymmetric transverse distribution in conveying zones is inherent to the granulator geometry.

Distribution of material between the screws is dependent on the fill level in the granulator. Raising the fill level in conveying zones improves distribution of material and induces mixing. Operating at higher fill levels will mitigate the inherent asymmetric distribution, however the higher mass loads in the granulator will affect granulation mechanisms and increases the risk of blockages occurring. This is implied by the average torque at steady state of 5.23 Nm at low fill level and 36.27 Nm at high fill level.

As some asymmetric transverse distribution is inherent to the process it can not necessarily be avoided, thus it is important to consider how it affects granulation mechanisms. Transverse loading will be uneven in that the driving screw carries more material than the loading screw. This means the driving screw does more work in conveying material, however the magnitude of this may be irrelevant when compared to the work carried out in mixing zones. A non-uniform transverse fill profile may establish in conveying zones leading into mixing elements. As the fill level rises in the approach to mixing zones, transverse distribution becomes more uniform, however for a non-cohesive material Figure 3.1 would imply uniform distribution is only established when the region is fully filled. The results of Lee et al [35] demonstrate that maximum fill is reached at the second kneading disc of the kneading block, but 100% fill level is only reached in this region with kneading blocks with 90° offset angle. Forwarding flow in kneading blocks is determined by a combination of kinetic and dispersive mechanisms, kinetic from the conveying action of the screw and dispersive following the axial fill profile of the block. If the transverse fill profile is non-uniform the kinetic force of the loading screw is lower and dispersive driven flow from the intermeshing region will have a greater tendency toward back flow. Given the differences in fill above and below the screws this may establish as "recirculation" of material between the upper and lower intermeshing regions of

kneading discs. This may be why lower axial mixing is observed by Kumar et al [34] at higher fill levels, kinetic force is high and the degree of backflow is reduced. Visualisation of this flow pattern could be achieved through modelling or an in depth PEPT study.

3.4.2 Size segregation in conveying zones

The size selective segregation of material in conveying zones results from the asymmetric transverse distribution and again can be mitigated by operating at higher fill level. Wetting of material in conventional liquid injection leads to non-uniform liquid distribution where larger granules contain more liquid as in Figure 3.5. Given the characteristic bimodal size distributions of granules produced by TSG this means granules are heterogeneous in both size and properties. If the action of conveying elements segregates these different particles it is important to consider how this affects the granulation process. Segregation of particles may reduce the degree of mixing and distribution of liquid. Primary agglomerates are formed at the site of liquid injection under immersion type wetting [24], variance in initial wetting results in a mixture of large wetted agglomerates and dry fines. Segregation of these two types of particles may result in separate flow streams and reduce their interaction, meaning wet particles mix primarily with other wetted particles and dry fines with other fines. Redistribution of liquid is restricted as wetted material is isolated. The differences in particles may be alleviated in kneading blocks due to their superior mixing action, however conceptually segregation of particles may establish in flow of "wet" and "dry" streams fed into the top and base of the kneading block respectively. Thus good radial mixing would be required in order to ensure liquid distribution.

Segregation establishes in long conveying sections operating at a low fill level, thus will only be apparent at the discharge depending on the positioning of mixing zones and final fill profile. This has implications for the use of in-line particle sizing: if segregation is established at the discharge optical sizing techniques may result in skewed size data dependent on the position of the detector. To avoid this the separated streams of particles should be collated or the entire discharge flow sampled.

Size selective segregation is a fill level dependent effect of conveying zone asymmetry. The free volume under low fill conditions allows for segregation to take place, therefore segregation can be controlled through fill level. Segregation of particles may not necessarily have a strong effect on mixing mechanisms but is a property of twin screw granulation that should be taken into consideration when establishing screw configuration.

3.4.3 Fill Level and liquid Distribution

From the results shown in Figure 3.6 it can be seen that the distribution of liquid is poor at low fill levels compared to high. The asymmetric, plug flow which establishes in conveying zones results in poor mixing of wetted agglomerates and dry fines and increases the mixing load of the kneading block. During nucleation material undergoes immersion wetting. Increasing the local fill level at the site of liquid injection improves the liquid distribution during nucleation. When the fill level at the site of nucleation is higher the liquid is injected into a greater instantaneous volume of powder material. Liquid is better distributed throughout the greater volume of powder, where under low fill intensely wetted agglomerates would form. Similarly the transfer of material between conveying screws in this region mixes the newly wetted powder and aids distribution of liquid to un-wetted material. The higher the local fill level the better the distribution and the more uniform final liquid distribution. Additionally the longer residence time of material at higher local fill level may aid in minimising any effect of liquid feed pulsation. In this study liquid was fed via an 8 roller peristaltic pump, due to the nature of peristaltic pumps some pulsation in liquid is always present. Longer residence times dissipate the pulse of liquid allowing it to become more uniformly distributed throughout the powder. This would otherwise result in wet and dry plugs of material, demanding good axial mixing from the downstream kneading block to ensure distribution. The quality of primary nucleation wetting affects the downstream mixing demand.

Feeding liquid directly onto the kneading block led to periodic surging of material discharged from the granulator. Fill levels are highest across kneading blocks, given the improvement in liquid

distribution found at higher fill level (Table 4) and the superior mixing action of kneading elements it would be expected this would result in superior dispersive mixing of liquid at nucleation. However the periodic surging of material arises due to the long residence times and poor conveying capacity of kneading blocks. Material in the block becomes intensely wetted changing the rheology and forming a viscous paste like substance resistant to forward flow. The pasted material forms a pseudo-blockage where dispersive forward flow is low. Sufficient kinetic force must be developed in the conveying zone upstream of the kneading block to clear the pseudo-blockage. Kinetic force increases as material accumulates in the conveying zone until it is sufficient to clear the pasted material, travelling as a plug of over-wetted lumps followed by a tail of fines. Once cleared, the pseudo-blockage will re-establish as the conveying fill level drops. Thus with this configuration the granulator never reaches true steady state. The material discharged does not contain true granules but instead a mixture of over-wetted lumps and ungranulated fines, with high variance.

Liquid distribution is most improved at high overall fill level as demonstrated by the differences in distribution in Figure 3.6. Despite the size distribution of granules remaining bimodal at high overall fill level the similar liquid distribution implies that granules across the size range are more uniform in structure and properties than those produced at low fill. There are three factors which lead to the improvement in liquid distribution, firstly the greater volume of powder gives more uniform immersion wetting during nucleation. Secondly maintaining the increased fill level throughout the conveying zone results in fully developed flow and induces mixing between the screws. Thirdly the higher overall mass load in the granulator increases compaction and consolidation of material. In addition to the mixing achieved in the conveying zone, primary agglomerates are restricted in size in the reduced free volume and are abraded through shear and collisions with other particles.

Breakage is higher at high fill level indicated by the greater proportion of fines, however the surfaces of particles in Figure 3.7 indicate greater compaction and the lighter surface colouration shows consolidation and incorporation of fines into the granule structure. Granules can be seen to be fragments of large elongated granules implying the 60°F kneading block mainly causes breakage of

primary agglomerates formed by nucleation wetting. The mixing ability of the kneading block is not sufficient to reincorporate material and promote growth through coalescence of granules. High fill levels increase consolidation and compaction of these granular fragments but optimisation of screw configuration is required to promote secondary growth of granules and overcome increased breakage rates. This is why proportionally more fines are present at high fill level despite the composition of granules being more uniform.

3.5 Conclusions

PEPT was successfully employed to validate measured transverse material asymmetry in the conveying zones of a twin screw granulator. Flow asymmetry is inherent to the granulator geometry but can be mitigated through control of fill level. Flow establishes as poorly mixed plugs of material travelling axially with minimal transverse mixing at low fill. Size selective segregation of particles occurs within conveying zones and further reduces the degree of mixing. The plug flow in conveying zones negatively affects liquid distribution at low fill level. Primary agglomerates formed by immersion wetting at nucleation travel as plugs and the mixing capabilities of 1D 60°F kneading blocks are insufficient to ensure redistribution of liquid. Raising the fill level at the site of nucleation reduces the variance in primary wetting. Maintaining high fill level throughout conveying zones induces mixing and improves liquid distribution. This work demonstrates that granule uniformity is dependent on wetting during nucleation. With 60°F kneading blocks the mechanism of formation is suggested to be primarily breakage in the mixing zone of large primary agglomerates formed during nucleation.

***Chapter 4* - The Granulation**

Process and Temperature

Sensitivity

4.1 Abstract

This chapter explores the impact of temperature on the granulation process and behaviour of common pharmaceutical excipients. The solubility of lactose, the main component in the formulation investigated is strongly correlated with temperature and many simple sugars used as pharmaceutical excipients share this characteristic. This increased solubility results in lower energies required for granulation at higher temperature and changes in granule size distribution as more liquid bridges may be formed. This chapter demonstrates that heat generated through mechanical work during granulation without adequate temperature control may lead to changes in granulation mechanisms and variable product. The interaction with and affinity for water of excipients across a range of temperatures is explored.

4.2 Introduction

Wet granule formulations present challenges in processing due to their complex flow behaviours. Handling of dry powders can be complex depending on multiple factors such as particle size and shape, wet granulation increases this complexity by adding liquid to the material and changing the material rheology. The rheology and behaviour of material is transitional as it changes from dry powder to wet granule, making prediction of flow and granulation mechanisms difficult. Careful control of process parameters is thus required in order to produce consistent granule. One of these parameters not typically explored in conventional wet granulation is temperature. While temperature control is required and employed in techniques such as hot melt granulation where it is required to melt solid binder particles, the influence over a continuous wet twin screw granulation has not been investigated.

Twin screw granulators have evolved from twin screw extruders. Temperature control is essential for many common extrusion processes such as plastic or food extrusion. As a result many twin screw

granulators are equipped with temperature control mechanisms, but are only used to maintain the equipment at steady state close to room temperature.

This chapter explores how temperature affects granulation mechanisms. A general trend of lower torque at higher operating temperature was observed. Results are highly dependent on the thermal behaviour of the individual formulation components. Granulators can generate a lot of heat through mechanical work during mixing, highlighting the need for careful temperature control to avoid changes in granulation mechanisms during continuous production.

4.2 Material and Methods

4.2.1 Granule Formulation

Initial experiments used a formulation of 75% Lactose (316/FAST-FLO[®], Foremost Farms, USA), 20% Microcrystalline Cellulose (Avicel PH101, FMC BioPolymer, Ireland) and 5% Hydroxypropyl Cellulose (Klucel EXF, Ashland Inc, USA) as binder.

Lactose and MCC are common pharmaceutical excipients and HPC a commonly used binder. While the behaviour of active material in pharmaceutical formulations will be different, the widespread use of these excipients provides useful information about the process behaviour.

As the solubility of HPC is dependent on temperature further granulation experiments were carried out using a blend of 80% lactose and 20% MCC in order to determine the thermal behaviour of the excipients without the influence of the binder.

Powders were blended for a minimum of 20 minutes in a Pascal lab mixer prior to granulation.

4.2.2 Granulation Experiments

Granulation was performed on a Haake 16 mm twin screw extruder (Thermo Scientific, Germany).

The granulator consists of a Rheocord torque rheometer and Rheomex twin screw extruder. Control, monitoring and recording of process parameters is through the Haake PolySoft operating system.

Powders were fed via a K-Tron T20 Volumetric twin screw feeder, distilled water was pumped into an injection port on the top of the barrel using an 8 roller peristaltic pump (REGLO Digital, Ismatec, Switzerland).

The granulator barrel consists of an upper and lower steel section, closing with a clamshell design and secured by bolts. The barrel temperature is maintained by circulating silicone oil throughout the upper and lower section. The temperature and flowrate of the coolant oil is controlled by a Haake F6 circulator and C35 refrigerated bath.

Before each granulation experiment the refrigerated bath was set to a set point temperature and the temperature of the barrel was left to equilibrate for up to two hours or until the readings of the barrel thermocouples had remained stable for 15 minutes. Granulation was performed with the bath at set point temperatures of 0, 20 and 80°C.

A set screw configuration consisting of two 90° 1D mixing zones was used for all experiments (11x 1D C// 4x 0.25D K 90°// 6x 1D C// 4x 0.25 D K// 6x1D C).

4.2.3 Granule size analysis

Granules were collected as they were discharged from the barrel of the granulator. Once a suitable mass of granules had been collected (~300 g) they were transferred to an oven where they were dried at 100°C for 2 hours.

The size distribution of dried granules was determined through image analysis using a QICPIC (Sympatec QICPIC).

4.2.4 Residence time distribution

The residence time distribution of the granulator was determined at steady state at both 20°C and 80°C. This was to confirm the granulator was operating at the same steady state at both high and low temperature. The Haake extruder is unsuitable for use with PEPT so the RTD was determined using an impulse response test with a nigrosin dye tracer similar to that used by Dhenge et al [30, 31].

Powdered Nigrosin dye (Nigrosin water soluble, Sigma-Aldrich, UK) was diluted in samples of the lactose/MCC/HPC formulation to form a 10% (w/w) mixture. Once the granulator had reached steady state operating at 2 kg/h feed rate, 0.3 L/S ratio and 200 rpm screw speed a 1 g pulse of the nigrosin mixture was introduced to the barrel powder inlet. Samples were collected from the barrel discharge every 5 seconds for 2 minutes. The RTD was determined from the distribution of the pulse of dye among these samples. The concentration of dye was measured using a similar method to that

for determining liquid distribution from dye concentration discussed in section 3.2.6. To determine the concentration of dye 0.5 g of each granule sample was dissolved in 10 ml of water and sonicated for 1 hour to ensure complete dissolution. The sample solutions were then centrifuged at 6000 rpm for 15 minutes in order to separate the insoluble MCC. The supernatant was drawn off and the concentration of dye determined by the absorbance at 565 nm using UV/Vis spectroscopy (Aquarius 7500, Cecil, UK). 565 nm is the wavelength of light where peak absorbance by Nigrosin occurs. Similarly to the use of nigrosin in determining granule liquid content in section 3.2.6, UV/Vis spectroscopy was used to determine the concentration of nigrosin. A calibration curve was obtained between concentration of nigrosin in water against absorbance by measuring the absorbance at 565 nm of a series of known concentrations of nigrosin. 565 nm is the wavelength where peak absorbance of light occurs in nigrosin. The concentration of nigrosin in each sample could then be determined by comparison of the absorbance at 565 nm. The residence time distribution was then calculated using equation (2-1) below, where dt is the sampling frequency, 5 seconds in this case.

$$E(t) = \frac{C(t)}{\int_0^{\infty} C(t) dt} \quad (2-1)$$

4.2.5 Rheology

To investigate the interaction of water with the individual excipients of the formulation rheological characterisation of lactose and HPC solutions was performed. A 4% HPC solution was prepared by heating distilled water above 43°C and adding HPC to form a suspension. Once all solids had been added the liquid was allowed to cool to form a solution and the correct final volume made up by adding additional water. A 25% lactose solution was prepared by dissolving lactose in distilled water at room temperature.

Rheological characterisation of solutions was carried out with a Discovery Hybrid HR-2 rheometer (TA Instruments, USA) using a 40 mm 4° smooth surfaced cone and plate geometry. The attached Peltier plate was used to accurately control the temperature of the solutions. First the rheology of

solutions was determined by obtaining flow curves under increasing shear rates from 0.1 to 100 reciprocal seconds with 10 points per decade over 180 s. Secondly the behaviour at different temperatures was determined by performing temperature sweeps at constant shear rate of 10 reciprocal seconds across a temperature range between 5°C and 80°C.

4.2.6 Dynamic Vapour Sorption

In order to determine how the dry powder excipients interact with water as solids Dynamic Vapour Sorption (DVS) was performed using a Dynamic Vapour Sorption Moisture Adsorption Apparatus (Surface Measurement Systems DVSA-STD, UK). DVS measures the interaction with water vapour as opposed to liquid water but was undertaken as a method of determining the materials affinity for water.

In DVS a small sample of the measured material is placed in a balance basket. The humidity of the surrounding environment is carefully controlled and the change in mass as the target material adsorbs water is measured. Sorption isotherms are determined by measuring the change in mass at 10% humidity intervals between 0% and 100% and desorption isotherms by the reverse.

4.2.7 Mechanical testing

To gain insight into the compressive behaviour mechanical testing of material was undertaken. The excipient formulation was placed in a plastic bag and 20% water was added. The bag was then sealed and gently agitated, this is to replicate the condition of material following nucleation before being fully mixed and granulated. The same procedure was followed with lactose only.

Spherical indentation was performed using an Environmental Mechanical Analyser (Instron MicroTest 5848, USA). Material was placed into wide glass crystallising dishes in order to give a large surface area for compression. The tester was fitted with an 80 mm rounded glass plate which was lowered onto the powder bed at constant velocity and the force required to compress the bed

measured. Measurements were performed at room temperature and after heating sealed powder samples to 80°C in an oven.

4.3 Results and discussion

4.3.1 Granulation at temperature

Granulation was performed in order to determine the steady state torque of the process operating at different temperature points. All other conditions were maintained the same. Granulation was performed at 200 rpm and 0.2 L/S ratio at material feed rates of 3 kg/h and 2 kg/h.

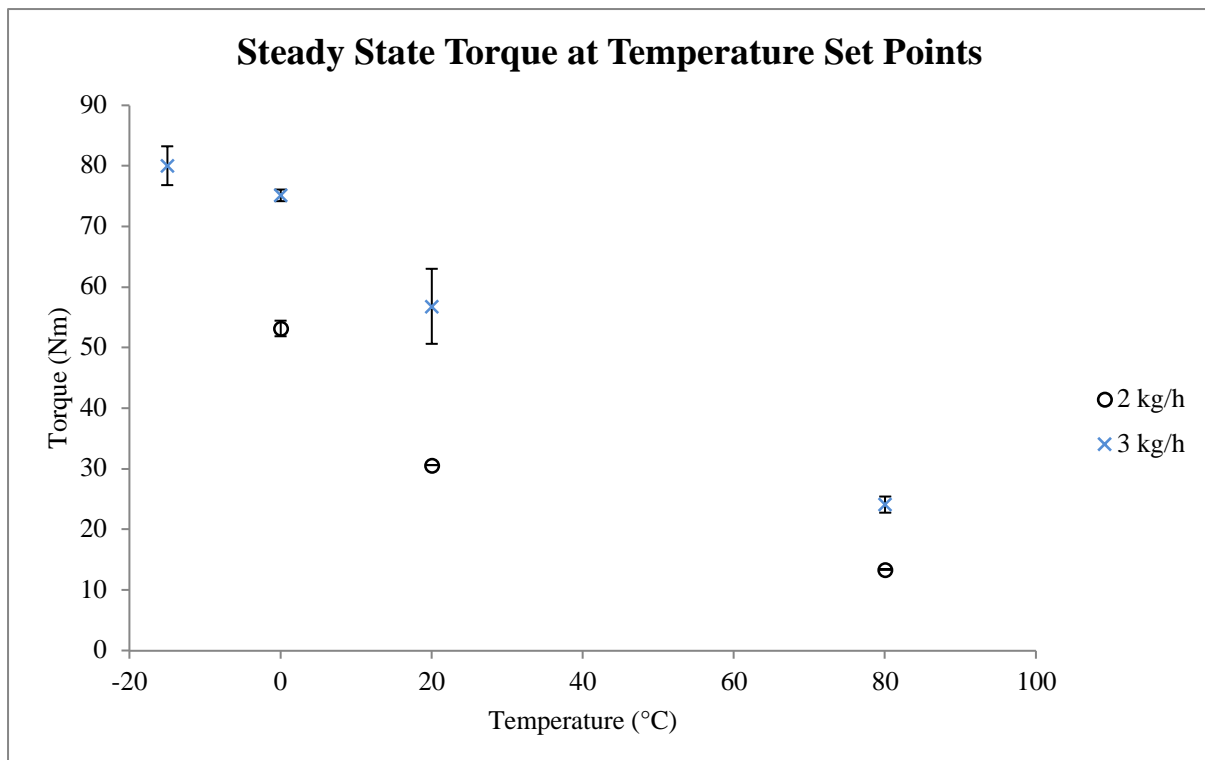


Figure 4.1 – Granulator steady state torque at different coolant temperature set points.

Figure 4.1 shows the granulator steady state torque at different coolant temperature set points. The absolute values for experiments at 3 kg/h are higher than those at 2 kg/h due to the greater mass of material in the barrel requiring more work to be done to mix and convey it. It can be seen that there is a decreasing trend in steady state torque with temperature for this formulation. The implication of this is that there is less work required to mix and convey material when it is hot compared to cool. The difference in torque operating at these temperature set points is quite large. At 3 kg/h and 0°C the granulator steady state torque is 76.1 Nm, while at 80°C it is 25.5 Nm, meaning only 33.5% of the

energy needed to granulate at the lower temperature is required. This may have implications for industrial use, where operating at higher temperatures could lead to reduced energy demands or less mechanical wear. However what implications this has on the process and the material must be considered. The extents of the temperature range explored were chosen arbitrarily as an extreme case and are not linked to any formulation need. However they highlight the changes in granulator performance with temperature.

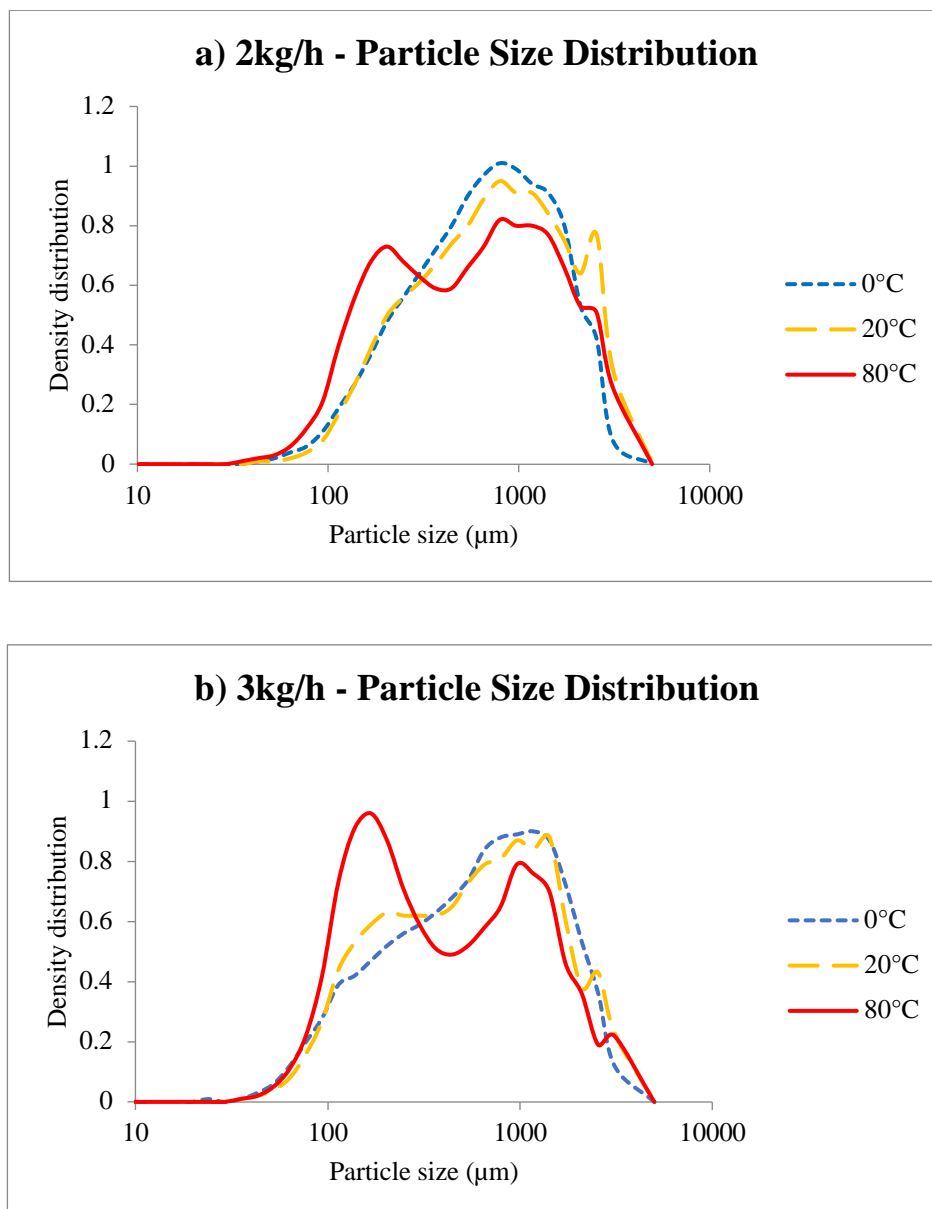


Figure 4.2 – Particle size distributions of granules made at 0, 20 and 80°C at a) 2 kg/h feed rate and b) 3 kg/h feed rate.

The particle size distributions of granules made at the different temperature steady states are shown in Figure 4.2. For both cases at 2 kg/h and 3 kg/h it can be seen that there is a transition from a monomodal size distribution at 20°C and below to distinctly bimodal at 80°C. This is clearest in the material granulated at 3 kg/h in Figure 4.2b. The granule size is most uniformly distributed at 0°C, at 20°C it can be seen that the proportion of fines is higher, producing a “shoulder” in the distribution at 200 µm. Finally at 80°C the proportion of fines is much higher, giving a highly bimodal distribution. The implication of this is that as the granulation temperature increases, the population of granules becomes more heterogeneous. Although the energy required to granulate at these temperatures is much lower, the physical properties of granules and their suitability for tableting may not necessarily be as good.

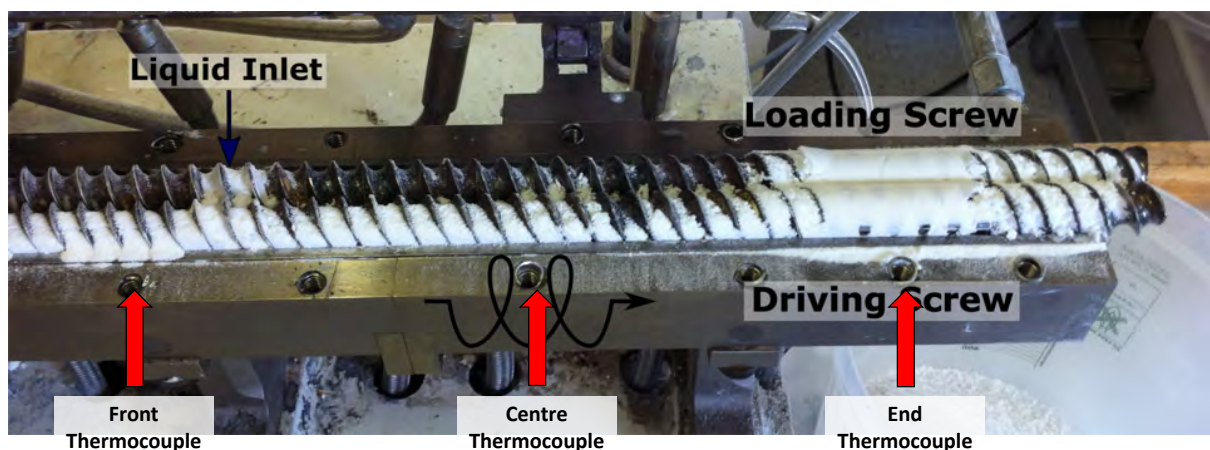


Figure 4.3 – Position of the thermocouples in the HAAKE twin screw granulator

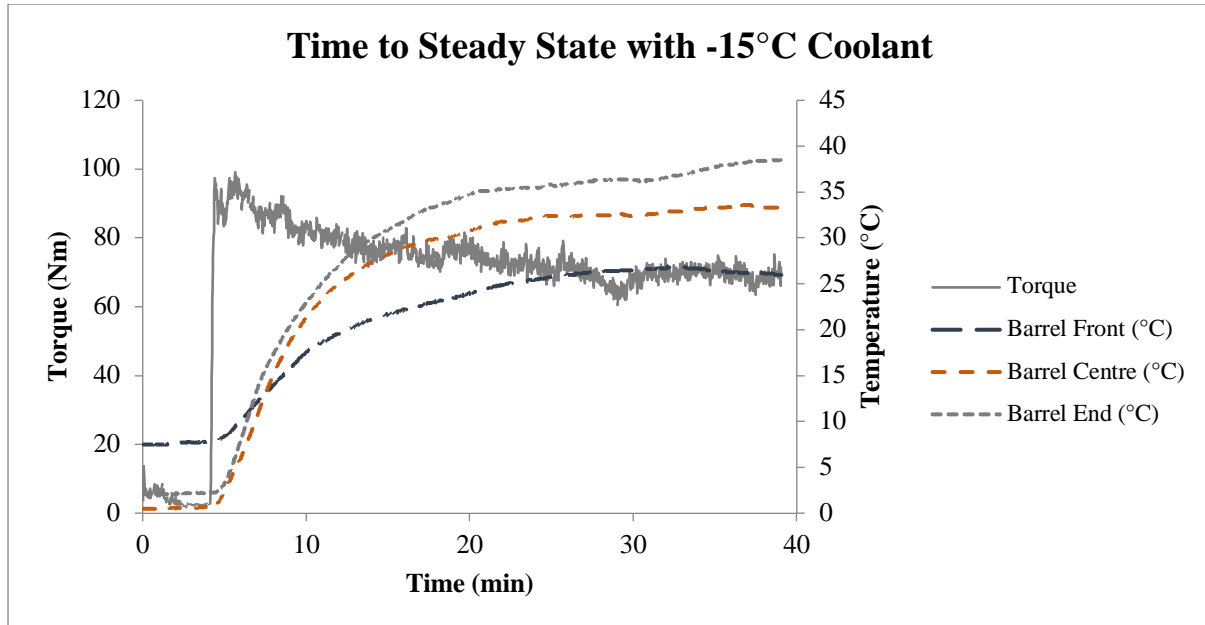


Figure 4.4 – Change in torque and temperature due to heat generated through granulation with a coolant temperature set point of -15°C .

Heat is generated during granulation from the mechanical mixing and compression of the granulated material. The amount of heat generated can be quite large when the granulator screws are arranged with an intensive mixing configuration, or when the granulator is operating highly loaded. Because this heat can be generated the time the granulation process takes to reach steady state may be increased. For example Figure 4.4 shows the time taken for the granulator to reach steady state with a coolant set point of -15°C . The granulator is equipped with three thermocouples distributed along the length of the barrel. The position of the thermocouples along the axial length of the HAAKE granulator are shown in Figure 4.3. From the data in Figure 4.4 it can be seen from the thermocouples at the centre and end of the barrel nearest the work zone that the granulator barrel changes in temperature from near 0°C to approaching 40°C over a period of 35 minutes. Across this period there is a drop in the granulator torque from a peak of 95 Nm at 6 minutes, soon after granulation is started, down to 68 Nm at 30 minutes where the torque plateaus. This means that the granulator does not reach steady state until around 30 minutes after granulation begins and the granule produced at the start and end of this period will be different. It should be noted that the

coolant system of the Haake granulator is undersized for the equipment and not very efficient, meaning it cannot compensate effectively for heat generated during production. While this is something of an extreme case, the impact of any change in temperature during start-up of an industrial process should be considered. In addition an industrial granulator should be equipped with a temperature control system that can adequately maintain a steady state temperature.

The work done in a rotating system can be calculated using the following equation

$$E = T\theta \quad (4-1)$$

Where E is the work done, or energy in Joules, T the torque in Nm and θ the angle of rotation.

The equation for power in a rotating system is then

$$P = T\omega \quad (4-2)$$

Where P is power with units Joules/second and ω the angular velocity.

Knowing the rotation rate during granulation the power may then be calculated from the measured torque.

Table 5 – Steady State torque and power across different process conditions with varying coolant temperature set points.

Feed rate (kg/h)	L/S Ratio	Screw Speed (rpm)	Temperature (°C)	SS Torque (Nm)	Power (J/s)
3	0.2	200	0	76.1	253.7
	0.2	200	20	50.6	168.7
	0.2	200	80	25.5	85.0
2	0.2	200	0	54.5	181.7
	0.2	200	20	30.6	102.0
	0.2	200	80	13.4	44.7
1.5	0.2	100	20	60.2	100.3
	0.2	100	80	27.3	45.5
2	0.3	200	20	35.6	118.7
	0.3	200	80	16.2	54.0

The power required for granulation at varying temperatures is shown in

Table 5. The required mechanical energy decreases at higher temperatures. The differences in power requirements would indicate differences in behaviour of the material or the way the granulator is operating. The potential to save energy in an industrial process is attractive, however balanced against a requirement to consume energy to generate heat this may not be feasible. The energy required to maintain temperature was not measured however it would be valuable to do this to enable an energy balance of the system to be performed such that a true power requirement could be determined.

Table 6 – Relative power required for granulation at 80°C compared to 20°C

Feed rate (kg/h)	L/S Ratio	Screw Speed (rpm)	Relative Power
3	0.2	200	50.4%
2	0.2	200	43.8%
1.5	0.2	100	45.3%
2	0.3	200	45.5%

It is of interest to note that despite a range of feed rates, screw speeds and liquid to solid ratios being explored, comparing the relative change in power at 20°C and 80°C shows a similar decrease. The difference in power required at 80°C compared to 20°C is shown in Table 6. Similar values are displayed for each condition and particularly for those at lower feed rates of 2 kg/h and under. It would be of interest to investigate the granulation power requirements across a range of temperatures to see if this factor scales.

4.3.2 RTD at different temperature

The increased torque at lower temperature was still observed when operating at different fill levels and different liquid to solid ratios, summarised in

Table 5. Implying that this difference in torque is a material property rather than being process specific. In order to confirm that there is not a change in the process when operating at different temperatures the residence time distribution was determined. Assuming no change in material properties, the process change when operating at different temperatures that results in higher torque would be if there was more material hold up in the barrel. The larger volume of material in the barrel means that the granulator has to work harder squeezing and compressing more material with each rotation of the screws. The RTD is an indication of the hold up of material in the barrel. A longer residence time meaning it takes longer for material to pass through the barrel so that at set feed rate at any given moment it contains more material. By measuring the RTD at different temperatures it can thus be shown whether the hold up of material in the barrel changes.

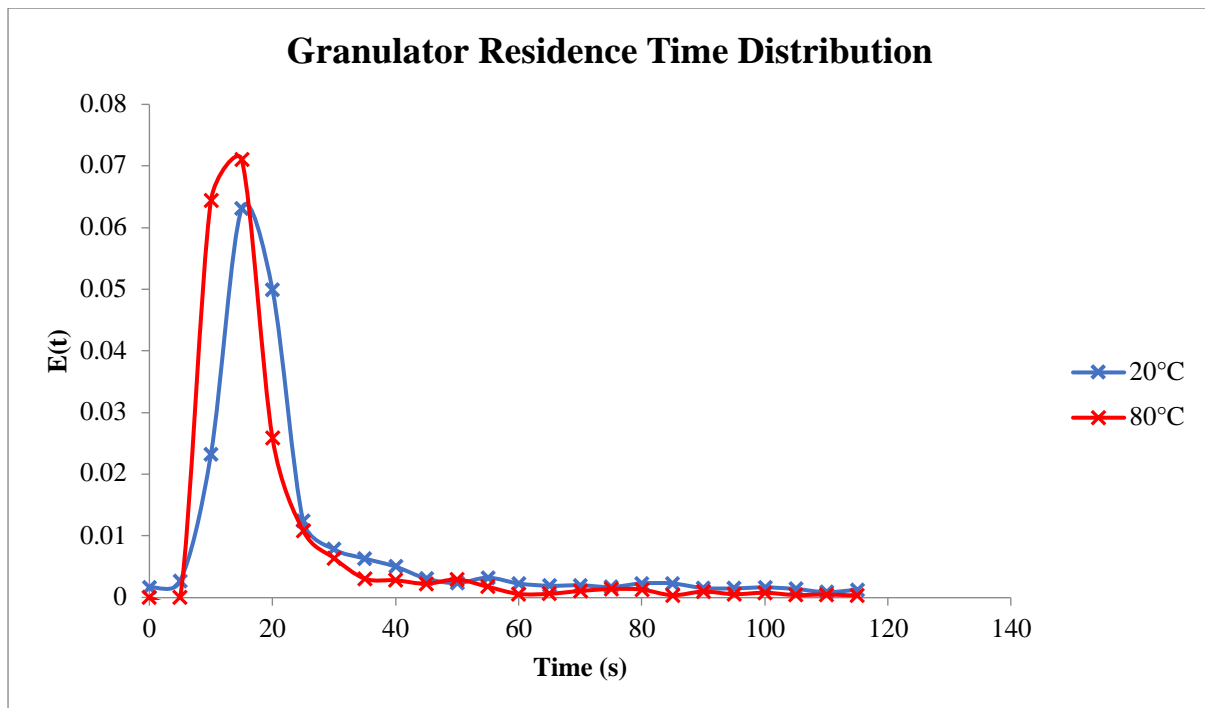


Figure 4.5 – Residence time distributions obtained using an impulse response test with the granulator operating at 2 kg/h feed rate, 0.3 L/S and 200 rpm at 20°C and 80°C set point temperature.

The residence time distributions for the granulator operating at 20°C and 80°C are shown in Figure 4.5. The RTD curves were obtained using an impulse response technique described in section 4.2.4 which has a relatively broad measurement interval of 5 seconds and thus limited accuracy. The RTDs

of both experiments are similar, with mean residence times of 26.6s at 20°C and 19.9s at 80°C. This indicates that the process is operating at the same steady state fill level and that the differences in torque, 35.6 Nm at 20°C and 16.2 Nm at 80°C, are due to a change in the material. It cannot be said with certainty that the RTDs recorded at 20°C and 80°C are the same due to the inaccuracy of the measurement technique. The 5 second time interval is fairly broad compared to the mean residence time of approximately 20 seconds. Given the higher mean residence time and shape of the distribution it could be argued that the elution of the tracer is slower at 20°C compared to 80°C, however again the sample frequency is not narrow enough to conclusively state this. The material feed rate for these experiments was 2 kg/h which is equal to approximately 0.56 g/s. In the impulse response technique a 1 g pulse of tracer is introduced to the granulator over as short a period as possible but in the region of one second. This would represent a significant increase in the material feed rate during this one second period. This plug of material may therefore disrupt the granulator steady state and thus the measured residence time not truly representative of the process. Given the flaws of this technique it may be worthwhile to repeat the experiments with a more accurate method of determining residence time distribution, such as through PEPT.

4.3.3 Hydroxypropyl Cellulose Rheology

The material properties of the different excipients in the formulation were explored to provide an explanation for the reduction in torque at higher granulation temperatures. Hydroxypropyl Cellulose is a polymeric binder which forms viscous gel like solutions with water. HPC undergoes thermoreversible gelation at a temperature of 43°C, at temperatures above this HPC will precipitate out of solution and form a low viscosity suspension [53]. This is illustrated in the temperature sweep of a 4% HPC (aq) solution shown in Figure 4.6. The viscosity of the solution reduces as temperature increases but drops considerably when the precipitation temperature is reached at 43°C. As the HPC precipitates out into a suspension the viscosity eventually drops to a level close to that of water.

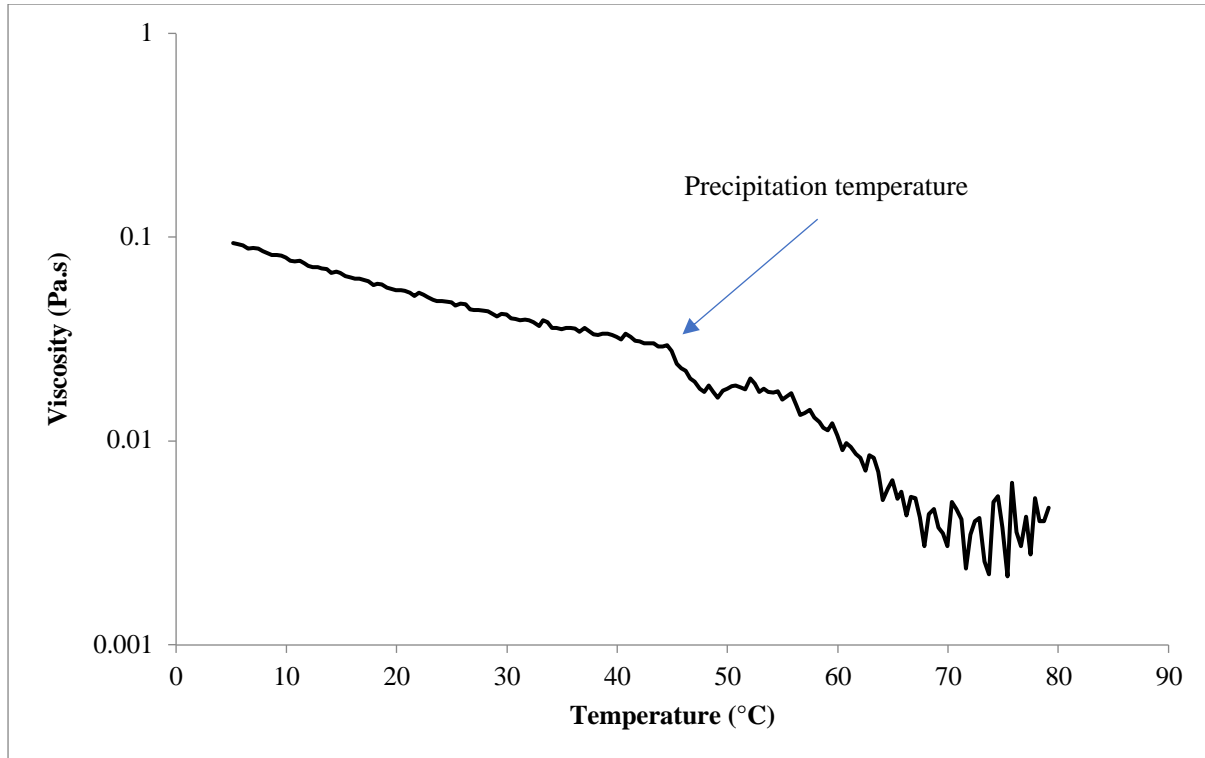


Figure 4.6 – Temperature sweep of a 4% HPC (aq) solution between 5°C and 80°C at 10 reciprocal seconds constant shear rate.

Initially this phase change of HPC appears to provide a good explanation for the lower torque at higher temperatures and the trend toward higher amounts of fines shown in Figure 4.2. Below the precipitation temperature the HPC binder particles will form sticky gels when the formulation comes into contact with water. Above this temperature the binder will remain solid and thus lose its binding capability. At 80°C the formulation is behaving as if there is no binder present, viscous forces are far lower, giving the reduced torque and higher proportion of fines as less particles bind together. The trend for lower torque between 0°C and 20°C in Figure 4.1 may then be explained by the reduction in viscosity of HPC with increasing temperature. Gels will be more free flowing reducing the energy required for mixing and granulation.

4.3.4 Granulation temperature response without binder

Further granulation experiments were performed with a formulation consisting of only lactose and MCC. This was in order to determine whether the rheological change with temperature of the HPC binder was alone responsible for the trend of lower torque at higher granulation temperature.

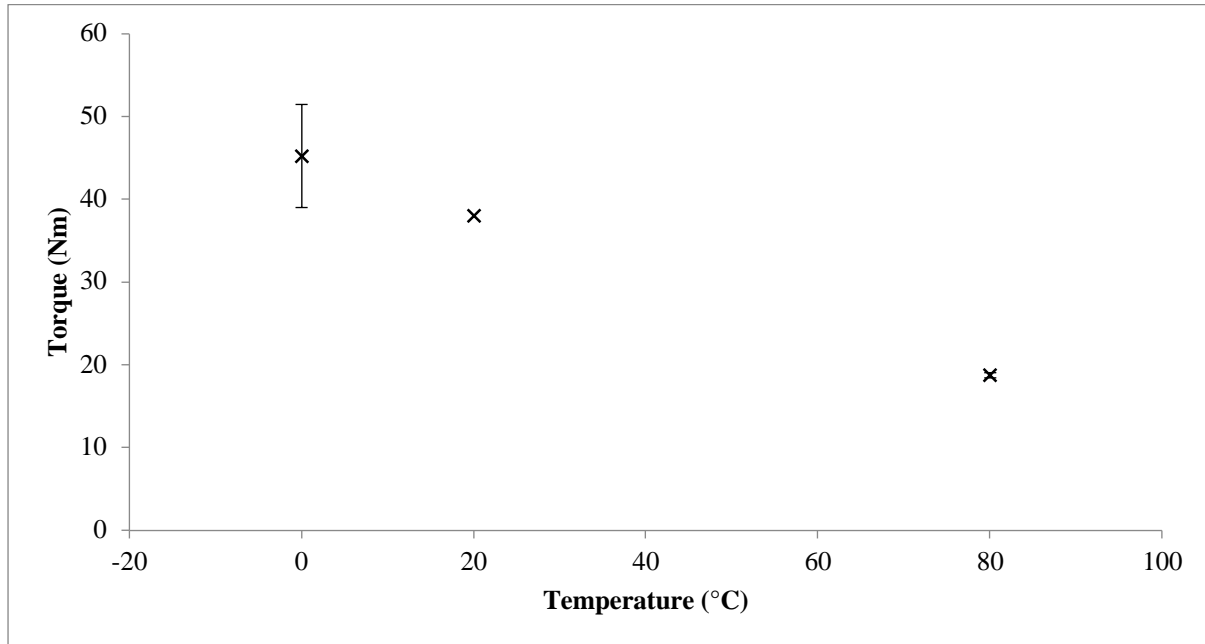


Figure 4.7 – Steady state granulator torque at coolant set point temperatures of 0, 20 and 80°C of a formulation consisting of 80% lactose and 20% MCC. Granulation liquid was water only, with no additional binder. Process parameters were 3 kg/h material feed rate, 0.45 L/S ratio and 200 rpm screw speed.

Figure 4.7 shows the steady state granulation torque at temperature set points of 0, 20 and 80°C for a formulation consisting of 80% lactose and 20% MCC. Note that the liquid to solid ratio is significantly higher for this formulation (0.45 L/S) compared to the formulation including HPC binder (0.2 L/S). A greater amount of liquid was required in order to produce granules with this formulation. The amount of liquid was increased incrementally to 0.45 L/S until the granules formed appeared visually close in size to those produced at 0.2 L/S with binder. Below 0.45 L/S this formulation would result in dry mixtures of powder and nucleation granules, demonstrating the role binders play in aiding granule formation. The data in Figure 4.7 shows that steady state torque is lower at higher granulation temperatures for the formulation without HPC. The absolute torque values are lower

than those for the HPC binder formulation shown in Figure 4.1 but this is likely due to the differences in amount of water added and the way each formulation interacts with liquid. The trend with temperature however is very similar, showing that the presence of HPC is not alone responsible for the reduction in torque with temperature. The drop in torque from 0°C (45 Nm) to 80°C (19 Nm) is still quite significant, the ratio of 80°C/0°C being 41% compared to 32% for the HPC formulation. The implication for this large reduction in torque is that one or both of the remaining materials (lactose and MCC) in the formulation contribute significantly to the change in granule rheology with temperature.

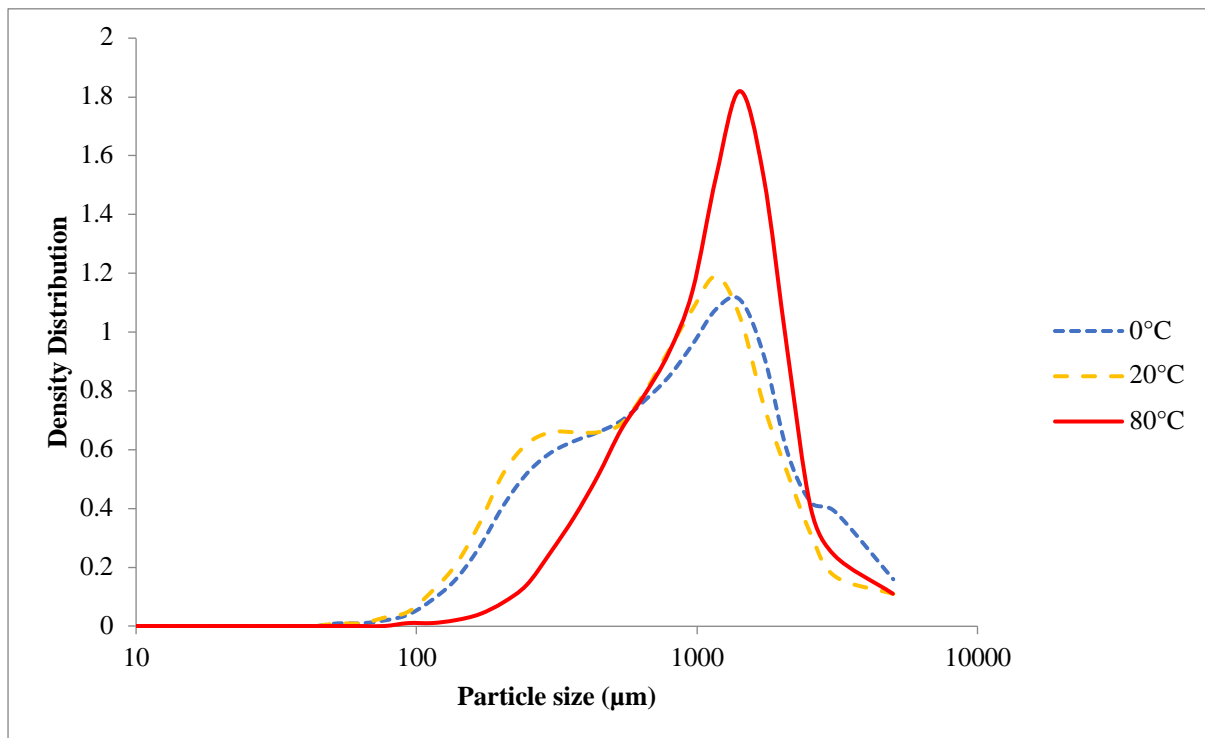


Figure 4.8 – Particle size distributions of granules formed at coolant set point temperatures of 0, 20 and 80°C of a formulation consisting of 80% lactose and 20% MCC. Process parameters were 3 kg/h material feed rate, 0.45 L/S ratio and 200 rpm screw speed.

Figure 4.8 shows the particle size distributions of the 80/20 lactose/MCC granules manufactured at different temperatures. What is interesting here is that the trend appears to be the opposite of that in Figure 4.2b, in that granules have a bimodal distribution at low temperature which becomes monomodal at high temperature (80°C). This is likely due to the higher overall liquid level. In the HPC

formulation at temperatures above its precipitation temperature the binder loses its binding functionality. Granules will only form from the interaction of the other excipients with water. As shown by the much higher L/S of the lactose/MCC formulation a much higher amount of water is required for this material to form granules. At 80°C the HPC formulation will behave like the lactose/MCC mix operating at 0.2 L/S thus only nucleation granules are formed, giving the higher amount of fines and bimodal distribution in Figure 4.2b. However in Figure 4.8 the system is always operating with a liquid level to produce viable lactose/MCC granules, so some change in the material at higher temperature is driving the formation of larger granules.

4.3.5 Lactose Rheology

Lactose is the only remaining water soluble excipient in the lactose/MCC formulation so rheological characterisation was undertaken in order to understand its behaviour in solution. A saturated 25% lactose solution was made up in order to try and establish conditions closest to those in the granulator where solids are in excess.

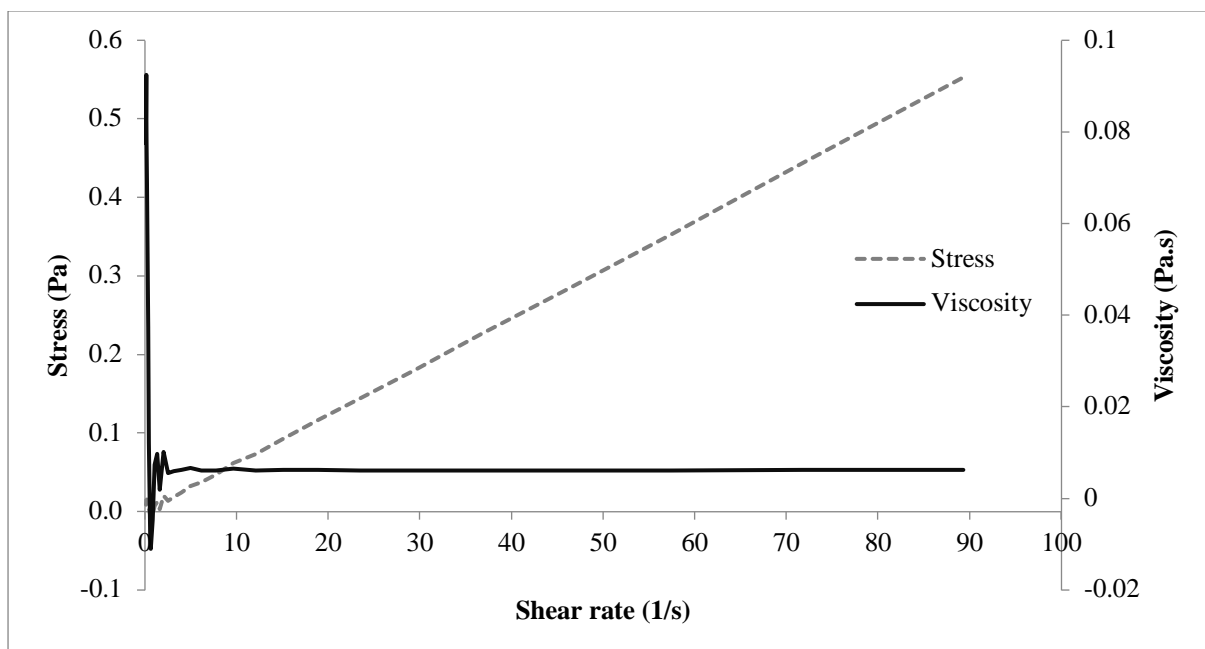


Figure 4.9 – Flow curve of a saturated 25% lactose solution (aq) showing Newtonian rheology.

Lactose solution is a Newtonian fluid as shown by the constant viscosity over increasing shear rate shown in Figure 4.9. The viscosity of the saturated lactose solution is low, close to that of water. Meaning that despite the high degree of solids incorporated into the liquid the flow behaviour is largely unchanged. In order to understand how this rheology changes with temperature a temperature sweep of the lactose solution was performed, the results of which are shown in Figure 4.10.

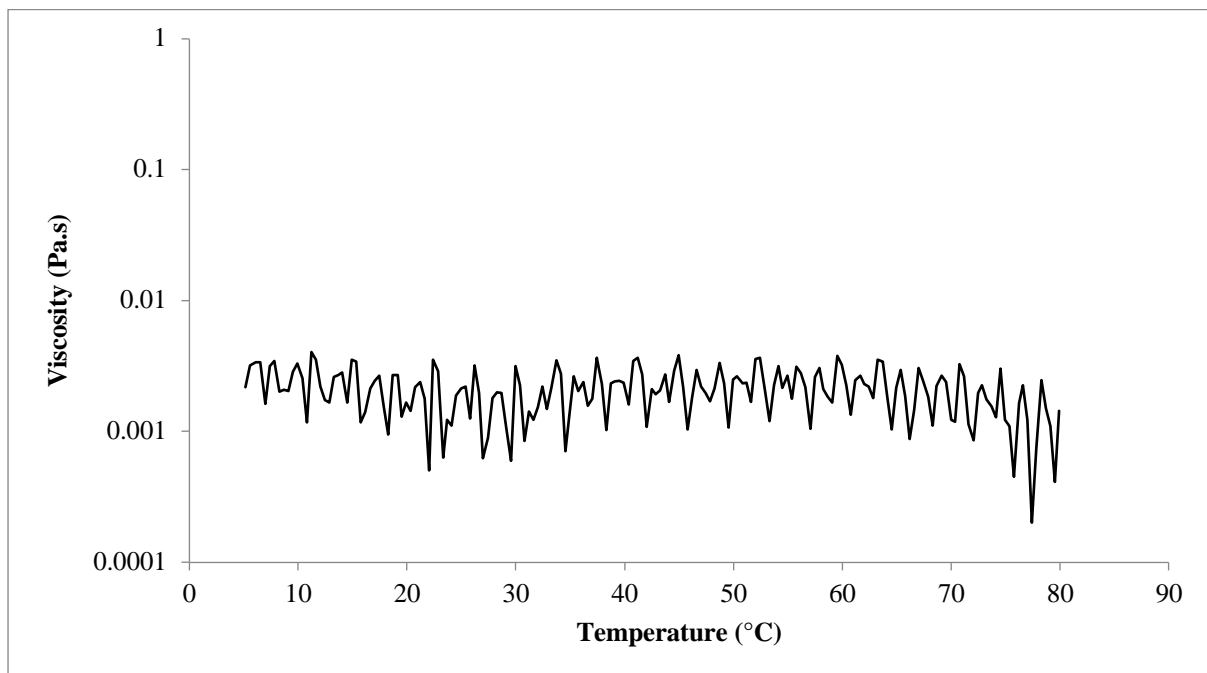


Figure 4.10 – Viscosity of a saturated 25% lactose solution (aq) across a temperature sweep between 5 and 80°C at constant shear rate of 10 reciprocal seconds.

The viscosity of the lactose solution appears to show an oscillatory response across the temperature sweep, however it is believed this is in fact due to the inability of the rheometer to measure the very small changes in force associated with the low viscosity. This means that the oscillation in the graph is a measure of the instrument accuracy rather than any fluid behaviour. The very low viscosity of the solution means there is very little resistance to the shear force generated by the rheometer. The stress sensor is unable to measure accurately at such a range and the oscillatory data is most likely a result of signal noise generated through motion of the geometry and not the material properties.

4.3.6 Dynamic Vapour Sorption

While the rheological characterisation of the excipients yielded valuable information because the technique examines excipients in solution it is debatable over how comparable it is to a granulation system where solids are in excess. In order to better understand how the solid excipients interact with water Dynamic Vapour Sorption (DVS) was undertaken. DVS examines the interaction of solids with water vapour rather than liquid water, so again is not truly representative to a granulation system, however it provides valuable information about the affinity for water of the excipients by characterising how hygroscopic they are.

The sorption and desorption isotherms for the three excipients in the formulation are shown in Figure 4.11. The isotherm for HPC in Figure 4.11c shows the high affinity for water that the material has, gaining close to 50% in mass through adsorbed water vapour at 100% relative humidity. The desorption isotherm lies closely in line with the sorption isotherm, showing that the material readily equilibrates with the surrounding conditions. The isotherm for MCC in Figure 4.11b shows how the material is hygroscopic despite being insoluble, adsorbing 25% of its mass in water vapour at 100% humidity. The hysteresis between the sorption and desorption isotherms is interesting, further demonstrating the hygroscopic nature of MCC in that it will readily adsorb and contain water. Finally the isotherm for lactose in Figure 4.11a is very interesting, showing that despite being highly soluble lactose has almost no interaction with water vapour. It is not until 100% relative humidity that there is a change in mass of the sample. At this humidity it is likely that water vapour has condensed on the sample as liquid and partially dissolved the lactose, hence the gain in mass. These results are interesting in showing the relative affinity of materials for water and providing clues for where it would go in a wet granulation system. As would be expected the HPC binder in the formulation readily adsorbs liquid. But what is surprising is the apparently low affinity of lactose for water considering its high degree of solubility. Implying it may not competitively absorb liquid over other excipients within the formulation.

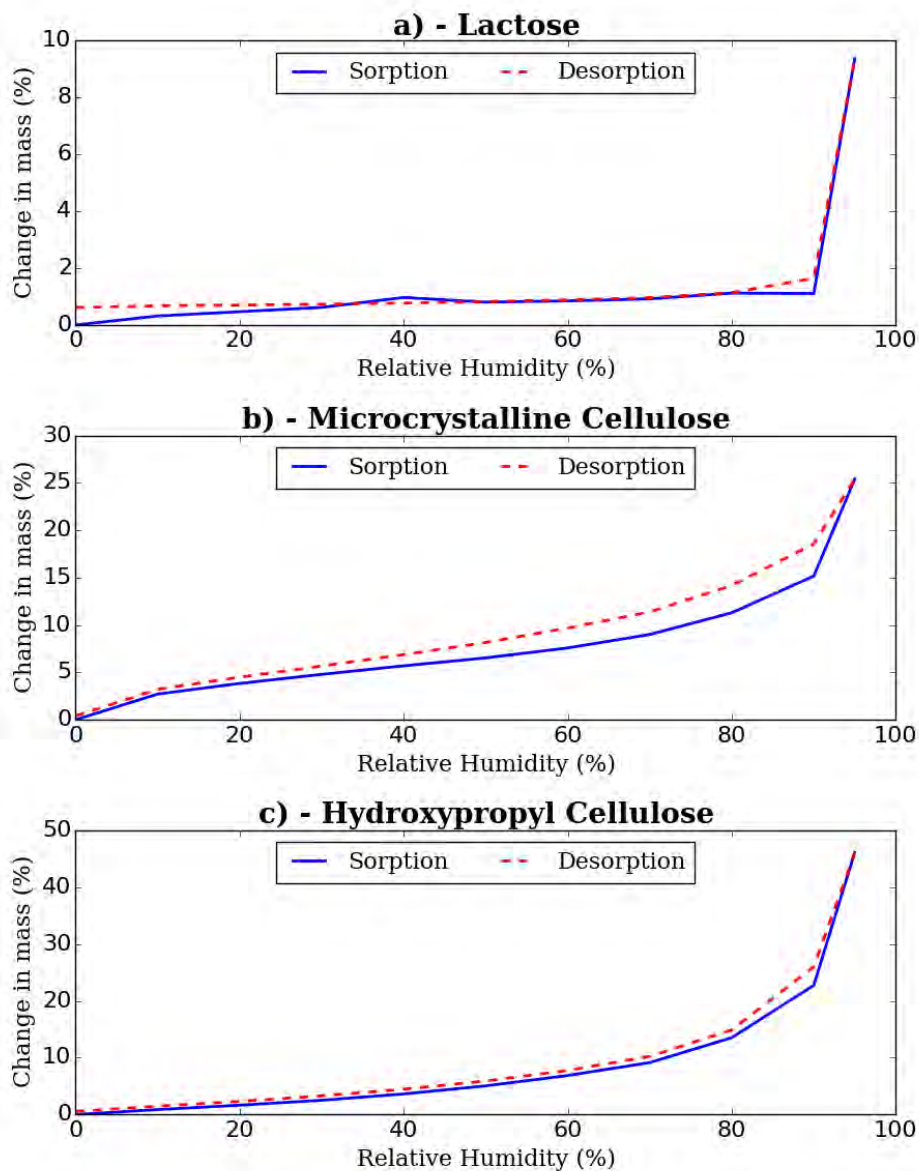


Figure 4.11 – Water vapour sorption and desorption isotherms at 25°C for a) Lactose, b) Microcrystalline Cellulose and c) Hydroxypropyl Cellulose

4.3.7 Mechanical testing

Mechanical testing was undertaken in order to understand the change in behaviour of the material at temperature. The lower steady state torque values at high temperatures shown in Figure 4.1 would suggest something like a thermoplastic effect, material becoming more pliable as it is hotter.

This is reflected in the stress strain curves for both the wetted binder formulation and wetted lactose shown in Figure 4.12.

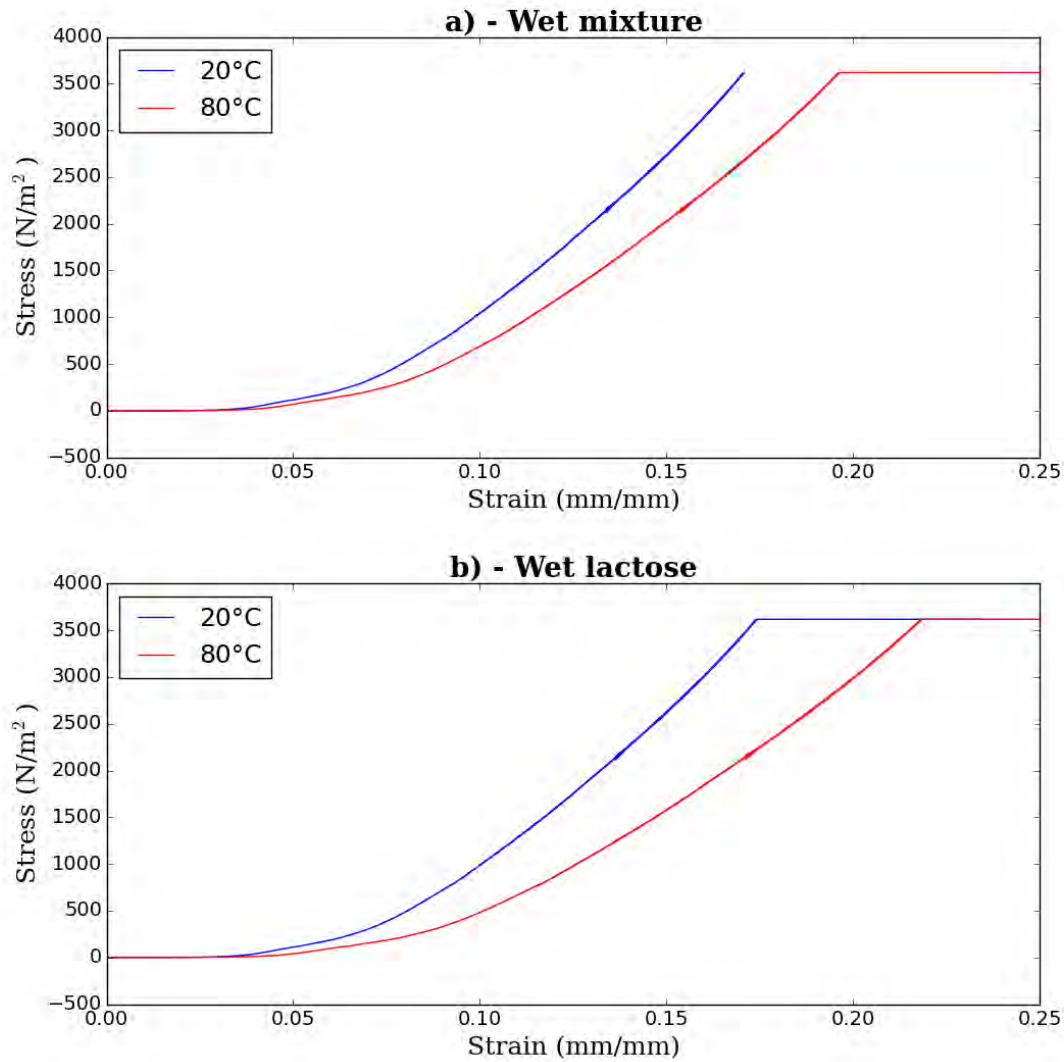


Figure 4.12 – Stress strain curves obtained through spherical compaction at 20°C and 80°C of a) 20% L/S wetted formulation mixture and b) 20% L/S wetted lactose

The stress strain curves obtained at 20°C and 80°C for the wetted formulation mixture and for wetted lactose both show the material to be more compressible at higher temperature. In both cases at higher temperature the deformation of material is greater for a given force. This reflects the

torque behaviour within granulation, with hotter material requiring less energy to mix and granulate.

Calculation of the area under the curve allows the comparison of the stress strain curves shown in Figure 4.12. First the data was processed in MATLAB to trim the periods where the probe was no longer moving but data continued to be recorded, represented by the horizontal lines of constant stress at the end of the curves. This was done so that only the representative stress data recorded during the displacement of the material was analysed. The area under the curve was then approximated using the MATLAB *trapz* function which approximates the area under the curve by fitting a series of trapezoids using the trapezoidal rule. For a curve between a and b with function

$$\int_a^b f(x)dx \quad (4-3)$$

The area under the curve can be approximated with the trapezoid rule where

$$T_n = \frac{b-a}{2n} [f(x_0) + 2f(x_1) + 2f(x_2) + 2f(x_3) + \dots + 2f(x_{n-1}) + f(x_n)] \quad (4-4)$$

Where T is the sum of n trapezoids, x_0 equals a , and x_1 through x_n are the equally spaced coordinates along the x-axis of the edges of trapezoids 1 through n .

The width of trapezoids was set by the measurement interval, which was approximately 9,500 evenly spaced data points across the measurement range. Given the high frequency of trapezoids this helps increase the accuracy of the approximation of area under the curve.

Table 7 – Approximated areas under curves of the stress strain curves presented in Figure 4.12

Material	Area Under Curve
Mixed formulation – 20°C	182.675
Mixed formulation – 80°C	209.925
Lactose – 20°C	186.286
Lactose – 80°C	233.589

Calculation of the approximate area under the curve of the stress strain curves presented in Figure 4.12 show similar values for the mixture and lactose at the same temperatures. This is not necessarily surprising as the formulation consists of primarily lactose (75%). Comparing the ratio of area under the curve between experiments at 20°C and 80°C gives 0.87 for the mixed formulation and 0.80 for lactose. It may be expected that the ratio between the curves would be similar to the ratio in differences in power during granulation at different temperature presented in Table 6. These values are quite different however with the power demand at 80°C around 45% of that at 20°C but the ratios of areas under curves being 115% larger at 80°C. While the power draw to granulate material and stress required to deform it are both measures of the energy required to manipulate it, it would not appear they are comparable. It may be worthwhile to investigate other techniques of mechanical testing to see if further insight could be gained into the changes with temperature and if these are similar to the differences in granulation power.

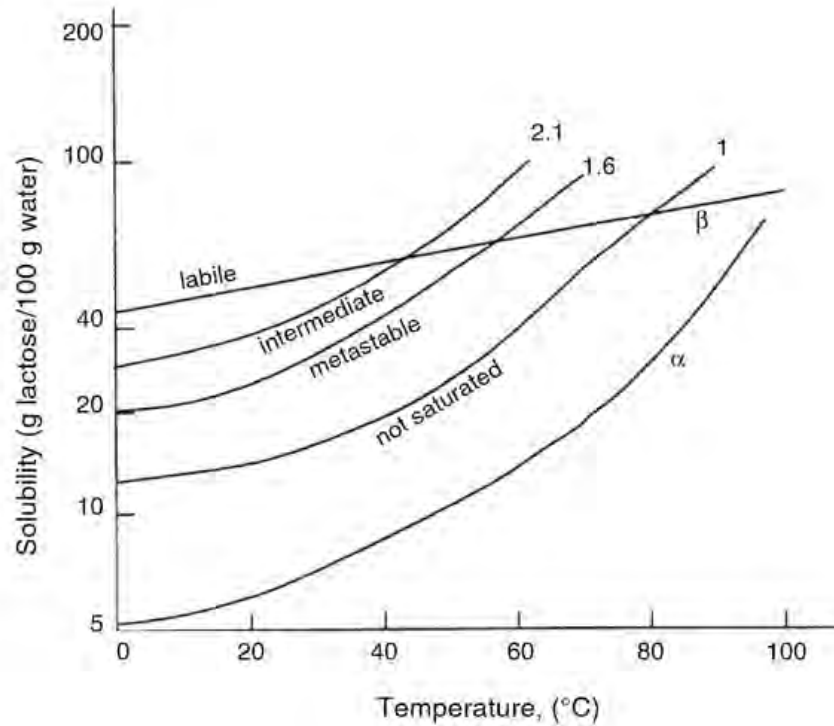


Figure 4.13 – Solubility of lactose in water. Recreated from Fox et al, Dairy Chemistry and Biochemistry, 2015

[54]

Solubility curves for the dissolution of lactose in water are shown in Figure 4.13. These show that the solubility of lactose in water increases considerably with temperature. The formulation investigated consists mainly of lactose and it is believed that the behaviour of lactose at various temperatures is primarily responsible for the torque phenomena observed within granulation. The solubility of lactose is highly correlated with temperature [54]. Lactose will readily dissolve into a saturated solution of increasing concentration as the temperature is increased. This increase in solubility is believed to lead to the reduced granulation torque at elevated temperatures. As more lactose can be dissolved within the same amount of liquid the system behaves at essentially a lower solids fraction. The competition for liquid is lower, particles are lubricated in flow and thus mixing becomes less mechanically demanding. When there is no HPC binder in the formulation the granule size distributions in Figure 4.8 appear to reflect the characteristic TSG transition from bimodal to monomodal at higher liquid levels. It is believed at 80°C here the effective higher liquid level allows

for more liquid bridges to form between particles, resulting in large monomodally distributed granules.

The HPC binder becomes insoluble at temperatures greater than 43°C, precipitating out of solution.

This leads to the resultant granule size distributions in Figure 4.2 where above 43°C the binder precipitates, loses its binding affinity and less large granules are formed.

4.4 Conclusions

The behaviour of the excipients at various temperatures can be seen to have considerable effect over the granulation process. While the observations here are specific to these materials, bulk pharmaceutical excipients are typically quite similar often consisting of simple sugar molecules. Thus it is likely that other excipients may display similar behaviours, particularly the increase in solubility of sugars in water with temperature. Control of temperature during the wet granulation process is often seen as unimportant compared to other more critical parameters such as overall liquid amount. However the changes in solubility of excipients with temperature may have strong correlations with liquid levels, effectively changing granulation mechanisms. An important point to consider is the amount of heat that can be generated through the granulation process alone. The mechanical mixing in granulation results in excess heat which is transferred to material. This has importance in twin screw granulation in the time it takes for the granulator to reach a true steady state, as demonstrated in Figure 4.4. The generation in heat may play an important role in other granulation techniques such as high shear wet granulation, where the impellor may transfer considerable energy into material. This temperature change across a batch may be an important point to consider for the understanding of granulation mechanisms or in construction of granulation models.

Quite considerable differences (approximately 45%) in the power required for granulation have been demonstrated between 20°C and 80°C. This has interesting implications towards application to an industrial process for the potential saving of energy. However comes with the strong caveat of the

additional energy required to heat and maintain temperature in the process. Mechanical characterisation of the formulation at 20°C and 80°C demonstrates differences in the behaviour of the material with greater deformation at the same stress at 80°C. Comparison of the ratio of areas of curves however does not show comparable changes to the power values in granulation. Given the differences between the systems, with granulation having higher stresses, shorter residence time, shear forces and a different thermodynamic profile to a static bed, this may not be surprising. It would however, be of interest to further characterise the differences in material behaviour with temperature. Examining the behaviour under stress at a range of temperatures between 20°C and 80°C would be of interest to see if a correlation could be drawn between the power required for granulation or the solubility of lactose. The solubility curve of lactose shown in Figure 4.13 for example shows an approximate four-fold increase in solubility of α -lactose between 20°C and 80°C, which is larger than the differences seen in granulation power and mechanical testing. It would be of interest to see if the solubility curve could be related to granulation power and add evidence to the theory that it is the cause of differences in power.

Finally, this chapter demonstrates that temperature can cause quite considerable changes in granulation systems, therefore it is important to consider control when scaling up to industrial systems.

Chapter 5 – Screw

configuration and degree of mixing

5.1 Introduction

Twin screw granulators have modular screws, allowing for transport and mixing elements to be arranged in numerous permutations. There has been little detailed work into how this arrangement, known commonly as the screw configuration affects the granulation process. This chapter seeks to address this gap in knowledge by systematically investigating the effect of screw configuration on granulation. A more detailed description of the types of screw elements and their impact to flow of material in granulation can be found in Chapter 3.1.

The flow of material through kneading elements is complex, determined by the length of kneading block, the angle of the elements and the push of material from upstream conveying elements. On top of this powder undergoes a transition as it passes through the block, becoming squeezed and compressed into granules, with changing flow properties. Understanding how these arrangements work is therefore key in building a screw configuration which results in granules of desired properties.

This work looks at how the length, angle and position of the kneading block affects granulation. Mechanisms of granulation are inferred through measurement of process conditions and granule characteristics and detailed analysis of flow through PEPT.

5.2 Materials and Methods

5.2.1 Granule formulation

The powder formulation used within these experiments consisted of 75% lactose (316/FAST-FLO[®], Foremost Farms, USA), 20% Microcrystalline Cellulose (Avicel PH101, FMC BioPolymer, Ireland) and 5% Hydroxypropyl Cellulose (Klucel EXF, Ashland Inc, USA). Prior to granulation experiments the formulation was prepared by mixing the excipients in 1 kg batches in a Pascal lab mixer for a minimum duration of 20 minutes.

5.2.2 16 mm Scale Granulation experiments

Granulation experiments were performed with the Haake Rheomex twin screw extruder (Thermo Scientific, Germany). The Haake extruder is equipped with a Rheocord torque rheometer which enabled recording of the motor torque during granulation through the Haake Polysoft software package.

The Haake extruder has a screw diameter of 16 mm and L/D ratio of 25:1. This relatively long screw length and large operating range allowed for many variations in screw configuration to be explored without over-torqueing the granulator motor.

Liquid was fed into the granulator through a liquid inlet port positioned above the screws, approximately 9 screw diameters from the base. An 8 roller peristaltic pump (REGLO Digital, Ismatec, Switzerland) was used to dose liquid. Distilled water was used as the granulation liquid at a liquid to solid ratio of 20%.

Granulation was performed at 200 rpm screw speed and 2 kg/h mass flow rate. Numerous different screw configurations were used and are summarised below, full details of the screw configurations investigated can be found in Appendix 1.

Table 8 – Summary of screw configurations used with the Haake TSG

Angle	Number of kneading elements											
30°F		2	3	4	5	6	7	8	9	10		
60°F		2	3	4		6		8		10		12
90°	1	2	3	4	5	6	7	8	9	10	11	12
30°R		2		4								

A range of screw configurations were investigated while maintaining all other process conditions.

The goal was to examine how the length of kneading block and kneading element offset angle affected granulation. To do this the number of kneading elements used in the kneading block was increased incrementally. For each configuration the process was allowed to reach steady state, so that the steady state torque could be measured and samples of granules taken. Wet granule samples were oven dried at 100°C for 2 hours prior to further analysis.

5.2.3 Granule analysis

The particle size distribution of granules was determined through image size analysis using a QICPIC system (Sympatec, UK). Approximately 5 g samples of granules were measured at a time. The granules are fed slowly by a vibratory feeder into the body of the QICPIC to ensure good dispersion of particles. The granules fall through a tube past a light source and the projected silhouettes captured via video. The images are then computationally processed in order to determine the size and shape of the individual granules.

The bulk density of granules was determined by measuring the mass of a fixed volume of granules.

5.2.4 PEPT

Positron Emission Particle Tracking (PEPT) is a technique developed at the University of Birmingham and is a powerful tool for non-intrusive visualisation of flow within actively running processes. PEPT was developed from Positron Emission Tomography (PET) and uses the same detection technology. While PET typically uses a gaseous radiotracer in order to image an area, PEPT differs in that only a single tracer particle is used. By tracking the position of the tracer within the bulk material over time PEPT can be used to determine velocity distributions [55], dispersion levels [56, 57] and shear rates. PEPT was used to study the flow of material during granulation by examining the 19 mm GEA twin screw granulator in operation. Unlike the PEPT data presented in Chapter 3 which reprocessed data from experiments performed by Lee et al [35], all PEPT data presented in this chapter was generated from novel experimentation.

In order to ensure that the particle motion is representative of material in the process the tracer needs to have similar properties to the bulk material. 100 μm ion exchange resin particles with 1100 kg/m^3 density were used in this study as they were similar to the primary powder. The tracer particles must be labelled in order for use. First water is activated by being bombarded by Helium-3 ions accelerated by a cyclotron. ^{16}O ions are converted to ^{18}F forming the radiotracer source. The ion exchange particles are then labelled by transfer of the ^{18}F ions to the particles. Particles are soaked in the activated water and ^{18}F ions are adsorbed onto the resin, resulting in a labelled particle.

The ^{18}F nucleus is unstable and undergoes beta decay, emitting a positron and a neutrino. The positron very quickly collides with a local electron, both are annihilated releasing two back to back 511 keV γ -rays. The γ -rays travel along the same line in opposite directions and are able to penetrate the stainless steel of the granulator barrel. The photons of the γ -rays are detected by scintillation cameras. By joining the photon pairs detected by opposing cameras a line of response is formed with its centre at the tracer. The tracer undergoes thousands of decays every second resulting in thousands of back to back γ -rays. By determining the intersection of these many lines of response

the position of the tracer is found. Tracer particles can be tracked to within 1 mm at frequencies of milliseconds [58]. Further details of PEPT and its applications can be found in references [56-61].

The 19 mm GEA twin screw granulator (GEA Niro, UK) was specially designed for PEPT, with the barrel machined down to minimise the attenuation of γ -rays. The granulator has an L/D ratio of 10:1 and a number of different screw configurations were examined in order to visualise the changes in material flow. Powder was fed via a volumetric feeder (T20, K-Tron Soder) at 2 kg/h feed rate unless otherwise stated. Water was used as the granulation liquid and delivered to the liquid injection port by an 8 roller peristaltic pump (REGLO Digital, Ismatec, Switzerland) at 0.2 L/S ratio. Screw speed was maintained at 200 rpm. Initially tracer particles were introduced to the barrel powder inlet, collected at the outlet and re-fed. Tracers were re-fed until the tracer lost activity beyond the point of being easily detectable or the particle was broken. To reduce the labour intensiveness of manually collecting and re-feeding tracer particles an alternate delivery method was developed. Hundreds of labelled tracers were formed and small quantities mixed into 1 kg batches of the powder formulation before being added to the feeder hopper. The feeder hopper was positioned outside of the camera field of view and shielded with lead in order to reduce the noise recorded. Tracers were then delivered through the normal operation of the feeder and granulator. When using this method the granulator was allowed to reach steady state before data collection began and the hopper periodically refilled in order to maintain the fill level. A summary of the screw configurations investigated with PEPT can be found in Table 9.

Table 9 – Summary of screw configurations for the GEA TSG investigated with PEPT. All at 2 kg/h feed rate (FR), 0.2 L/S and 200 rpm screw speed unless otherwise stated

Stagger Angle	Configuration				
90°	3x 2KE 90°	2x 4KE 90°	2x 6KE 90°	8KE 90°	10KE 90°
60°F	2x 4KE 60°F	2x 6KE 60°F	8KE 60°F	10KE 60°F	
30°F	6x 0.25D KE 30°F – (1.8 kg/h FR)		3x 0.5D KE 30°F – (1.8 kg/h FR)		

Raw PEPT data was processed using the track.exe program developed by the University of Birmingham School of Physics. This produced a data file of cartesian coordinates of detected tracer positions throughout the experiment. Before each experiment began a calibration was performed where a tracer particle was positioned on a fixed point for 3 minutes, then moved to a second fixed point for another 3 minutes. This insured that the experimental data gathered could be matched to the granulator geometry. As each experiment was recorded as a continuous period the data required processing in order for useful information to be extracted. Code was written in MATLAB to process the extracted data into useful form. First the data required splitting into individual passes of a tracer through the granulator. This was performed by trimming data spatially around a detected tracer entering and exiting the granulator geometry. Coincident passes, where two or more tracers entered the field of view concurrently were removed. Some manual processing was then required to remove passes where tracers became stuck or broke apart. Once the dataset of individual passes had been created it was processed in MATLAB in order to determine residence time.

5.3 Results and discussion

5.3.1 Effect of kneading block length

Experiments were performed where the length of kneading block was increased incrementally in order to determine the impact on granulation. It was hypothesised that the mixing intensity would increase with kneading block length and this increase in degree of mixing would lead to less variability in the final product.

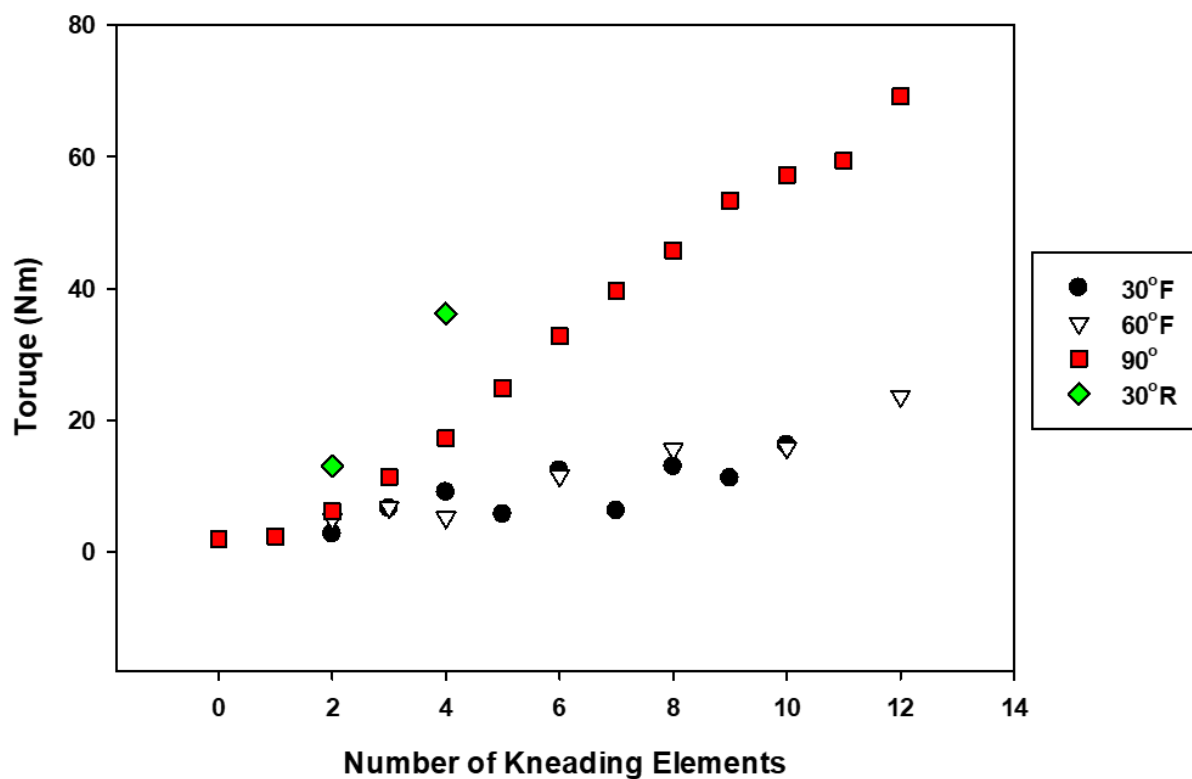


Figure 5.1 – Steady state granulation torque values for increasing lengths of kneading block. Process parameters were 2 kg/h material feed rate, 0.2 L/S and 200 rpm screw speed.

Figure 5.1 shows the steady state torque during granulation for increasing lengths of kneading block. Note that the granulator is calibrated for baseline torque during setup and the above values are absolute torque values from during granulation. The torque values increase proportionally with length of kneading block for all the different angles investigated. Only a small number of kneading

elements (4) could be used when offset at a 30° reversing angle at these process conditions. Attempts to use more elements would lead to blockages forming and over-torquing of the granulator drive motor. 30°R angles produce the greatest amount of backflow, while this may be desirable in extrusion processing for generating pressure, they are not necessarily useful in granulation where materials are less plastic and more likely to form blockages. Driving force from upstream conveying elements is required to ensure flow through reversing kneading blocks. This driving force is generated by the mass of material pushed forward through rotation of the conveying elements. The degree of force is dependent on the volume of material and speed of rotation. However these two factors also contribute to the overall degree of reverse flow within the mixing zone. A careful balance of process conditions is then required to ensure flow through reversing elements. Because of this, bar specific circumstances, reversing geometries do not appear optimal for granulation processes.

The increase in torque for 90° kneading blocks in Figure 5.1 is much higher than that of the 30° and 60° forwarding geometries. The increase in steady state torque with length of kneading block is roughly approximate for the two forwarding geometries. This would imply the degree of mixing is higher with 90° elements.

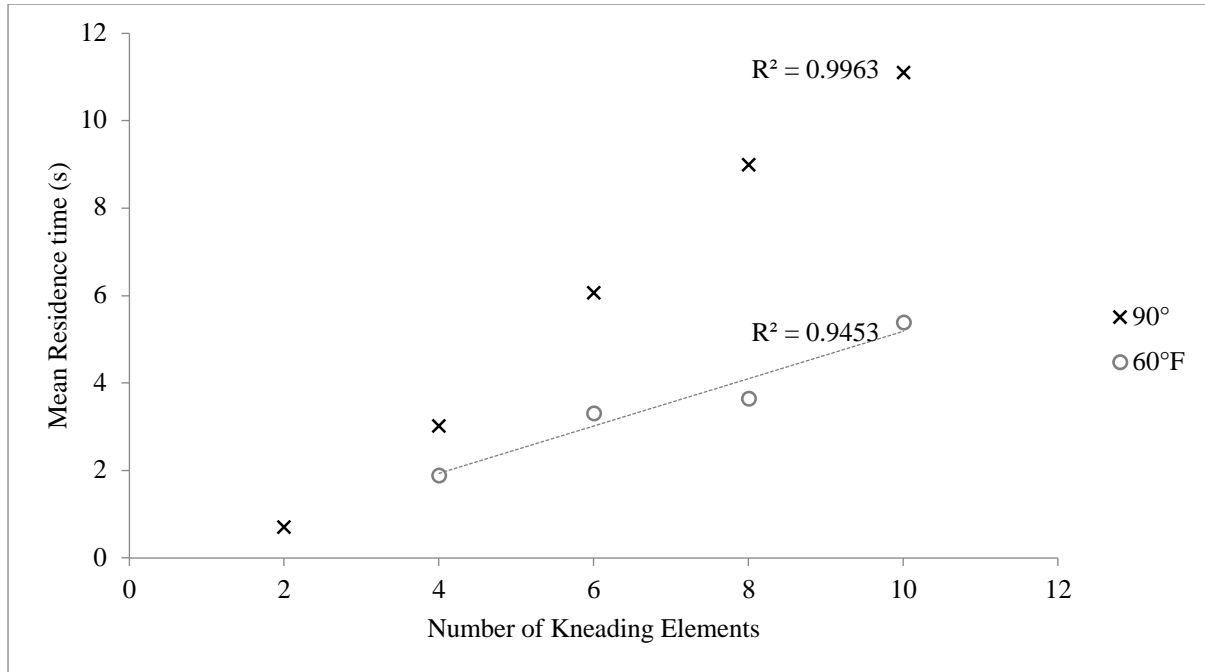


Figure 5.2 – Mean residence times determined across the kneading block for 90° and 60°F screw configurations through PEPT analysis of the GEA 19 mm TSG. Process parameters were 2 kg/h material feed rate, 0.2 L/S and 200 rpm screw speed.

Figure 5.2 shows the mean residence times across the kneading block for 90° and 60°F screw configurations. These residence times are based on the time for material to pass through the mixing zone only and ignore conveying zone residence times. As would be expected the mean residence time increases with the length of kneading block used. 60°F configurations have shorter residence times than 90° configurations due to their greater conveying capacity. What is interesting to note is that the general trend for increasing residence time is similar to that for increasing torque shown in Figure 5.2. While these results for steady state torque and average residence time are obtained on different granulators and are thus not directly comparable, the trends exhibited are expected to be similar for both.

The linear trend shown in both Figure 5.1 and Figure 5.2 would imply that the process response for an increasing length of kneading block is easily predictable. However an upper limit is expected to

this correlation where very long lengths of kneading block result in such high impediment to flow that blockages form in real world systems.

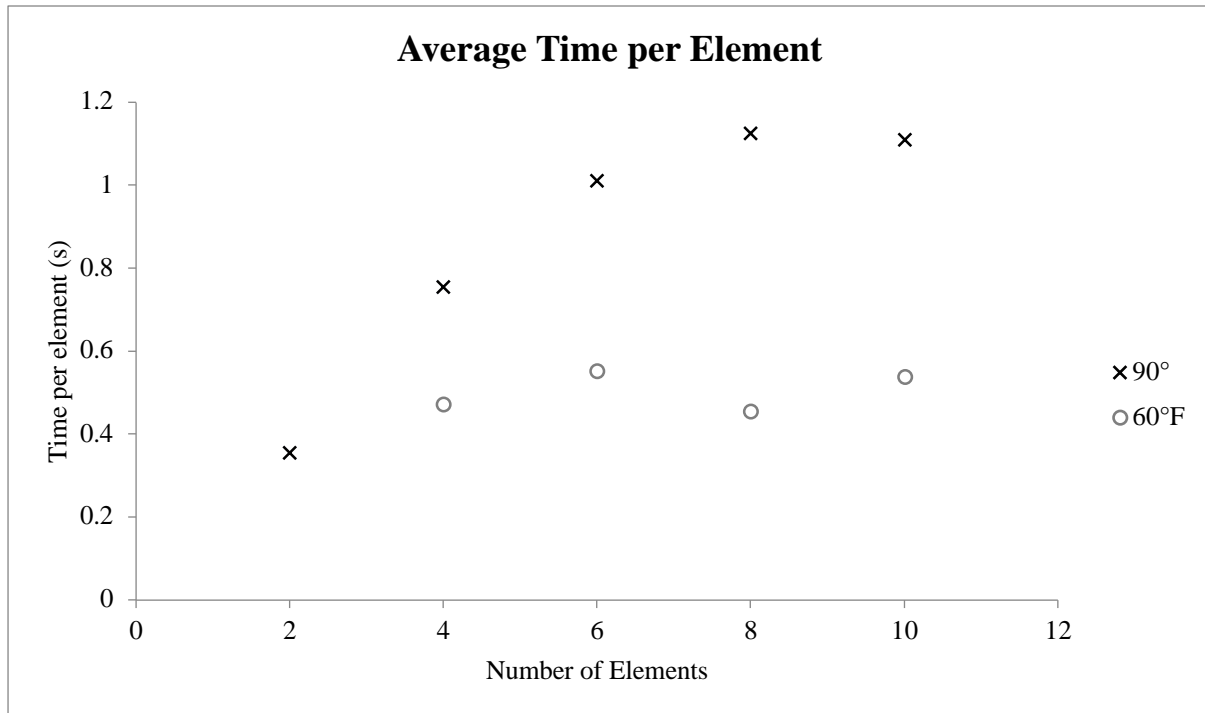


Figure 5.3 – Average time per element in the kneading blocks of 90° and 60°F screw configurations obtained through PEPT analysis of the GEA 19 mm TSG

Figure 5.3 shows the average time per element from the mean residence times obtained in Figure 5.2. There are distinct differences in the relationships between the 60° forwarding geometry and neutral 90° elements. There is little change in the average time per element for 60°F geometries as the length of kneading block is increased. This would imply that changes in kneading block length do not affect the individual element residence time and instead the overall residence time come from the length of kneading block alone. In contrast the neutral 90° elements display an almost logarithmic relationship between the element residence time and length of kneading block. This increase in element time implies that the fill level across the element is similarly increasing. The plateau at 8 to 10 elements suggesting that a maximum fill level has been reached. In contrast the small differences exhibited by 60°F geometries suggest that these elements are operating at a constant fill level.

5.3.1.1 Change in Granule properties

The prior section investigated how the process responds to changes in screw configuration, this section explores the product response in terms of granule properties to increasing lengths of kneading blocks.

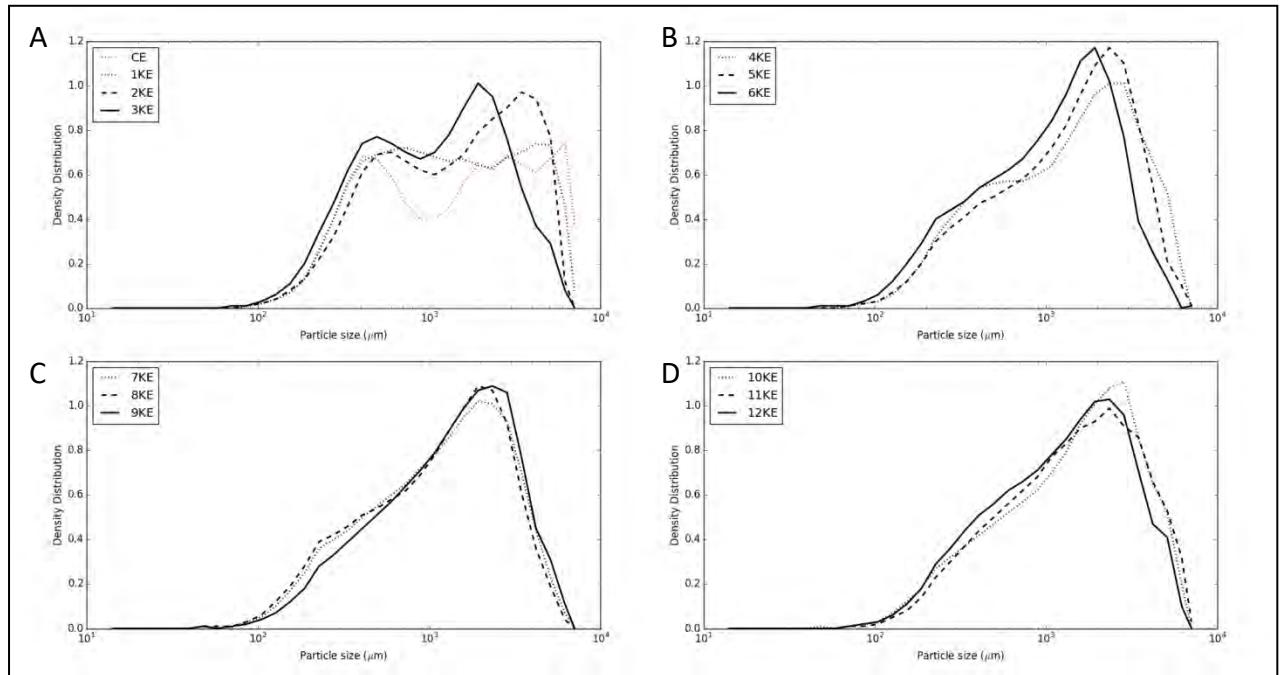


Figure 5.4 – Particle size distributions of granules produced using increasing lengths of 90° kneading blocks with the Haake TSG. Note that the length of kneading block increases through A-B-C-D.

Figure 5.4 shows the particle size distributions for granules made with the Haake TSG using 90° kneading blocks. With low numbers of kneading elements the size distributions reflect the characteristic bimodal size distributions associated with twin screw granulation. However as the number of elements used increases a transition in the size distribution can be observed. The size distributions narrow and eventually become monomodal with 5 kneading elements. Size distributions are relatively consistent between 6 and 10 kneading elements but display a slight broadening above this.

The ability to achieve this shift in distribution from bimodal to monomodal through screw configuration provides a useful tool in process design. Previous work has only reported on achieving

this shift to monomodality through increasing the liquid to solid ratio during granulation [32, 39, 62]. Coupled with the linearity in torque response exhibited in Figure 5.1 the ability to predict where this shift in size distribution will occur will aid determination of optimum granulation conditions. It is of interest to note that the main mode within the particle size distributions lies around the same approximate value of 1400 μm . Larger granules are produced when short mixing blocks with less than 3 kneading elements are used. These are believed to be large agglomerates formed at nucleation from the uptake of liquid, where subsequent mixing is not intensive enough to disperse these agglomerates into smaller individual granules. The establishment of this mode about 1400 μm with longer mixing sections appears to be characteristic of the granulator mixing elements or combination with the formulation properties. The exact mechanism for the formation of these granules is not understood, but is perhaps a function of the size of the intermeshing region between kneading elements. With longer mixing sections it would be expected for breakage rates to be increased as each granule experiences more chopping and shearing motions. However as there is no significant reduction in the frequency of this mode it may imply that granule growth and breakage rates remain in balance, or that granule formation and size is a function of the granulator kneading element geometry.

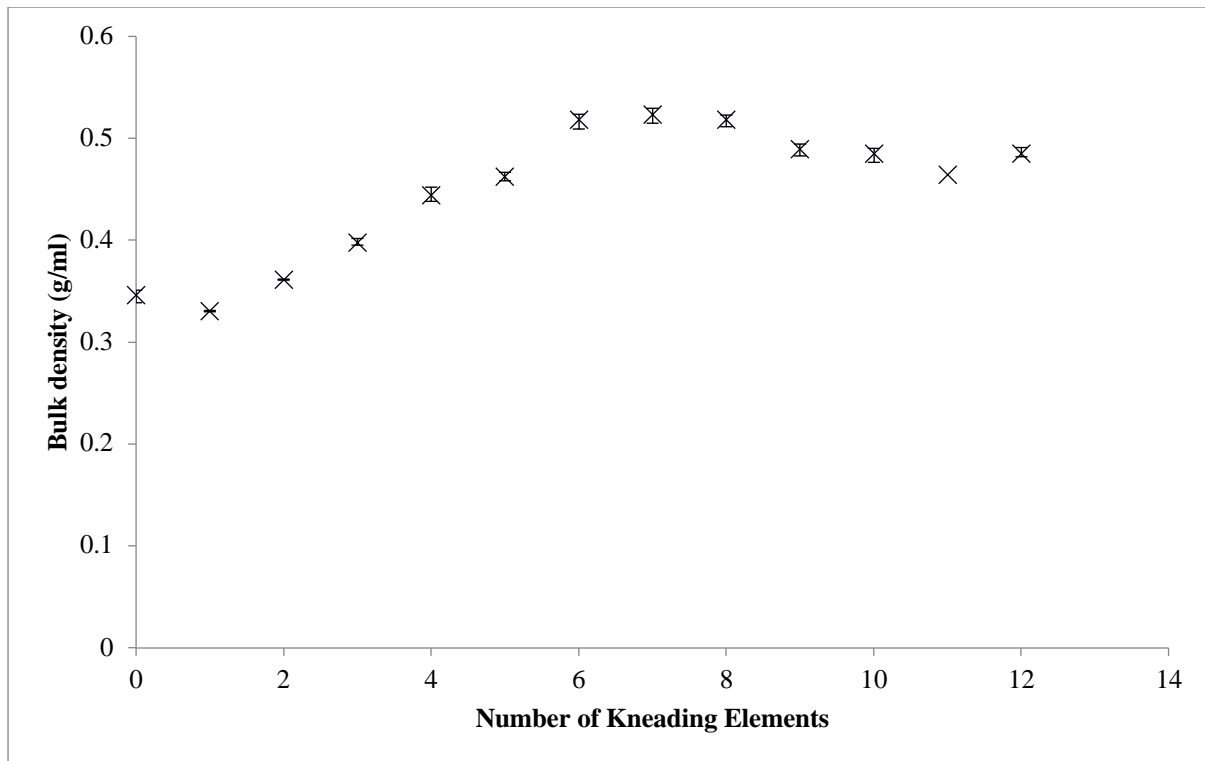


Figure 5.5 – Bulk densities of granules produced with increasing lengths of 90° kneading blocks using the Haake TSG. Error bars represent the extremes of measurements made in triplicate

The bulk densities of samples of granules produced using 90° kneading blocks are shown in Figure 5.5. The density of granules increases with the number of kneading elements used, reaching a plateau between 6 – 8 elements at approximately 0.5 g/ml before decreasing when further elements are used. It is of interest to note that the bulk density of granules produced using conveying elements only is higher than that with a single pair of kneading elements and is perhaps related to the difference in shape of granules formed. The density of the primary powder formulation was 0.51 g/ml however the density of granules formed was in general lower and only at parity with the densest samples of granules produced. This is somewhat in contrast to high shear wet granulation where longer residence times/mixing times result in more compacted, denser granules, generally much more dense than the primary powder formulation. The relatively low bulk densities observed for twin screw granulation in this case may be in part explained by the formulation used and size and shape of granules. The primary powder formulation consisted of mainly spray dried lactose particles

of diameter 100 μm . The lactose has good flowability, one of the acceptance criteria for its use as a pharmaceutical excipient, to produce API blends suitable for tableting. This good flowability and narrow particle size distribution means the lactose particles will naturally pack fairly close together resulting in higher bulk densities compared to other more fluffy pharmaceutical powders. Secondly the granules produced by twin screw granulation are fairly large as can be seen by the mode about 1400 μm in the particle size distributions in Figure 5.4. On top of the high frequency of these large granules, the size distributions are relatively broad even when monomodal. Because of this it is believed that the large irregularly shaped granules prevented close packing in the bulk phase resulting in the relatively low bulk densities. To better understand this, the tapped density of granules could be investigated or the skeletal density measured through pycnometry.

The initial trend for increasing bulk density of granules would appear to match with the measured increase in steady state torque in Figure 5.1 and narrowing of size distribution in Figure 5.4. The more intensive mixing resulting in more compaction of granules, incorporating higher proportions of fines and producing denser granules. The plateau and subsequent decrease in granule bulk density can be explained by the temperature during granulation. Long kneading blocks result in excess heat generated through mechanical work and the frictional effects of material flow. High temperatures can be generated during the granulation process as described in chapter 3 and the Haake granulator cooling system is not efficient at maintaining a set point temperature.

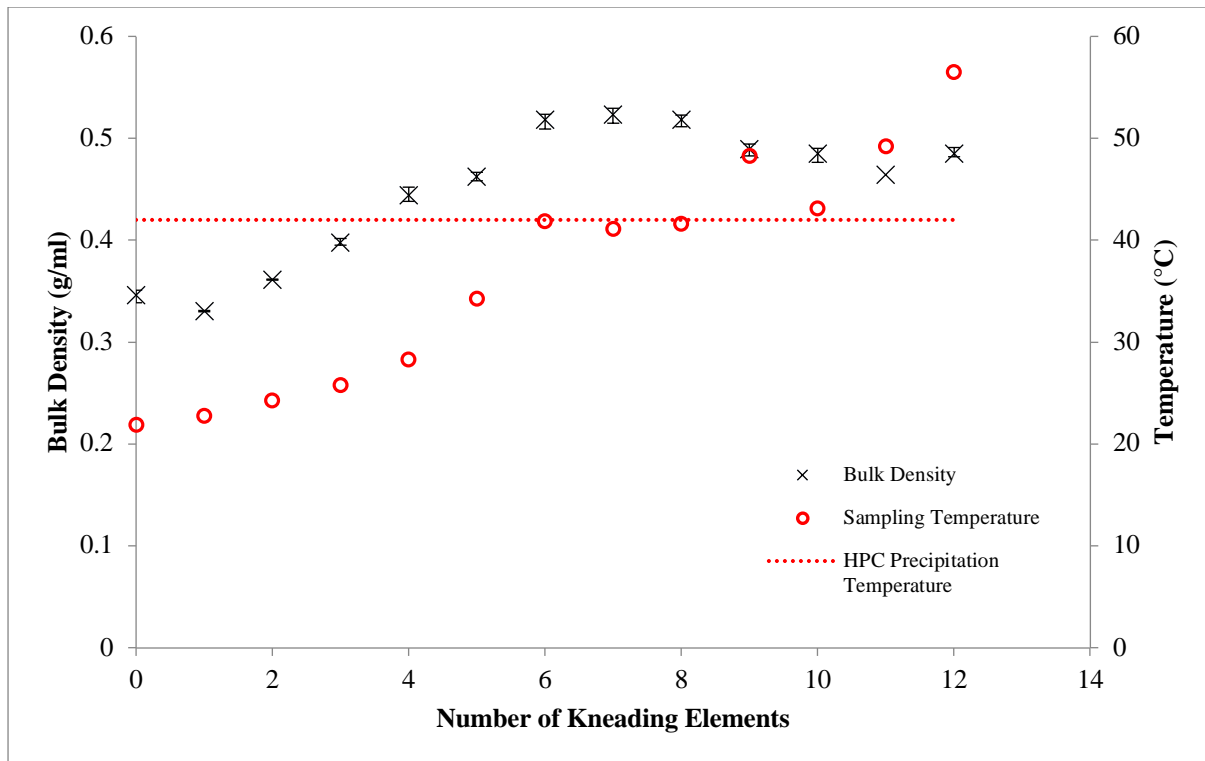


Figure 5.6 – Barrel temperatures at time of sampling and bulk densities obtained for granules produced using 90° kneading blocks with the Haake TSG.

Figure 5.6 compares the bulk densities of granules with the granulator barrel temperature at the time of sampling. It should be noted that granule samples were taken when the process was observed to be at steady state (constant motor torque) and not at any set time and are not directly comparable with each other. The higher the number of kneading elements used, the more rapidly heat is generated and higher final temperatures are reached. As can be seen from Figure 5.6 when the granule bulk density is highest between 6 and 8 kneading elements, the barrel temperature is just below the precipitation temperature of the HPC binder as described in chapter 3. When longer kneading blocks of 10 or more kneading elements are used the barrel temperatures at sampling are all above the HPC precipitation temperature. Thus it is likely that for these formulations the HPC has lost its binding affinity at this stage of granulation. This would explain the broadening in size distribution as shown in Figure 5.4 and is likely responsible for the drop in bulk density of granules. The change in bulk density for increasing lengths of kneading block is expected to be affected by

temperature for the formulation investigated. So it may be possible that more dense granules could be produced with longer kneading blocks with different formulations where materials remain malleable, or where the equipment is adequately cooled to prevent temperature increases.

This section has focussed on the granulation properties of 90° kneading blocks of increasing length. 90° kneading blocks exhibited the largest change to steady state torque and residence time while being able to maintain a granulation process. This is believed to be due to their neutral flow properties allowing for higher degrees of fill compared to forwarding geometries, while not providing such an impediment to flow to cause blockages such as with 30°R elements at these conditions. Within the range of kneading block lengths explored no one optimum configuration was found. With the specific formulation and process conditions used a relatively narrow monomodal granule size distribution could be made with 6 to 8 elements as shown in Figure 5.4. Based on the hypothesis that a homogenous population of granules indicates a well mixed product the results would suggest that a robust mixing process is achieved with this configuration. Further increase in length would be expected to result in a higher degree of mixing but complexity is added by the greater temperatures generated.

While an optimum universal kneading block length cannot be specified the work in this chapter demonstrates the relationships between kneading block length and process and granule properties. The strong relationships show that the granulation process can be predicted, which makes choice of kneading block length a useful tool in process design. Instead of using a standard 1D kneading block length, it can instead be tailored to meet desired granule or process conditions. A formulation requiring low water volumes with naturally bimodal size distribution could be shifted to monomodal through an increase in kneading block length. Similarly granulation of a highly compressible or temperature sensitive formulation prone to blockages or overheating could be optimised through reducing the length of kneading block used and thus the mixing stress the material undergoes. Screw configuration is often an area left unexplored in twin screw granulation research, possibly due to the

complexity suggested by the many possible permutations. This work demonstrates that changes in screw configuration result in logical and predictable responses and shows the use for process design.

5.3.2 Kneading Block Angle

Granules made using forwarding geometries show less of an improvement in the bimodality of size distributions compared to 90° elements. The nature of forwarding elements is that material will be conveyed in the direction of axial flow through rotation of the screws. Due to the conveying nature the hold up time within mixing zones is lower as demonstrated by the comparative residence time of 60° and 90° elements shown in Figure 5.2. As the residence time is lower the duration of mixing is similarly lower for these geometries. This would support the theory that more intensive mixing leads to more homogenous granules.

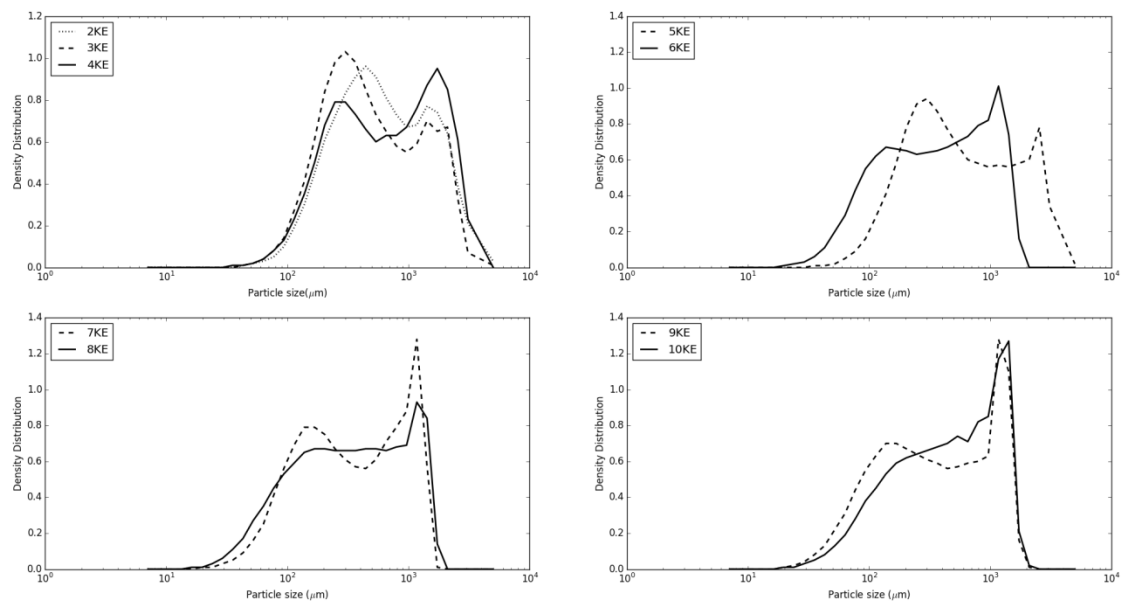


Figure 5.7 – Granule size distributions made with increasing lengths of 30°F kneading blocks

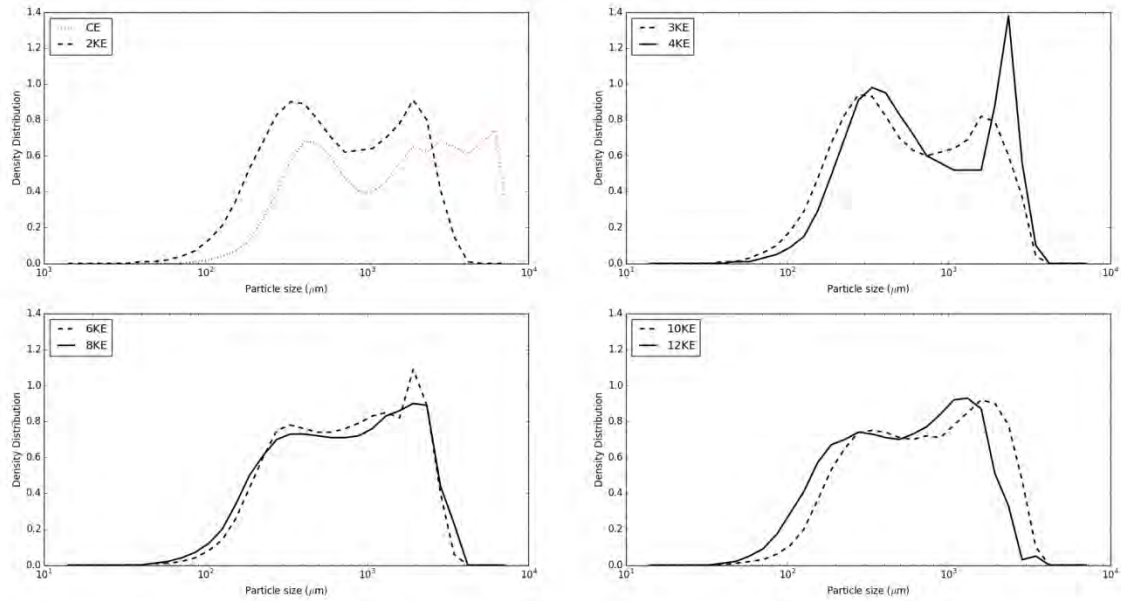


Figure 5.8 – Granule size distributions made with increasing lengths of 60°F kneading blocks

The size distributions made with 30°F and 60°F kneading elements are shown in Figure 5.7 and Figure 5.8 respectively. Granules made using 60°F elements show only slight reduction in bimodality with increasing length, with the proportion of fines decreasing and larger granules increasing. The change between a kneading block consisting of 2 elements to 12 elements is fairly minor with the size distributions sharing a similar range and profile. There is relatively small change in torque seen with the increasing length of kneading block so it is difficult to assess what impact longer lengths of 60°F kneading blocks have from particle size distributions alone. Because such little change in size distribution is seen it may be that longer kneading blocks provide no advantage for promoting mixing. However size distribution is not necessarily a direct reflection of degree of mixing and so this would be worthy of further investigation.

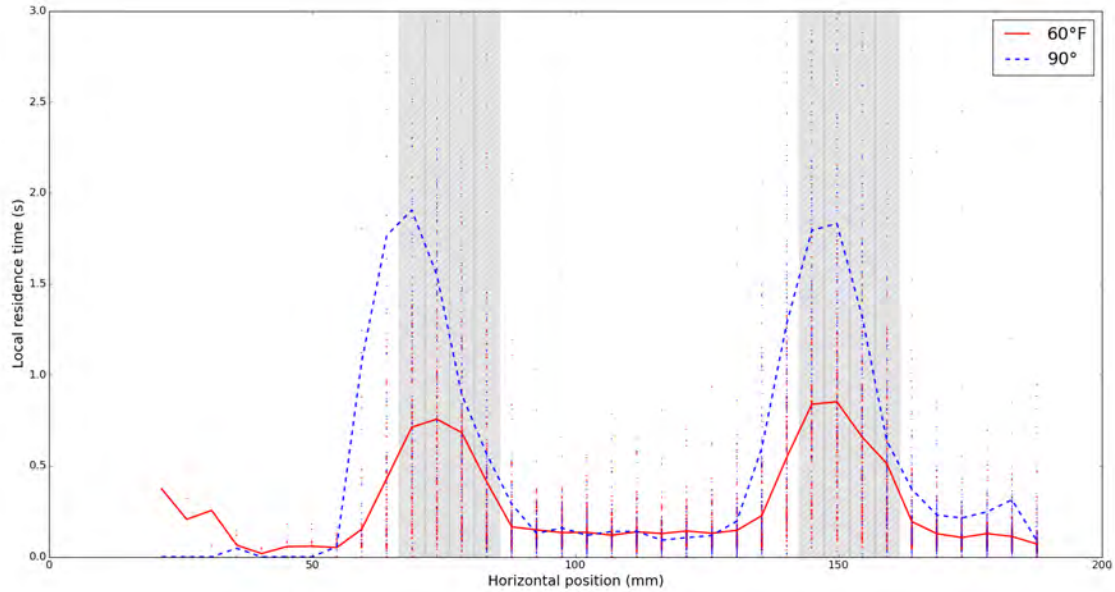


Figure 5.9 - Local residence time per 0.25D element along the axial screw length of the GEA TSG with two 1D kneading blocks obtained through PEPT analysis, showing the difference in residence time between 60°F and 90° elements. Red and blue dots represent individual residence times per pass of the tracer for the 60°F and 90° screw configurations respectively. The mean local residence times are shown by lines. Note the grey hatched area represents the position of the kneading blocks. Process parameters were 2 kg/h material feed rate, 0.2 L/S and 200 rpm screw speed

Figure 5.9 shows the comparative local residence times (proportional to fill level) along the axial length of the GEA TSG equipped with 60°F and 90° kneading blocks but otherwise identical configurations. As would be expected the residence times of the 90° screw configuration are longer than the 60°F configuration. Comparing the two configurations it can be seen that the time spent within the kneading block of 60°F elements is always lower than that of 90° elements. What this implies is that the fill levels here are consistently lower, meaning that the 60°F elements cannot be operating fully filled.

It is of interest to note the fill profile which establishes across the kneading blocks. The local residence time is highest at the start of the mixing zone and decreases further along the kneading block. This shows that under these conditions the kneading block does not operate fully filled. It

would be expected that as the overall fill level is increased, through increase of feed rate or reduction in screw speed, that the fill profile across the kneading block would change. The evolution of the fill profile and effect on the granulation process would be worthy of further exploration through PEPT. This would provide useful information on the process operability range of twin screw granulation, such as whether the kneading blocks can operate fully filled, the choking point of the granulator or information on mixing mechanisms.

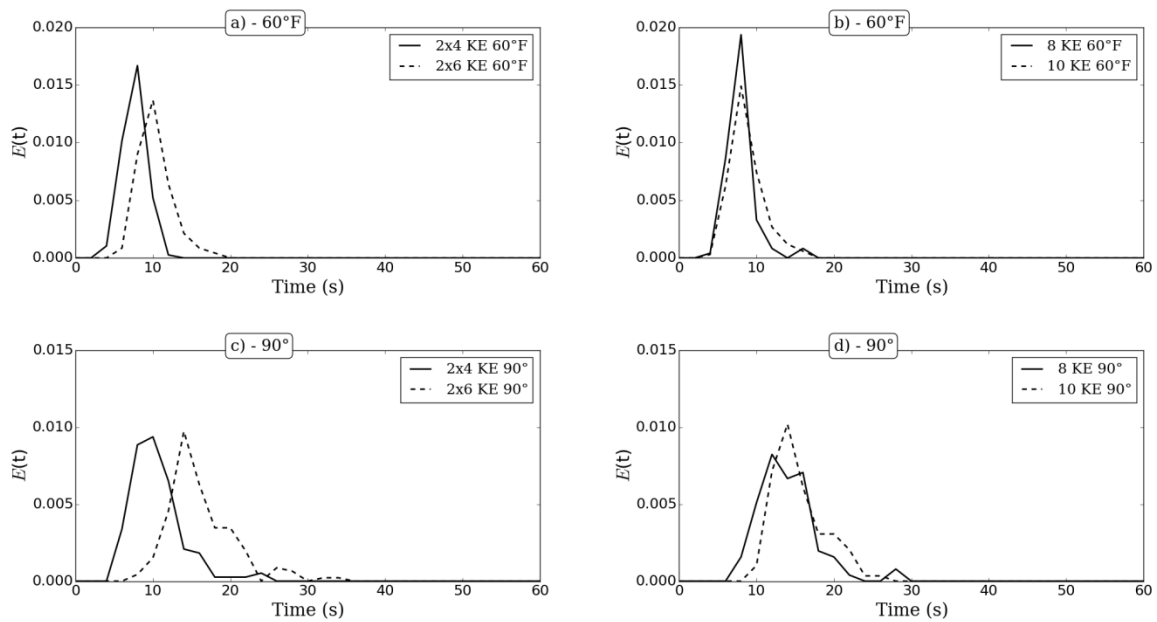


Figure 5.10 – Residence time distributions obtained through PEPT analysis of the GEA TSG. a) & b) with 60°F screw configurations, c) and d) with 90° screw configurations.

Figure 5.10 shows the residence time distributions for 60°F and 90°F screw configurations. The RTD curves were determined using the modified form of the residence time distribution equation (2-1) described by Lee et al [35] where:

$$E(t) = \frac{a(t)/\delta(t)}{\sum a(t)} \quad (5-1)$$

Where $E(t)$ is the residence time distribution, $a(t)$ is the number of passes with residence time between t and $t + \delta t$ and $\Sigma a(t)$ is the total number of passes. The modified form of the residence time distribution equation accounts for the differences in the form of tracer used for PEPT. PEPT uses individual tracer particles rather than a dispersible tracer whose concentration can be measured. The residence time distribution is then a probability distribution for a tracer to have exited the granulator at time t based on the population of passes through the granulator.

As screw configurations using 4 and 6 element kneading blocks were equipped with two kneading blocks while those with 8 and 10 were equipped with one the evolution of the RTD with kneading block length cannot be directly extrapolated. However the RTDs clearly show the differences in flow between 60°F and 90° elements. 60°F screw configurations all have sharp narrow RTDs while 90°F screw configurations are much broader in comparison. This highlights the differences in degree of mixing achieved by the different elements. The narrow RTD curves of 60°F screw configurations would imply low axial mixing compared to the 90° configurations.

5.3.3 Arrangement of screw configuration

The arrangement of screw configurations has not been explored in detail for twin screw granulation. Screw designs typically follow a basic pattern of a nucleation zone and subsequent mixing zone to result in agglomeration and breakage. Where the mixing zone is positioned relative to the nucleation zone has largely been unexplored, apart from certain examples such as the recommendation of Van Melkebeke et al [16] to include a conveying element after the kneading block,.

While it may be expected that adding liquid directly onto the mixing zone would result in robust mixing for granulation the exploration of this in chapter 2 demonstrated that the resultant long hold up time leads to surging and unsteady state operation. This is due to plugs of material forming and being cleared by build up of upstream pressure. As little mixing occurs within conveying zones it could be expected that the properties of wetted material do not change and should be delivered to the mixing zone in the same state independent of the length of conveying zone. Some preliminary

experiments were performed using the Haake twin screw granulator in order to determine if the position of the kneading block on the screws affects the granulation process.

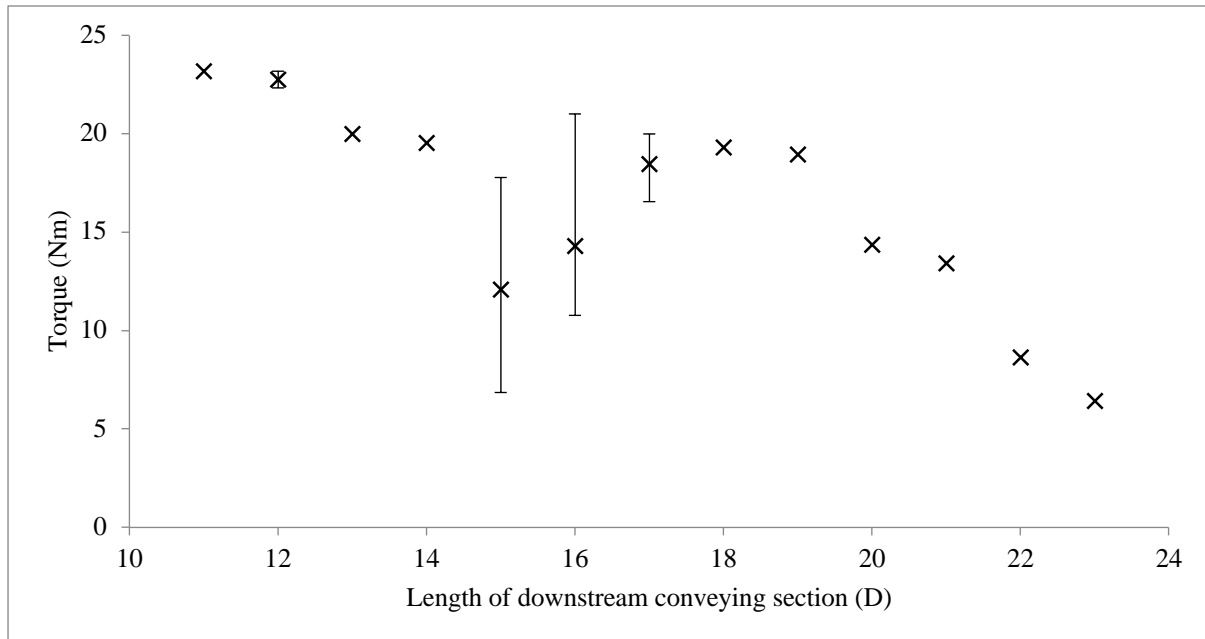


Figure 5.11 – Steady state torque values for a 90° 1D kneading block with increasing lengths of conveying section between liquid injection port and kneading block. The liquid injection port is located at 9D and these represent 1-13D lengths of conveying section before the kneading block. Obtained on the Haake TSG running at 2 kg/h material feed rate, 200 rpm screw speed and 0.2 L/S ratio. Note D refers to the screw diameter of 16 mm

Figure 5.11 shows the steady state granulation torque obtained when the kneading block was shifted incrementally downstream. The liquid injection port was fixed at approximately 9D from the base of the screws. There appears to be a general trend of lower steady state torque for longer lengths of conveying sections. These results are not conclusive as not all experimental conditions were repeated to give a full dataset. In addition where triplicate experiments were performed for 15, 16 and 17 D conveying sections a high degree of variability is observed in the results. However these results are presented as they show an interesting trend and would be worth expanding upon. A possible factor which may have influenced the high variability in the repeated experiments is the cleanliness of the barrel when the experiments were performed. A set of experiments was

performed when the barrel was clean and resulted in the lower torque values. An additional set was performed the next day after the barrel had been left dirty overnight, including the accumulated extrudate layer and high torque values were obtained. Drying and hardening of the extrudate layer overnight may have increased the frictional resistance on the screws and reduced the effective free volume of the granulator meaning more work was required to sustain granulation. This is only circumstantial evidence, but the impact of extrudate build up during granulation on process variability, particularly following manufacturing interruptions, or following batch to batch changeovers should be considered in industry.

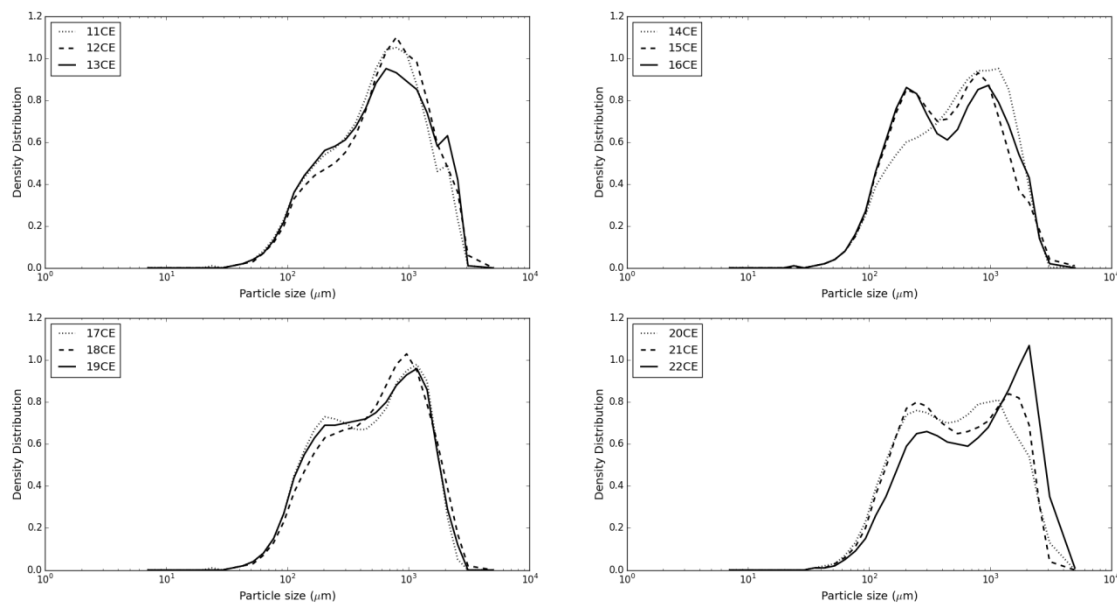


Figure 5.12 – Particle size distributions of granules made with increasing lengths of upstream conveying elements (CE). Manufactured on the Haake twin screw extruder equipped with a 90° 1D kneading block, running at 2 kg/h material feed rate, 200 rpm screw speed and 0.2 L/S. Each conveying element is 1D (16 mm) in length, the total screw length is 25D.

The resultant particle size distributions for granules made under the conditions in Figure 5.11 are shown in Figure 5.12. The distributions can be seen to be initially monomodal when the kneading block is positioned close to the liquid injection port (approximately 9D). As the kneading block is positioned further downstream there is a transition in size distribution, with the proportion of fines

increasing, eventually becoming distinctly bimodal when placed near the end of the screws. Coupled with the trend of lower torque with longer upstream conveying section in Figure 5.11 this would suggest that the degree of mixing at the end of the screws is lower, resulting in the under-granulation represented by the size distributions.

The screws configurations used in this series of experiments all consisted of exactly the same elements and only the position of the kneading block was changed. It may be expected that the kneading block would perform in the same way, however there is a process change that occurs with its position. The cause of this process change is likely an evolution in the material properties. When the kneading block is positioned close to the liquid inlet, material is wetted during nucleation and then is very quickly delivered to the mixing zone resulting in good dispersion and a homogenous product. When a long upstream conveying section is used there is a longer period for liquid to become isolated within nucleation granules before it arrives at the mixing zone. Dhenge et al [63] have demonstrated that conveying screws alone result in a mixture of large crumb like wetted nuclei and small dry fines. By maintaining this long conveying section leading into the mixing zone this heterogenous mixture becomes well established, and indeed may be subject to the segregation effect discussed in Chapter 3 3.2. It may be that material is then delivered to the mixing zone as a stream of dry fines which largely bypass the kneading block through the clearance and soft nuclei granules which are sheared, chopped and compressed into the final granules. It may be interesting to see if this effect is observed on granulators of narrower clearances, smaller than the primary particle size (200 μm clearance and approximately 100 μm particle size in this case). Alternatively this change in degree of mixing may be as a result of the fill profile which establishes around the mixing block. Being positioned close to the liquid inlet raising the local fill level at nucleation and providing improved nucleation liquid distribution as discussed in section 3 3.3. Visualisation of the differences in fill level could be achieved through PEPT analysis and would be worthy of future investigation. Finally it may be that the mixing effects of conveying elements on granules post the kneading block are greater than expected. With a long downstream conveying section carrying sticky

granules inducing a secondary mixing stage. While this work would need expanding upon to fully understand the mechanism the results would suggest that the granulation mixing zone should be positioned closely downstream of the liquid inlet to achieve optimum mixing.

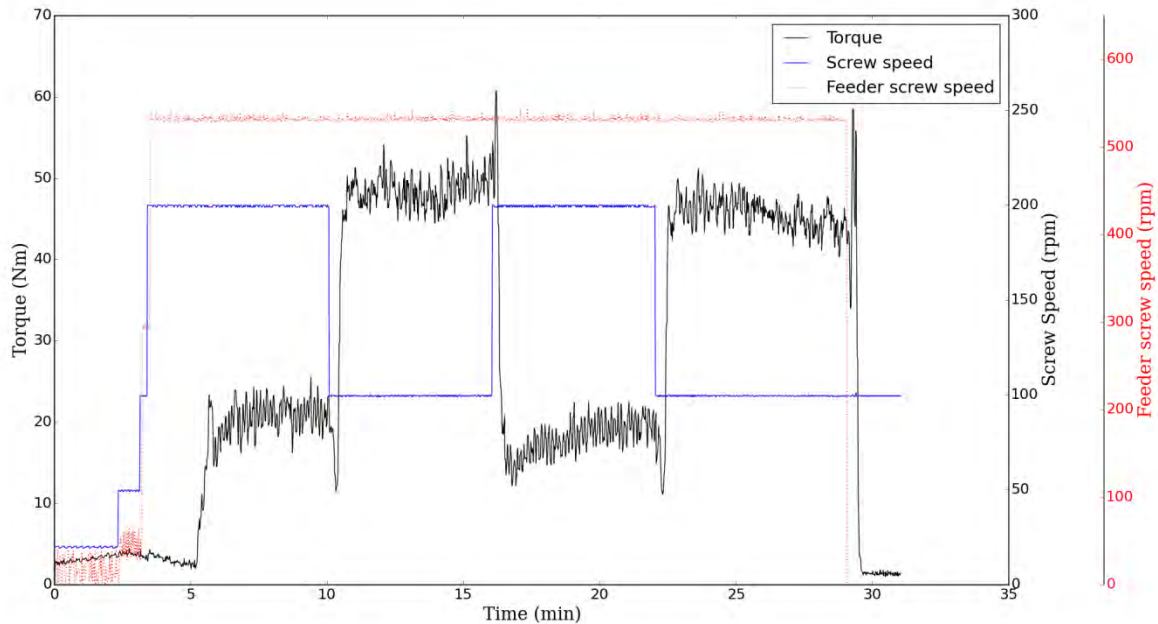


Figure 5.13 – Granulator torque, screw speed and feeder screw speed alternating between 200 rpm and 100 rpm screw speed to show granulation steady state torque at the different speeds. Material feed rate is constant at 2 kg/h, 0.2 L/S ratio and the screw configuration incorporated a 1D 90° kneading block (17x1D C// 4x0.25D K 90°// 7x1D C).

The series of experiments exploring the kneading block position all used screw configurations with the same elements but in different arrangements. It would be expected that the overall fill level would be the same for each configuration. The steady state fill level should be controlled by a combination of the material feed rate, screw speed and resistance to flow provided by the screw elements. This can then be measured by a constant torque signal, indicating the process steady state. However as the feed rate, screw speed and flow resistance were all theoretically constant in these experiments the differences in torque values in Figure 5.11 rather than being an effect of the material and process response are in fact an indication that the process is able to reach varied steady states. In order to test this hypothesis an experiment was performed to establish whether the

process returns to the same steady state torque level following the change and then return of process parameters. The results of this are shown in Figure 5.13. The granulator was run at a constant 2 kg/h material feed rate and 0.2 L/S ratio. Initially the granulator was allowed to reach steady state at 200 rpm, indicated the levelling of the torque output. Once at steady state at approximately 10 minutes the screw speed was decreased to 100 rpm and allowed to reach the new steady state at the now increased fill level. The granulator very quickly reached a level torque value, indicating the new steady state and was allowed to run for around 5 minutes. At 15 minutes the screw speed was increased to the original 200 rpm to see if the granulator returned to the original steady state torque value. After 5 minutes the screw speed was once again lowered to 100 rpm to see how the torque of the two 100 rpm periods compares. The torque values for the two 200 rpm periods are approximately equivalent with an average of 20.3 Nm and 18.4 Nm respectively. The two 100 rpm periods have approximately equivalent torque values with averages of 48.5 Nm and 45.6 Nm respectively. This implies that in both cases the process returned to the same steady state. Thus it is likely that the process will always operate at the same state for a given set of process conditions. The differences in torque values observed in Figure 5.11 are then caused by change in material properties induced by the position of the kneading block and the local fill level which establishes around it.

5.3.3.1 Sequential mixing zones

The section above explores how the position of the kneading block affects granulation. Given that mixing sections are typically fairly short compared to the overall length of the screws ($1D/25D$) this leaves many possible permutations in screw configuration. The previous section provides evidence to show that the position of the kneading block relative to the liquid injection port affects granulation mechanisms. A point to also consider is how the mixing mechanisms of multiple kneading blocks change depending on their arrangement downstream of each other. The majority of PEPT screw configurations used two or more mixing zones in order to increase the mixing data

density. However this also has the advantage of allowing the differences in flow through the upstream and downstream kneading block to be compared.

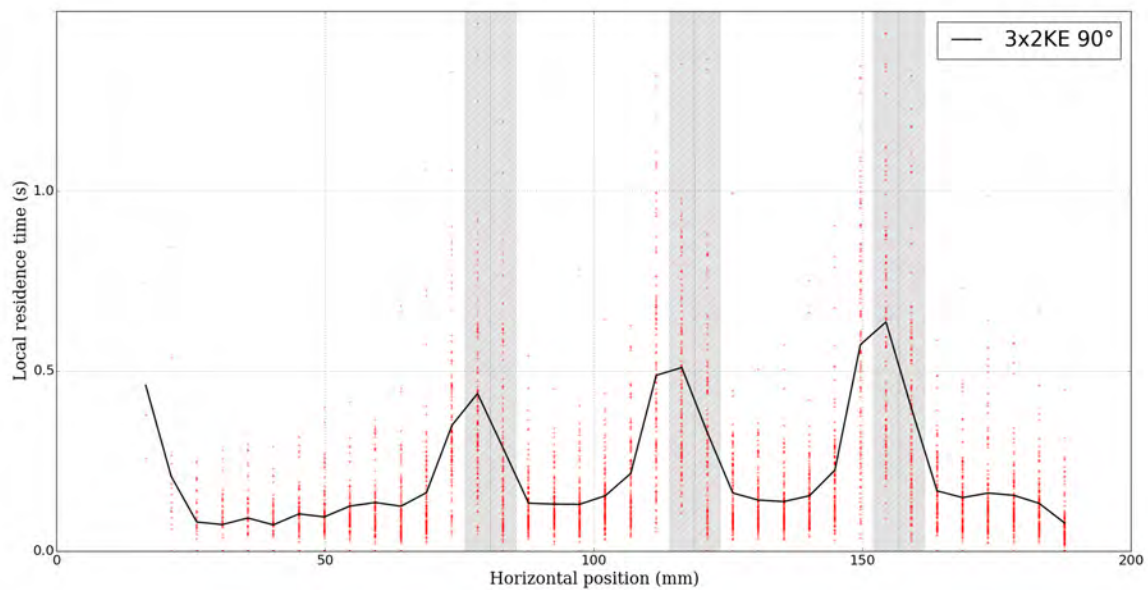


Figure 5.14 – Local residence times per 0.25D element along the axial length of the GEA twin screw granulator obtained through PEPT analysis. The screw configuration consisted of three kneading blocks each 0.5D in length, separated by 1.5D conveying sections (4x0.25D K 30°F// 2x1.5D C// 2x0.25D K 90°// 1x1.5D C// 2x0.25D K 90°// 1x1.5D C// 2x0.25D K 90°// 1x1.5D C). Red dots represent the individual residence times per pass of the tracer and the average overall residence time by the solid black line. Grey hatched areas represent the positions of the kneading blocks.

Figure 5.14 shows the local residence times along the axial length of the GEA granulator screws containing three identical 0.5D 90° kneading blocks. It can be seen from the height of the peaks across each mixing zone that the residence time across each kneading block increases the further downstream it is. The mean residence times across each kneading block from upstream to downstream are 0.72, 0.84 and 1.03 seconds respectively. This increase in residence time implies a rheological change in the material, becoming more viscous and sticky as it is squeezed and compressed. The implications of this rheological change are that it could be used to control the mixing mechanisms during granulation. For example a high intensity mixing zone could be included

closely downstream of the liquid injection port to ensure good liquid distribution. Subsequent mixing zones could be of less intensive design in order to achieve a bulk density required for tablet compression, or achieve required dissolution rates.

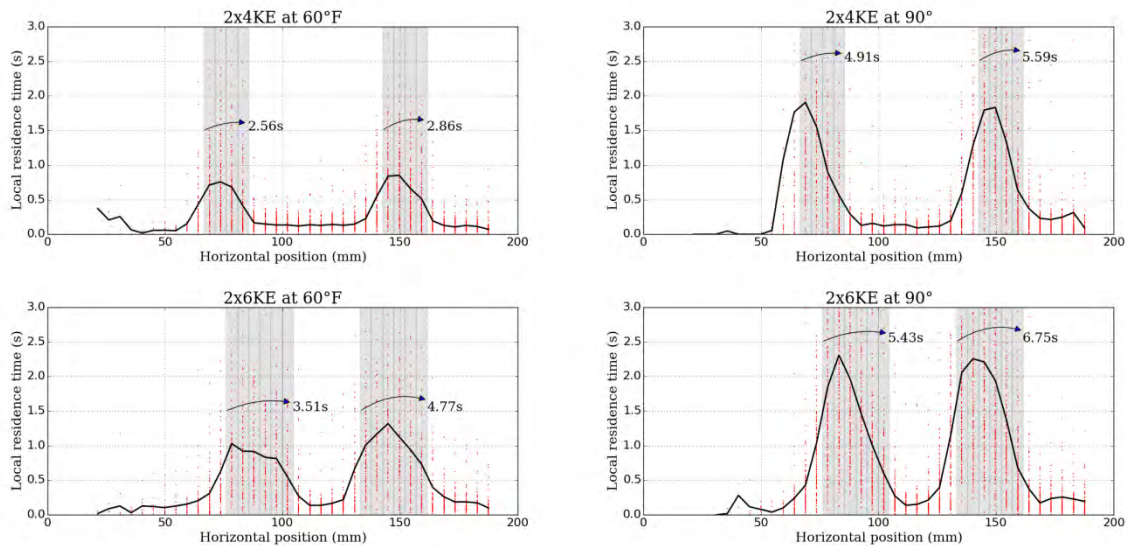


Figure 5.15 – Comparison of local residence times across sequential mixing zones for 60°F and 90° kneading blocks. Obtained through PEPT analysis of the GEA TSG at 2 kg/h, 0.2 L/S and 200 rpm. Black lines are the mean local residence time, representative of the local fill level, grey hatched areas show the position of the kneading blocks.

Figure 5.15 shows the local residence times across sequential mixing zones for 60°F and 90° kneading blocks. For each of these screw configurations the residence time across the secondary mixing zone is longer than the first. Again this implies a rheological change to the material, as it becomes more cohesive the longer it has been mixed. It is of interest to note that unlike the local residence times shown in Figure 5.14, there is not a significant increase in the peak local residence time between the primary and secondary mixing zones. Instead the increase in residence time across the mixing zone is due to the broadening of the distribution across the kneading block.

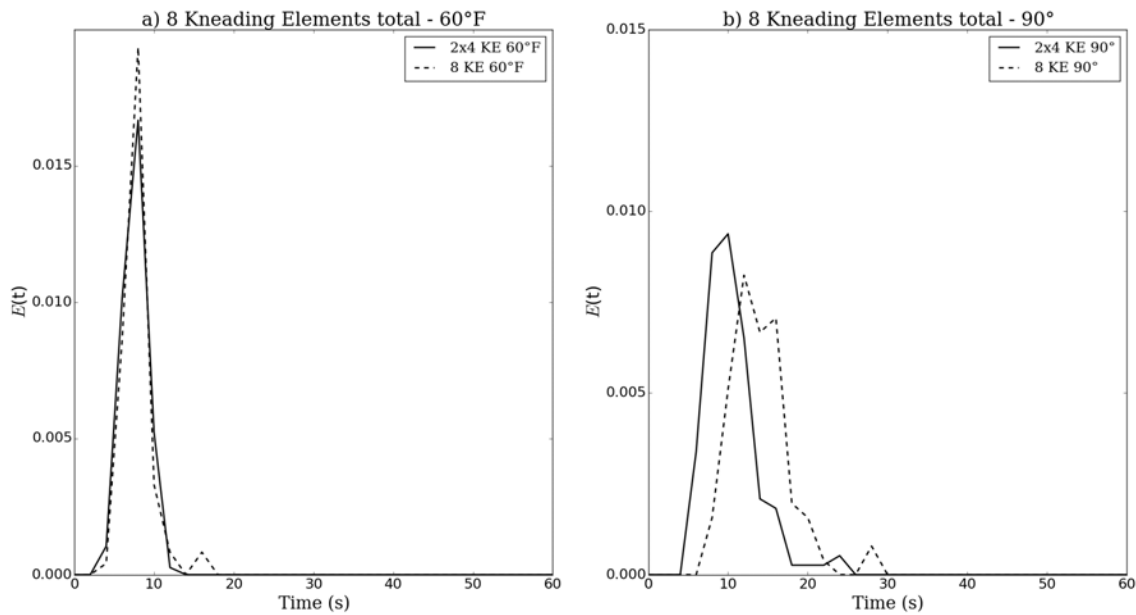


Figure 5.16 – Residence time distribution curves for screw configurations consisting of 8 kneading elements total comparing the distributions when kneading elements are arranged as a single kneading block to two separate 4KE kneading blocks at a) – 60°F offset angle and b) – 90° offset angle

Table 10 – Mean residence times of screw configurations consisting of 8 kneading elements total but with different kneading block arrangement

Kneading block arrangement	Mean Residence time (s)	
	60°F	90°
2x4	6.59	9.52
8	6.91	12.89

Figure 5.16 compares the residence time distributions of screw configurations consisting of 8 kneading elements arranged as a single kneading block to two separate kneading blocks. Interestingly at 60°F offset angle in Figure 5.16a the RTD curves are nearly identical, implying that the degree of axial mixing is very similar. This would suggest that under these process conditions the behaviour of each screw configuration is very similar and are likely to result in similar granules. This would also suggest that a fairly high number of kneading elements would be required in order to

result in axial dispersion with 60° elements. Unlike the 60° kneading blocks the two RTD curves for the 90° screw configurations are clearly different. When arranged as a single kneading block the mean residence time is longer and the curve is broader implying more mass holdup and a higher degree of axial dispersion. This is supported by the mean residence times of the different arrangements shown in Table 10. The mean residence times of the 60° configurations are very similar, while for 90° elements the mean residence time is almost a third longer for the single kneading block. This would suggest that to achieve robust mixing it is better to arrange elements as single long kneading blocks rather than as a number of short ones. However this may not be suitable for all formulations, particularly where over-densification may be an issue.

5.3.1.2 Kneading element width

The width of individual kneading elements is typically fixed and reliant on what equipment is available from the supplier, with 0.25D wide kneading elements being commonplace between manufacturers. It is not known why this width has been selected, having a relatively small element width means that kneading blocks can be kept fairly compact. This means that often long lengths of the screws consist of conveying elements. While this may be advantageous for hot melt extrusion processes, where long conveying sections can be employed to ensure adequate heating and generation of pressure, these are not required for granulation. It may be advantageous to develop twin screw granulators of shorter lengths in order to improve hygiene through ease of cleaning. While 0.25D kneading elements are the default width for both the Haake and GEA twin screw granulators, the modular screws allow elements to be placed in parallel at the same angle, effectively creating a single element with twice the width. There is no known processing advantage to using 0.25D wide elements so the effect of changing the width of kneading elements was explored.



Figure 5.17 – Comparison of two 1.5D 30°F kneading blocks on the Haake TSG. a) – 6x 0.25D elements and b) – 3x 0.5D elements (arranged as pairs of 0.25D elements)

Figure 5.17 shows an example of how kneading elements can be arranged to create wider elements. Both kneading blocks pictured are 1.5D in length and consist of 6 0.25D kneading elements. In Figure 5.17a these are arranged conventionally to form a 30°F kneading block. In Figure 5.17b the kneading elements are arranged in parallel pairs to form a 30°F kneading block consisting of 3x 0.5D kneading elements. In order to determine if the width of kneading elements impacts the process granules were initially made using the Haake TSG with the screw configurations shown in Figure 5.17. A point to consider is the differences in conveying capacity between the wide and narrow elements. One turn of the screws gives effectively twice the rotation of the kneading block in Figure 5.17a than b, thus the conveying capacity would be expected to be greater.

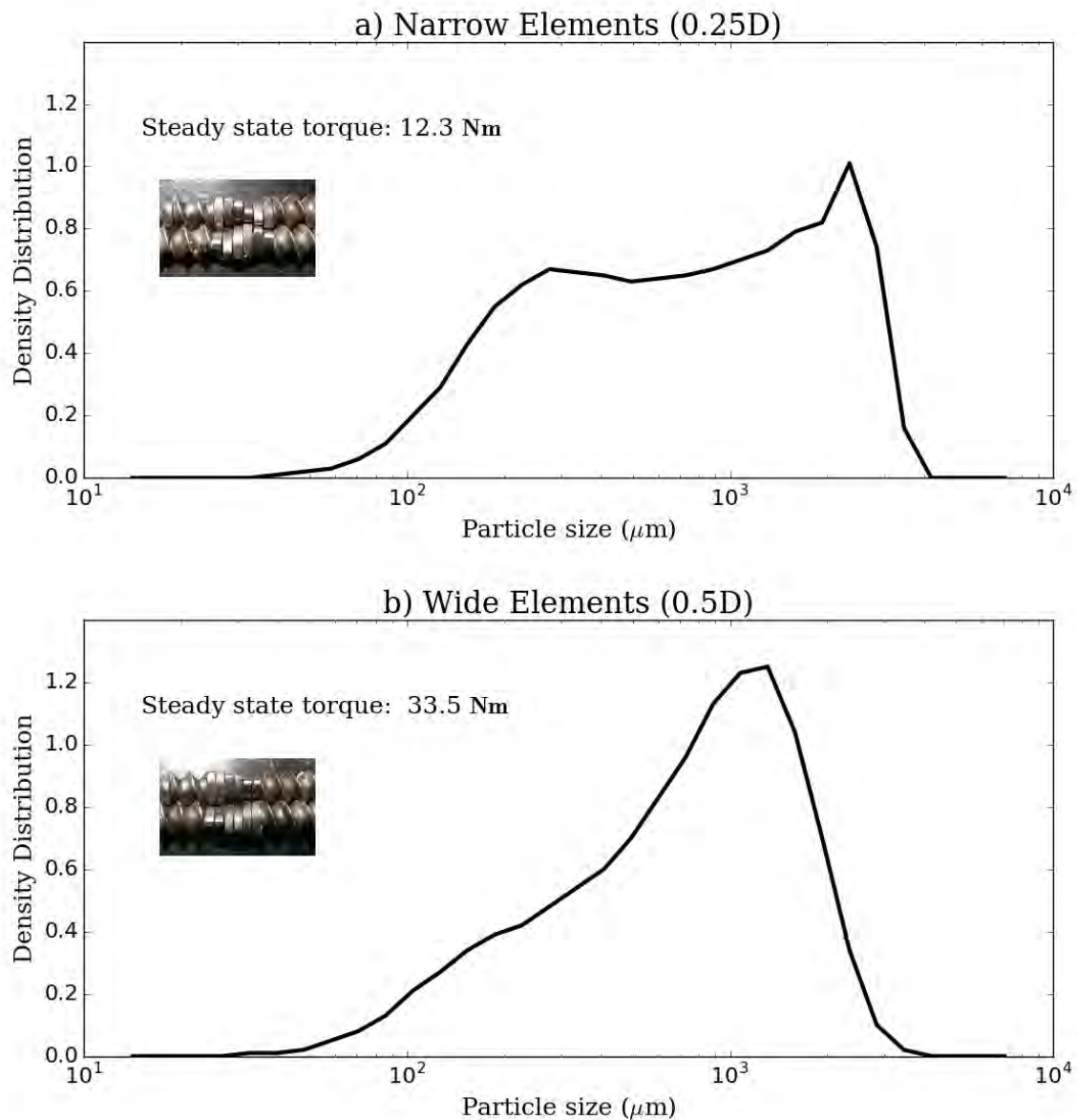


Figure 5.18 – Resultant particle size distributions of granules made using the Haake TSG at 2 kg/h material feed rate, 0.2 L/S and 200 rpm screw speed. Mixing zones consisted of a single 1.5D kneading block arranged at a 30° angle with a) six 0.25D kneading elements (1x0.5D C// 19x1D C// 6x0.25D K 30°F// 4x1D C) and b) three 0.5D kneading elements (1x0.5D C// 19x1D C// 3x0.5D K 30°F// 4x1D C).

The difference in size distribution for granules made using the kneading block arrangements in Figure 5.17 are shown in Figure 5.18. Both experiments were performed under the same process conditions and the screw configurations consisted of the same elements and same length of

kneading block, with the only difference being the width of the individual kneading elements. 30°F kneading blocks are non-intensive mixing zones, resulting in low torque values and broad bimodal granule size distributions even when a high number of elements are used as shown in Figure 5.1 and Figure 5.7. This is again shown in the size distribution in Figure 5.18a where granules have a broad range in size. Figure 5.18b shows the granule size distribution when the width of kneading elements is doubled. Here despite the kneading block being arranged at 30°F the granule size distribution is monomodal and comparatively narrow. The steady state torque with this configuration is much higher, 33.5 Nm with 0.5D kneading elements compared to 12.3 Nm with 0.25D elements. This coupled with the narrow size distribution implies that the mixing intensity is far greater with the wider elements.

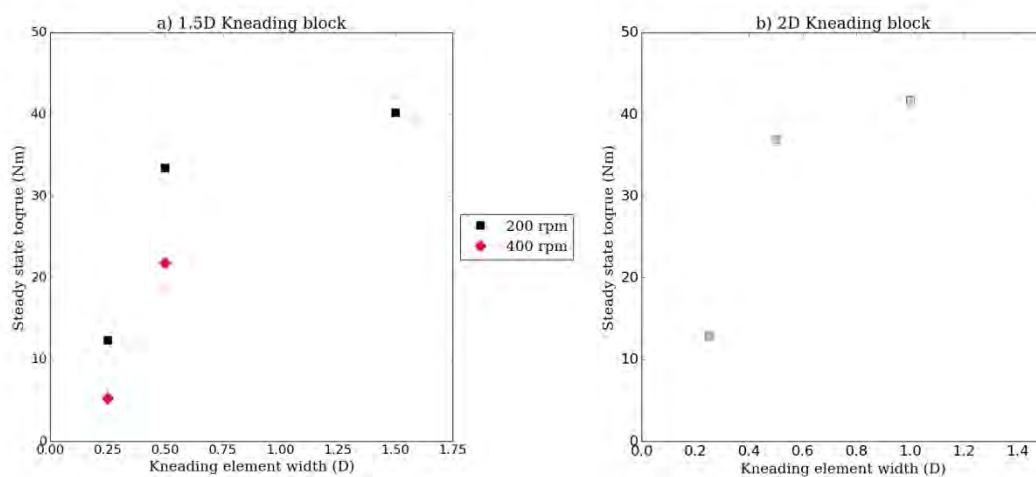


Figure 5.19 – Steady state torque values generated on the Haake TSG using different widths of kneading elements a) with a 1.5D kneading block and b) with a 2D kneading block

Figure 5.19 shows the steady state torque values during granulation with the Haake TSG using various widths of kneading elements. A 1.5D kneading block was used with element thicknesses of 0.25, 0.5 and 1.5D and a 2D kneading block with element thicknesses of 0.25, 0.5 and 1D. In both cases increasing the width of the kneading elements from the standard 0.25D to 0.5D led to a considerable increase in the value of steady state torque. However further increase in width led to much smaller increases in torque. This may imply a plateau will be reached where the increased

resistance to flow from these very wide elements means that the entire kneading block is operating fully filled.

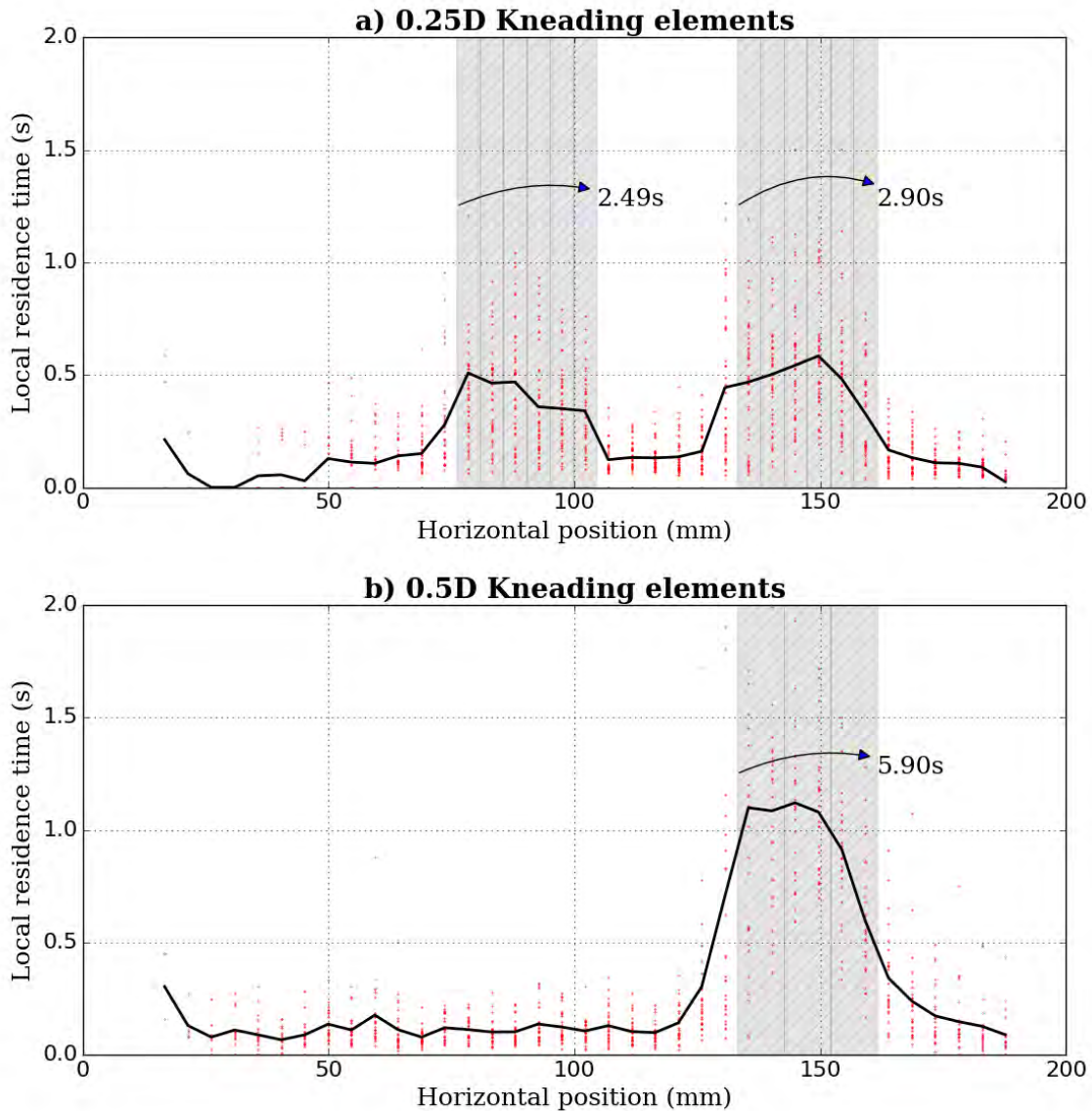


Figure 5.20 – Local residence times and representative fill level across screw configurations consisting of 30°F 1.5D kneading blocks obtained through PEPT analysis of the GEA TSG at 1.8 kg/h material feed rate, 0.2 L/S and 200 rpm. a) using standard 0.25D kneading elements b) using 0.5D kneading elements

In order to assess how the change in width of kneading elements affects the flow of materials during granulation PEPT was performed on the GEA TSG with screw configurations consisting of 0.25D and 0.5D kneading elements. The wide elements resulted in an aggressive screw configuration which the

granulator motor was not adequately sized for, this led to frequent blockages at the standard 2 kg/h material feed rate. To prevent further blockages the material feed rate was reduced from 2 kg/h to 1.8 kg/h for this set of experiments. As wide elements result in such aggressive screw configurations they may not be suitable for use with all materials, such as those which are highly compressible. The local axial residence times and representative fill levels obtained through PEPT are shown in Figure 5.20. The wide 0.5D KE kneading block can be seen to be highly filled across the first two kneading elements and steeply profiled across the last. This would imply the wide kneading elements produce a high resistance to flow and the transfer of material between elements is restricted, despite the conveying nature of the 30° offset angle. The residence time across the wide element kneading block is considerably longer, more than twice that of the narrow elements. Interestingly however longer residence times are generated using equivalent length kneading blocks with 90° offset angle lengths as can be seen in Figure 5.15, averaging 6.09 seconds for 90° 0.25D elements compared to 5.9 seconds for 30° 0.5D kneading elements. The difference in material feed rate may contribute to this longer residence time. The peak local residence time across the wide kneading elements is only slightly longer than 1 second, this is again lower than the peak local residence times observed in Figure 5.15 with 90° 0.25D kneading elements, where times greater than 2 seconds are observed. Assuming comparable bulk density this would imply that the wide element kneading block is only operating partially filled, at about 50% of maximum fill level. The observed results in torque and size distribution would suggest that the robust, intensive mixing can be achieved across the same length of kneading block by increasing the width. This high intensity mixing may not be suitable for all materials or granulators due to the strain imposed on equipment but it does provide another avenue for adapting screw configuration to meet required process demands.

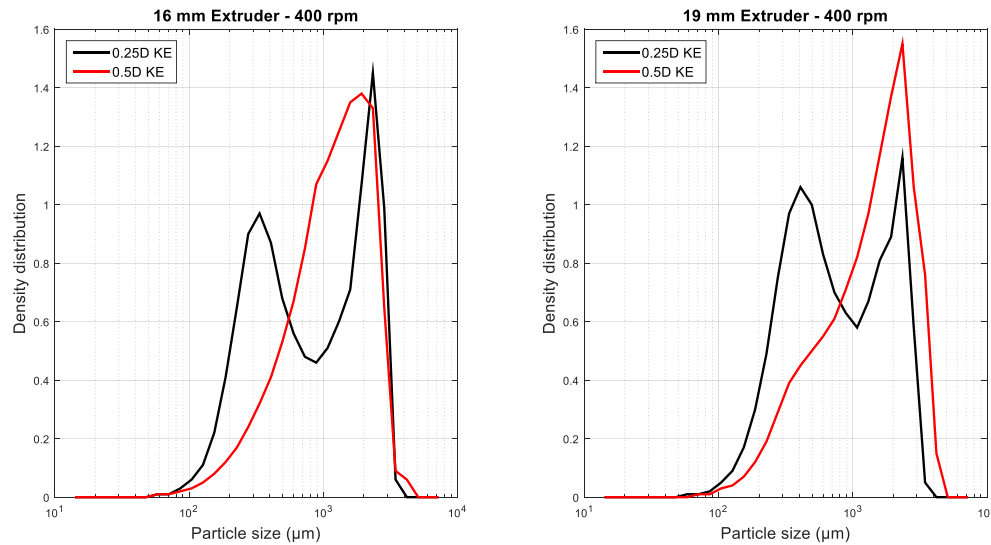


Figure 5.21 – Comparative granule size distributions made with narrow 0.25D kneading elements and wide 0.5D elements on the 16 mm Haake granulator and 19 mm GEA granulator. Granulation was performed at 2 kg/h material feed rate, 0.2 L/S and 400 rpm screw speed.

Figure 5.21 shows the particle size distributions for granules made using both the 16 mm Haake and 19 mm GEA twin screw granulators with 0.25D and 0.5D kneading elements. Both granulators see a shift in size distribution from bimodal to monomodal with wide elements. This shows that the shift in distribution takes place across different production scales and is not limited to one granulator. The size distributions for both granulators are very similar, the D50 values for the narrow elements are 785 and 693 μm for the Haake and GEA granulator respectively and 1224 and 1480 μm for the wide elements. As these values are so similar it would imply that at these fill levels the granulator scale has small impact on the properties of granules. Instead it is the material properties, liquid to solid ratio and screw configuration which determine granule size. However it should be noted that the granulators were operated at relatively high speed in order to reduce load on the motors and thus the overall fill level is likely to be low in both cases. When the granulators are operating at higher throughputs the scale is likely to have larger impact.

Table 11 – Mercury porosimetry results for granules made using narrow and wide kneading elements

	16 mm		19 mm	
Element width	0.25D	0.5D	0.25D	0.5D
Bulk density (g/ml)	0.6841	0.8485	0.6495	0.9339
Porosity (%)	58.03%	40.61%	59.68%	36.29%

The porosity of granules made with wide and narrow kneading elements was determined through mercury intrusion porosimetry (Autopore IV Mercury Porosimeter, Micromeritics) and the results are shown in Table 11. Both at the 16 and 19 mm scale there is a considerable increase in the bulk density of granules when using wide elements over narrow. The bulk densities with narrow elements are higher than those observed in Figure 5.6, but this may be due to the much higher accuracy of measurement through the porosity technique. Granules made using wide elements are very dense, have low porosity and therefore may not be suitable for compression. Interestingly denser granules are made with wide elements at the 19 mm scale than at 16 mm. This may be because the overall length of these kneading blocks is longer and thus granules experience a longer period of compression as they flow through.

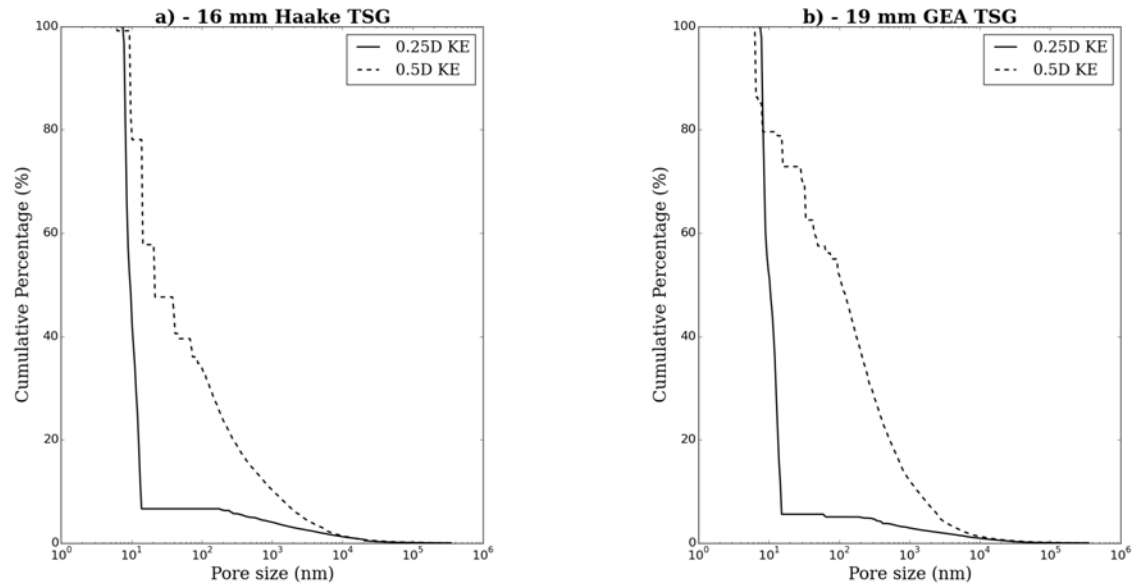


Figure 5.22 – Cumulative pore size distributions obtained through mercury intrusion porosimetry comparing granules made using a 1.5D kneading block with wide to narrow kneading elements a) – at 16 mm scale and b) – at 19 mm scale

Figure 5.22 shows the cumulative pore size distributions of granules made using narrow and wide kneading elements, obtained through mercury intrusion porosimetry. It is of interest to note that narrow kneading elements result in evenly sized pores at nanometres scale. In contrast wide kneading elements show a much wider distribution in pore size, including macrovoids at micrometer scale. This difference in pore size distribution is observed at both 16 mm scale as shown in Figure 5.22a and 19 mm scale in Figure 5.22b. This would suggest that despite wide element granules being more dense the average void size is larger. This may be due to the intensive mixing caused by these elements compressing the powder so that the porosity of the primary particles is lost and only intragranular space remains. In contrast the comparatively low densification seen with narrow kneading elements means the primary powder particles maintain the majority of their base porosity, seen by the sharp rise at 10 nm. It would be of interest to compare how well these granules can be compressed into tablets, as the high densification caused by wide kneading elements may render granules unsuitable for tableting.

The impact of changing the kneading element width is an interesting observation and it raises questions around the appropriateness of the design of kneading elements for granulation. The increase in measured torque and the lower porosity of granules with wide elements would suggest material undergoes much higher compression. It is not known whether the material would undergo less compaction with narrower elements but it would be of interest to investigate. The increased compression is likely as a cause of the wider element face, as these intermesh material is squeezed between them. The larger area of the wide element face means material must travel further to escape the intermeshing region as it is squeezed and extruded and so is compressed more. In theory there is no preferential axial force generated by the faces of two individual elements coming together and forward flow is maintained by the pressure like push of material conveyed from upstream. The angle kneading elements are arranged however does impact the axial flow as forwarding elements have a bigger gap downstream than upstream. As two elements intermesh material can be squeezed out into this gap downstream where it would be blocked by the position of the upstream element. Comparing kneading blocks of wide and narrow elements shown in Figure 5.17 it can be seen that the kneading block goes through effectively twice the rotation with narrow elements compared to those twice as wide. As less of a conveying motion is passed to material this may be a contributing factor to material being held up in the kneading block. Examining the mean residence times across the blocks shown in Figure 5.20 shows times of 2.49 and 2.90 seconds for narrow elements and 5.90 seconds for wide. With the doubling in element width the residence time of the block is slightly more than doubled. It would be expected for the residence time and compression to decrease further as element width decreases and conveying capacity increases. Conveying elements are effectively made of an infinite number of thin slices of kneading element arranged at constant angle. However it would be of interest to explore how thinner elements could be applied to granulation. Thin blocks of 90° elements may generate more shear forces. Single lobed thin elements without an intermeshing region could result in high shear zones with low compaction, it would be valuable to explore how this could be applied to granulation.

5.4 Conclusions

This chapter investigated screw configuration and its impact on granulation mechanisms and material flow. 30°F and 60°F kneading block offset angles lead to relatively low levels of mixing compared to 90°F, where 90°F offset kneading elements appear to provide the most robust mixing. Steady state torque and mean residence time both increase linearly with the length of kneading block. This implies that process conditions can be easily predicted during process design when developing a suitable screw configuration. The average time per element increases logarithmically for 90° elements, implying a point of maximum fill where the resistance to flow results in a limited maximum flow rate. Granule size distributions shift from bimodal to monomodal with increasing lengths of 90° kneading blocks. Showing screw configuration is an effective way of achieving a homogeneous product. There is some improvement with forwarding screw configurations but granule size distributions remain broad even with long lengths of kneading block. The residence time distributions of 60°F screw configurations show little axial dispersion even with relatively long lengths of kneading block. In contrast 90° kneading blocks display a much greater degree of axial dispersion, showing the much higher degree of mixing.

The position of the kneading block on the screw appears to impact granulation mechanisms. Kneading blocks positioned far downstream of the liquid inlet port have low steady state torque values and broad, bimodal granule size distributions. However when positioned closely downstream of the kneading block, despite having the exact same elements, much higher steady state torque values are reached and it results in homogenous granules with monomodal size distribution. This may be as a result of promoting mixing at nucleation and liquid distribution which induces secondary mixing in the downstream conveying zone. Alternatively the poor mixing of downstream kneading blocks may be a result of the segregation of wet and dry material in the upstream conveying section. Because the same steady state torque levels are reached when process parameters are changed and then returned to initial point it suggests the granulator always operates at the same steady state for

a given set of process conditions. Thus the changes observed with arrangement of the screw are a direct result of the position of the kneading block.

Sequential mixing zones see an increase in mean residence time across each downstream kneading block. This shows the rheological change in material properties as it becomes stickier the more it is mixed. This can be used as an aspect of screw design, by matching mixing intensity of the kneading block to the evolving material properties along the axial length of the screw. The performance of screw configurations with two separate versus one single kneading block, but same total number of elements was examined. 60°F kneading blocks show almost identical RTDs and levels of axial dispersion, implying very similar granulation conditions for the different configurations. In contrast with a single kneading block 90° elements show a higher degree of axial dispersion and more robust mixing compared to two separate kneading blocks. However over-densification may be an issue with such lengths of kneading block and certain formulations.

The width of individual kneading elements shows high impact on granulation. By increasing the width of individual kneading elements high degrees of mixing can be achieved with the same length of kneading block. Monomodal granule size distributions can be achieved with wide 30°F kneading elements which would otherwise result in heterogeneous product. However these are aggressive configurations which densify material to a large degree, so their use may be restricted to suitable formulations and granulators. Interestingly despite the aggressive nature PEPT results show that these configurations do not operate fully filled.

The modular nature of twin screw granulator screws offers numerous permutations for screw configuration. By systematically examining the changes in process and granule properties this piece of work demonstrates the correlations with screw configuration and provides the tools for establishing a robust screw design.

***Chapter 6* – Quantifying
Distribution**

6.1 Quantifying Distribution through X-Ray Micro-Tomography

The previous section discussed the degree and quality of mixing correlated to screw configuration. Mixing is inferred through measurements such as mixing energy in the form of process torque or the shape of the residence time distribution. These techniques are very useful but do not necessarily describe the final distribution of material within product. Understanding the distribution in final product is useful in that it can be used to infer back to the mixing which occurred in the system. In a real world example drug content in pharmaceutical tablets is a crucial factor which must be maintained within a specified range for safety and efficacy. The ability to understand how the mixing in a process results in distribution in final product is valuable in understanding the mechanisms taking place. Quantifying distribution such as the example of drug content in pharma can be destructive, where the content is chemically assayed. In granulation where shape and structure of granules and resultant tablets is very important the ability to measure distribution and relate it to the granule structure would be valuable. This section explores some initial work into developing a technique to achieve this.

Dispersion was measured in Chapter 3.2.6 by looking at the distribution of a dye tracer across the granule size range. This is a fairly coarse technique as the detection accuracy is limited by the concentration of tracer which can be used and it only examines differences in distribution between size classes. To improve the resolution in measurement the use of X-ray micro-tomography (XRCT) (Skyscan 1172, Bruker) with a suitable tracer was explored. XRCT is a non-destructive imaging technique which provides 3 dimensional information of an object. The benefit of XRCT is that information on the internal structure of materials can be obtained at very high resolutions (2 μm per pixel). XRCT works by measuring the attenuation of X-rays as they pass through the sample of interest. A fixed X-ray source is used and the sample is positioned between the X-ray source and a CCD camera. The strength of the X-rays reaching the camera is measured. The sample is rotated

through 180° and X-ray images are taken at intervals, this builds a series of slices through the sample. These images are then reconstructed computationally in order to build a 3 dimensional model of the sample.

XRCT relies on the difference in densities of materials in order to differentiate them within a sample. Because the individual components of the formulation, lactose, MCC and HPC all have very similar densities XRCT is unable to resolve them from each other. A high density tracer can be introduced into the granulation process to act as an effective contrast agent for XRCT images. By scanning the resultant dosed granules the dispersion of the tracer can be measured within individual granules as well as across the granule population.

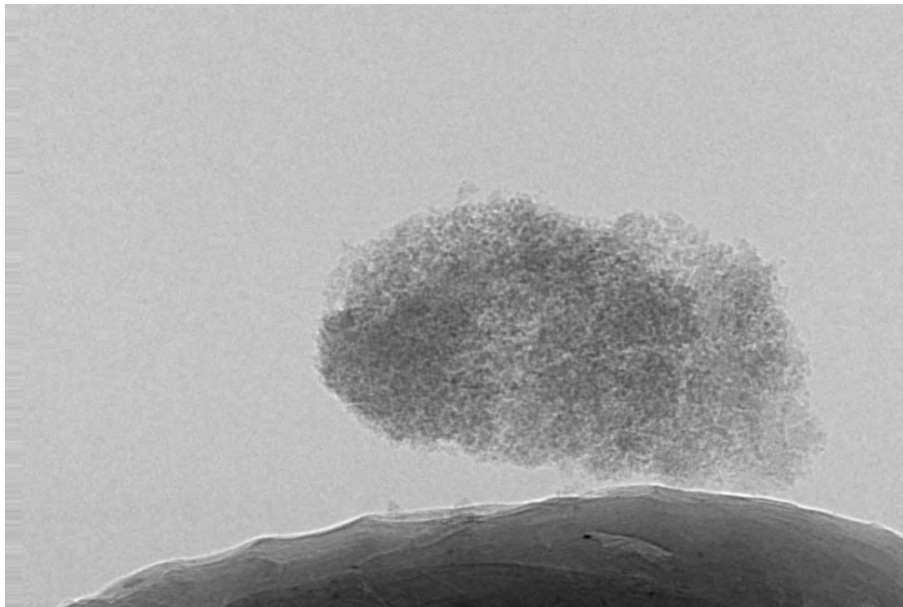


Figure 6.1 – Raw X-ray image of a 1 mm granule

Figure 6.1 shows an example of the X-ray images obtained through XRCT. This image is of a 1 mm granule scanned at a 4 μm per pixel resolution. The granule can be seen to be fairly porous as voids in the internal structure can be seen from the lighter areas of the image. While the image provides structural information about the granule the differences in its material composition cannot be seen.

44 μm Iron particles with density of 7.8 kg/m^3 were selected for use as an XRCT tracer. As the density of iron is far greater than that of the formulation it can be easily differentiated from bulk granule material. Granulation experiments were performed using the Haake TSG running at 2 kg/h material feed rate, 0.2 L/S and 200 rpm screw speed, with screw configuration [11x1D C// 4x0.25D K 90° // 6x1D C// 4x0.25D K 90°// 6x1D C]. The granulator was allowed to reach steady state and a 1 g pulse of iron tracer particles were added to the granulator powder inlet. Granules were collected at the barrel outlet until no more iron was visible in the material. The granules were then dried at 100°C for 2 hours.

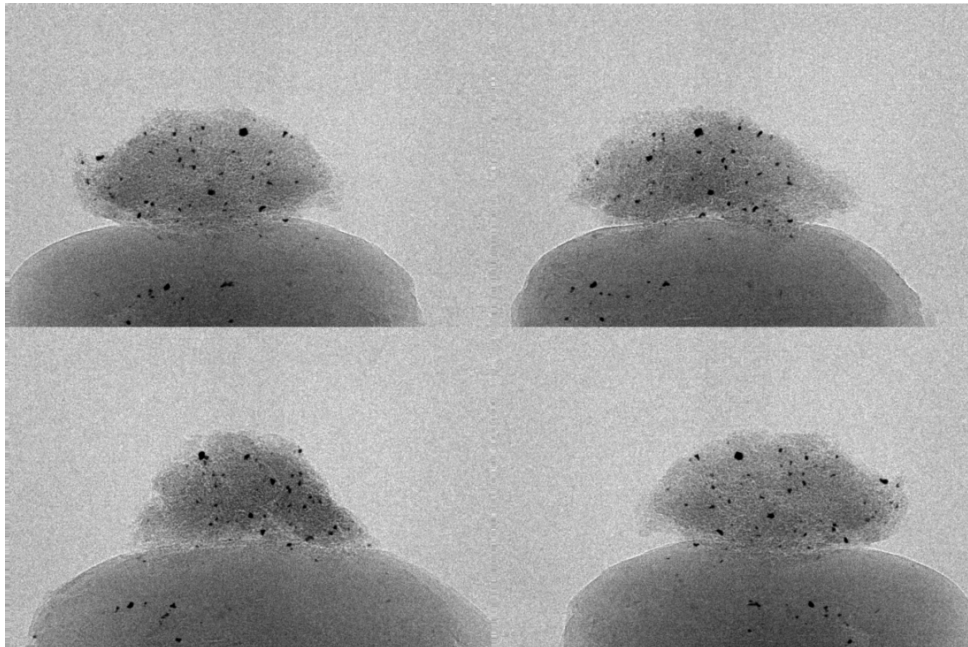


Figure 6.2 – Granule containing iron tracer particles showing 4 stages of rotation. Iron particles are the dark black areas in the image

Figure 6.2 shows one of the granules formed following the introduction of the iron tracer pulse to the granulation process. Iron particles can be easily differentiated from the bulk granule phase due to their much darker colour in the image. The iron particles can be seen to be distributed relatively evenly throughout the granule structure.

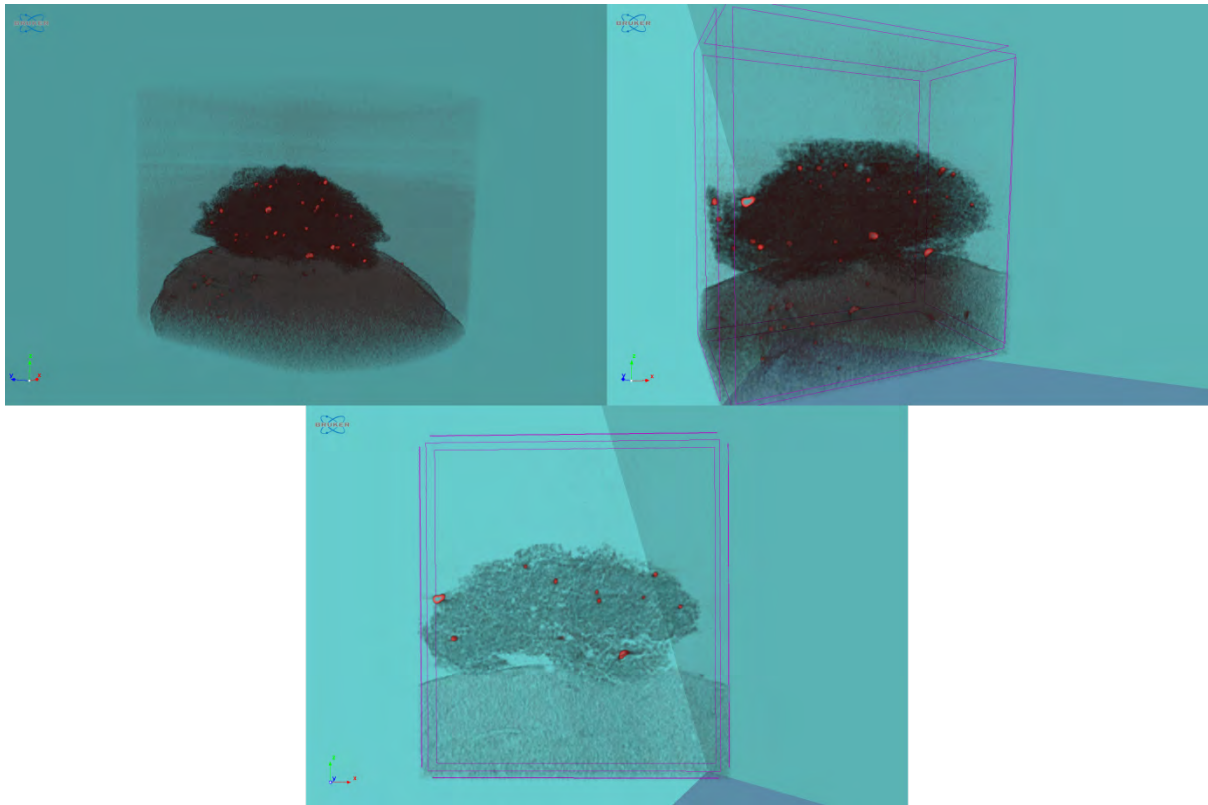


Figure 6.3 – 3D volume reconstructed from the X-ray images of an iron tracer dosed granule, the iron particles have been coloured red for identification

The reconstructed 3D volume of the iron dosed granule is shown in Figure 6.3. The iron particles have been coloured red to aid visualisation and can be seen distributed throughout the granule bulk phase. These images provide interesting qualitative information about the granule shape and tracer distribution but more work would be required to develop quantitative understanding. The advantage of XRCT is that it allows imaging of the internal structure of a sample. These images can then be reconstructed as a volume and freely manipulated. This allows the generation of views such as the bottom image of Figure 6.3, showing a “2D” slice through the granule. Indeed the 3D volume itself is created from a stack of vertical slice images similar to this. Images such as these lend themselves well to automated image processing, where there is good sharp contrast between the tracer particles and remaining material. Images could be processed sequentially as successive slices. By overlaying a grid on the image the concentration, distribution and position of the tracer particles relative to the bulk granule phase can be measured. A quantitative measure of distribution within

the granule may then be determined from these parameters, which provides information on how well mixed a system is to achieve this. Because XRCT equipment is adaptive in scale, groups or clusters of granules could be measured this way as well as individual particles. This would allow quantification of distribution on both an intra-granule and inter-granule level.

The iron particles used as tracers are very effective contrast agents for XRCT and have good potential for use in measuring the solids dispersion that occurs during granulation. There are however some issues associated with the use of these iron particles as tracers. The iron is vastly more dense than the other granular materials and its attenuation of X-ray beams is much greater. In order to compensate for this and capture images comparatively powerful X-ray beams must be used than would be for imaging of normal granules. There is little attenuation of these powerful X-rays by the bulk granule material and so little information on its physical properties may be gathered. Essentially the volume of the material may be visualised but not at a sensitivity to show differences in density. There are also problems associated with using these particles as tracers within the granulation process. In order to obtain these XRCT images the iron tracer particles were delivered in a small pulse through the barrel powder inlet. To measure the continuous steady state mixing properties of the granulator the tracer must be fed continuously. This would require the consistent feeding of very low volumes of solid particles. This is very challenging to achieve with existing technologies, vibratory feeders are difficult to control to accurate feed rates and other solids feeding technologies have a tendency to pulse at low feed rates. Finally the argument may be made of whether the mixing of iron particles is representative of mixing within the granulation process. Because the iron particles are much more dense, non-plastic and have completely different hygroscopic properties to the excipients it would not be expected for their flow behaviour to be the same.

Given these issues with using solid iron particles as tracers the use of Potassium Iodide (KI) was explored as an alternative. Potassium Iodide (Sigma Aldrich, UK) is a water soluble crystalline solid regularly used as a contrast agent for staining biological samples for use with XRCT. KI is highly

soluble in water forming a non-viscous solution. The granulation liquid was replaced with an aqueous KI solution as a method of tracer delivery. This has benefits over the iron particles previously used as the liquid could be delivered at consistent, reliable flow rates. The physical properties of the KI solution leave it very similar to water and are thus expected to have low impact on the granulation process. Granulation experiments were repeated on the Haake TSG at 2 kg/h material feed rate, 0.2 L/S and 200 rpm screw speed.

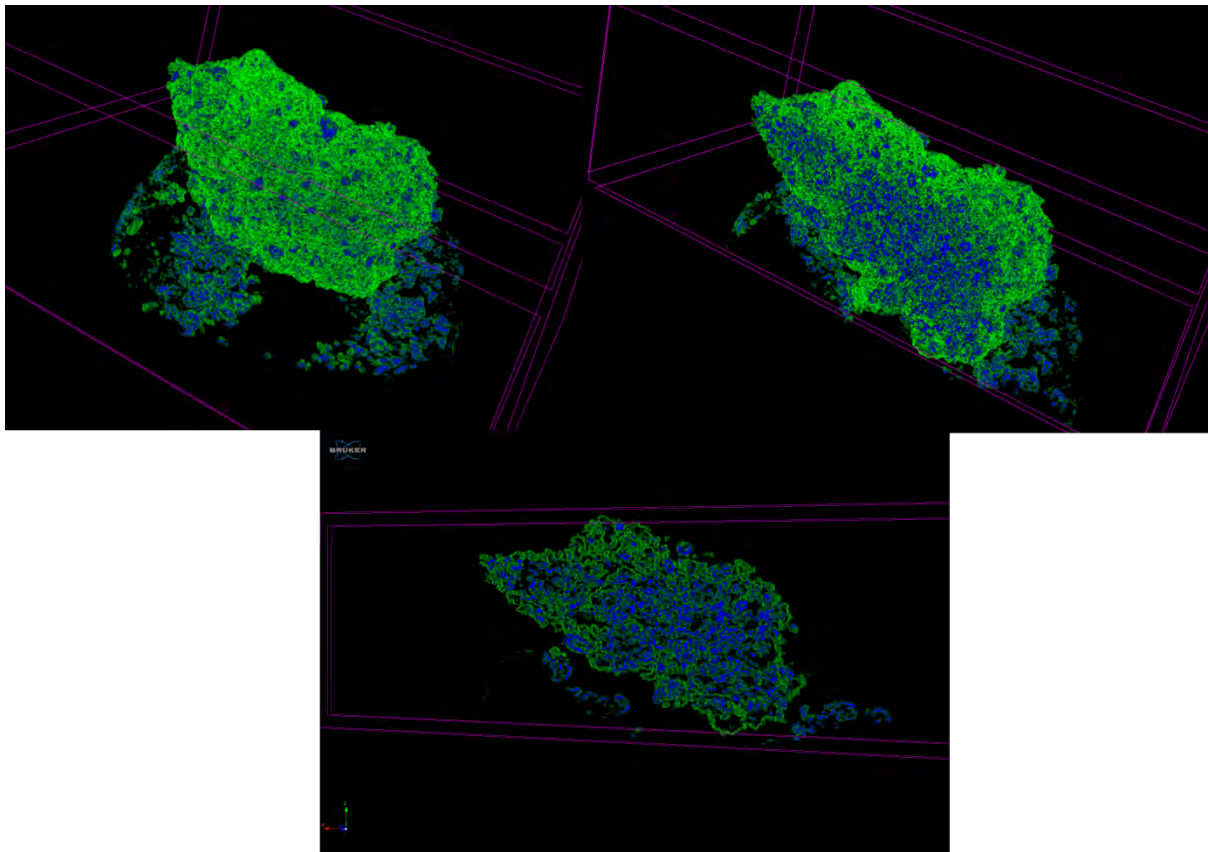


Figure 6.4 – Reconstructed 3D volume of a granule made using Potassium Iodide labelled water as tracer solution, areas of low attenuation are coloured in green, areas of high attenuation are coloured blue. Clockwise from top left, the entire reconstructed volume, half the volume sliced through the centre of the granule, and a 2D slice through the centre of the granule

The reconstructed XRCT images of the granules made using KI tracer are shown in Figure 6.4. Areas of high X-ray attenuation which represent the location of the KI tracer have been coloured blue. Areas of low attenuation which have little to no KI tracer have been coloured green. These images

show the KI tracer to be primarily in the centre of the granule. What these images effectively show is the distribution of liquid during the formation of the granule structure, with the KI remaining in the location of the water as it is evaporated off. These images then show the granule to be a wetted core with an outer layer of dry material. Looking at the internal structure of the granule it can be seen to consist of blue (wetted) particles linked with green (dry) material. This supports the proposed formation mechanisms of wet granulation. Coalescence of granules can be seen in the bridging between the internal smaller particles. Consolidation is shown by the layering of dry fines around the outside of the granule structure. These images provide strong evidence of the distribution of water in wet granulation and its role in determining granule structure. Application of this method may provide a powerful tool in building deeper understanding of the mechanisms of wet granulation as high resolution non-destructive images of the internal liquid distribution can be obtained. Similar image processing techniques proposed for analysing the iron tracer images could again be used here but would require some development work with the tracer concentration and X-ray energy. Currently the distribution of liquid has been inferred from regions of greater attenuation within the granule structure, however assumptions have been made that KI from water is directly responsible for this. It is possible that KI has been distributed evenly throughout the granule and the differences in attenuation are simply a result of more compact areas, however this is unlikely when looking at the contrast of un-dosed granules. There is however an assumption made that the labelled blue areas are indicative of KI from water. To make any quantitative assessment of water a calibration method would need to be developed based on the attenuation of various dilutions of KI solutions which have been allowed to dry. The sensitivity of XRCT may not allow for differentiation of these however.

The images obtained through XRCT presented here are only of qualitative value and represent the result of a limited investigation exercise. However the compelling results would highlight the potential of using XRCT for in depth characterisation of wet granulation processes.

***Chapter 7* – Conclusions and
Future Work**

Twin Screw Granulation continues to be developed in order to meet a need in the pharmaceutical industry. Granulation remains a fundamentally required process in order to produce certain drug formulations. Where a formulation cannot be developed to meet product quality criteria, granulation is a process which can modify physical properties to meet these.

There is a real movement toward the development of leaner, greener and more efficient processes in pharma. The continued investment, research and adoption of continuous technologies such as Twin Screw Granulation in this traditionally slow to evolve industry being a prime example.

Twin screw granulators are available across multiple scales, from small research units, to pilot plant units and full scale industrial equipment. Indeed particularly in the last instance these units are being marketed specifically as granulators and not extruders capable of granulation from which the technology evolved. The question then remains, if the technology exists at industrial scale and there is a desire to implement it, what is preventing widespread adoption. Ultimately it would suggest that the status of the technology is not sufficiently advanced to be directly implementable. An existing manufacturing process cannot simply have a batch granulation operation “swapped out” for a continuous process. Significant development work would have to be undertaken in order to determine the process parameters to produce comparable product. Crucially, while significant work has been undertaken, much summarised in Chapter 2 of this thesis, the understanding of the relationship between equipment and process parameters is not fully robust. Hence manufacturing development work would be more of a trial and error approach rather than following Quality by Design principles. The onus is then on the scientific community to build the understanding of relationships and mechanisms and is what this thesis seeks, in part, to do.

Much of this thesis seeks to understand the flow and mixing characteristics of Twin Screw Granulators. Twin screw granulators have evolved from twin screw extruders, however the properties of materials typically processed are vastly different. As a generalisation, extrusion in food, metal, ceramics and plastics will see the transformation of a solid material into a fluid state

whereupon it is forced through a die under pressure forming a dense solid of the desired shape. Granulation sees the agglomeration of particles into discrete solids where porosity is desirable. As a result granulators must be run starved of material as the inherent pressure building design of the equipment leads to compaction. Compaction leading to undesirably low porosity or dense solids causing blockages in the granulator. The flow of material through a granulator is therefore quite different to that of an extruder. This leads to some interesting observations such as the preferential loading of material on a single conveying screw under starved conditions such as that in Chapter 3. This flow pattern is believed to result in heterogeneity in the material, particularly as conveying zones are where water or binder liquid is typically added. This variance in product is observed to decrease with increasing fill level, suggesting better mixing performance with higher material loading. This is without optimisation of the mixing zone of the granulator but would suggest that the mixing performance of a kneading block is dependent on the fill level across it. While perhaps not surprising, this would indicate that a balance must be made between filling a kneading block to ensure good mixing while avoiding over-compaction or blockages. An added layer of complexity coming from the fact that the arrangement of screw elements impacts the local fill level across individual and downstream elements, not just the ratio of material feed rate to screw speed. Future work would seek to better understand the interaction between different elements and the characteristic changes between fill level, residence time and mixing performance, possibly through a PEPT study. Additionally it would be of benefit to understand the importance of liquid/solid mixing at nucleation and the impact this has on granules. Particularly as it is concluded that the formation mechanism of 60°F kneading blocks is primarily breakage of agglomerates formed during nucleation. This would be achieved through exploration of different mixing configurations at the liquid injection site or different methods of liquid injection. Initially this should use only conveying screws downstream, but should be expanded as the impact of nucleation mixing may be overshadowed by subsequent mixing. The liquid tracer method could be developed to use a more sensitive

characterisation and quantification method such as through High Performance Liquid Chromatography.

Significant work has been undertaken around understanding the impact of temperature on the granulation process and the changes in material properties which are linked to this. The granulator operates at significantly lower steady state torque at higher temperature despite otherwise identical processing conditions. This implies that less mechanical energy is required for granulation at higher temperatures. This would suggest that energy savings could possibly be made by operating at elevated temperatures however a full energy balance would need to be performed in order to confirm the validity. As temperature has such a marked impact on steady state torque it would be of interest in future work to investigate through PEPT if there is any impact on the fill level and residence time of the granulator. It is believed that changes in the physical properties cause the change in steady state torque and not a change in fill level, however it would be beneficial to confirm this through PEPT.

There are physical differences in the particles formed at low and high temperatures and it is believed these differences are largely due to the solubility of the excipients used. The formulation investigated consists of common pharmaceutical excipients, lactose, MCC and HPC as binder. HPC undergoes thermoreversible gelation in water at 43°C. At temperatures higher than this HPC will precipitate out of solution and lose its binding ability. Without the functionality of the binder the growth and formation of granules will be reduced. Lactose increases significantly in solubility at elevated temperature. Thus it is believed that temperature encourages the formation of liquid bridges and granule growth. As pharmaceutical excipients are chemically similar to HPC and lactose, with common cellulose based binders and sugar like bulking materials, it is believed that these same effects would be seen across a range of materials.

Crucially observations have been made around the generation of heat as a byproduct of granulation, from the mechanical action of the screw mixing zones. As the mixing zone effectively becomes a

heat source it takes time for the system to thermally equilibrate, observed at up to 35 minutes in the experiments run. Throughout this period the torque changes, steadily lowering as temperature increases and not reaching a steady state until this 35 minute point. This would have implications in pharma for example where a product may be validated in the steady state region and thus requires a long and wasteful start-up time. As the excipients' behaviour changes depending on temperature a temperature profile along the barrel is likely to impact granulation mechanisms. Sufficient temperature control should therefore be in place to ensure that heat generated through mechanical action can be mitigated. Alternatively in a granulator with very accurate temperature control it could be possible to use a temperature profile as an additional control factor in granulation, impacting rate mechanisms at certain points. Applied temperature control is worthy of future investigation.

As this behaviour with temperature is very much material dependent it would be of value to test this hypothesis across more materials in other formulations. Additionally while this single mixing geometry has been shown to generate heat under these conditions it would be interesting to see how this compares to other mixing geometries and whether the rate of heat generation could be correlated with mixing intensity.

A core part of this thesis is focussed on screw configuration and building the relationship between arrangement and flow of material through the granulator. This has been achieved through systematic PEPT analysis of screw configurations. Data has been used to infer the fill level of the granulator and residence time distribution, from which degree of mixing may be inferred.

This has been the first study to systematically characterise the impact of kneading block length. It has been demonstrated that both torque and residence time increase proportionally with kneading block length. This would suggest a predictable relationship between kneading block length and degree of mixing. This is supported by the observed changes in granule population, with granules becoming more homogenous in size with increasing kneading block length. The hypothesis being that good mixing leads to homogenous granules. However axial mixing has important impact in

minimising variability and can help smooth out changes in feed rates. While much of this work has looked at the quality of mixing can be achieved with various screw configurations this is not necessarily translatable into quality of granule. For example somewhat of a trend is observed of increasing bulk density with kneading block length. Dense granules may be poorly compressible and not form suitable tablets in pharmaceutical application. Therefore it would be valuable in future work to correlate mixing performance with drug product quality attributes, such as compressibility, the strength of resultant tablets and their dissolution rate, using appropriate formulations or analogues. The trend of increasing density is impacted by the high temperatures generated in long mixing zones, which highlights the need for good temperature control discussed earlier.

The angle of the kneading block has been investigated and shows that the behaviour of 30°F and 60°F kneading blocks show similar trends with increasing length to those of 90° blocks described above. Torque, residence time and granule size homogeneity all increase with kneading block length implying more mixing. These values are much lower than in 90° blocks, suggesting that forwarding geometries are much less intensive in mixing. However this may have advantages in avoiding over-compaction of granules. Direct comparison of the residence time distributions of the same arrangements of 60°F and 90° kneading blocks shows the low level of axial mixing in 60°F geometries. Suggesting it may be difficult to scale a process which requires some degree of axial mixing.

One area of interest has been how the arrangement of screw configuration impacts the flow of material and properties of granules formed. Preliminary results suggest that the position of the first kneading block relative to the liquid injection port has an impact on granulation mechanisms. When positioned closer to the site of liquid injection higher steady state torques are observed which become lower the further it is placed downstream. Along with higher torque values more homogenous granules are formed, suggesting a better mixed system. This may be a result of the segregation effects of conveying zones discussed in chapter 3. The implication is that the position of

the kneading block relative to the nucleation site is important in determining granule formation. It would be valuable to expand on these findings in future work to better understand the importance of nucleation and post nucleation mixing. While feeding liquid directly onto a kneading block has been shown to disrupt the granulator steady state and result in periodic surging, it would be of interest to explore different geometries.

One of the benefits of PEPT is that it allows information to be gathered from inside an active process. This has allowed the generation of novel data demonstrating how the residence time increases across downstream mixing zones. This implies a change in the material properties impacting the powder rheology. It would be valuable to correlate this with the evolution of granules across these different mixing zones, if a suitable and reliable method of in-process sampling could be developed. In theory this would suggest that mixing zones of varying intensity could be matched to evolving granule properties axially as part of granule design.

Furthermore data has demonstrated that a single kneading block has a much broader residence time distribution compared to two half blocks arranged sequentially. This demonstrates that good axial mixing is best achieved with long mixing blocks rather than multiple, with the risk of densification. Future work should include analysis into the interaction of screw configurations containing different angle kneading blocks. For example the change in material properties over sequential mixing zones would suggest that a 60° block with 90° downstream block would perform differently to a 90° block with downstream 60° block. Exploring this may add a useful tool in intelligent screw configuration design.

Novel results have been obtained showing the different performance of kneading blocks of the same length made up of made up of kneading elements of different width, 8 mm compared to the standard 4 mm. Much higher torque is measured using wide elements and the resultant granules are very dense. However at the same conditions this can shift the size distribution of granules from bimodal to monomodal. This may suggest intensive mixing and compaction compared to narrower

elements. Though very intensive, the residence times of these wide element configurations are comparable to 90° blocks of the same length. This may suggest that axial mixing is not significantly greater and in fact wide elements simply result in greater compaction. These observations with wide elements pose some interesting questions around the possible uses of even narrower elements. Should these result in even less compaction it may be a viable method of producing more porous granules. Indeed for a given length of kneading block a plug of material will experience more chopping, shearing motions with narrower elements. This would certainly be worthy of future investigation and would be a good starting point for modifying screw element design to tailor for granulation.

This investigation into the mixing performance of kneading elements demonstrates how they may be utilised to increase mixing rates, however it brings a question of how well the fundamental design is suited for granulation. The typical bilobe elements common across many twin screw granulators are the same as are used in extrusion. These work best when fully filled and generate good axial mixing. However their intermeshing design naturally results in compaction of material and the holdup of material means limited lengths of kneading block are possible before blockages occur. Over-compaction is to be avoided in granulation as compressibility is a required property for tableting. A homogenous granule population is desirable to ease variability in downstream processing. In a continuous system such as TSG this cannot be achieved by extending a mixing time such as in a batch process and thus must be achieved by improving the quality of mixing. While this is possible with kneading elements it is linked to compaction and densification. A key aspect of future work would therefore be to explore different mixer element designs and their impact on the granulation process. It would be of particular interest to develop elements which preferentially generate shear forces over compression, perhaps through the use of single lobe thin elements.

PEPT is a very valuable technique and has enabled the generation of some novel information on Twin Screw Granulation. While this thesis has focussed on an experimentalist approach it is hoped

that the data and understanding generated could be applied to future modelling of the granulation process.

In conclusion Twin Screw Granulation is a technology with great potential for application in industrial continuous wet granulation. Screw configuration is an underexplored area and is the focus of much of this thesis. Characterisation of the process and PEPT have built some key knowledge of fundamentals of process operation. It is hoped that the correlations and trends brought to light within this body of work contribute to the future understanding, control and application of this process.

References

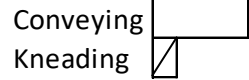
1. Shotton, E. and D. Ganderton, *THE STRENGTH OF COMPRESSED TABLETS*. Journal of Pharmacy and Pharmacology, 1961. **13**(S1): p. 144T-152T.
2. Cao, Q.-R., et al., *A formulation approach for development of HPMC-based sustained release tablets for tolterodine tartrate with a low release variation*. Drug Development and Industrial Pharmacy, 2013. **39**(11): p. 1720-1730.
3. Department of Health and Human Services U.S. Food and Drug Administration, *Pharmaceutical cGMPs for the 21st Century - A Risk-Based Approach*. 2004.
4. Dhenge, R.M., et al., *Twin screw granulation: Steps in granule growth*. International Journal of Pharmaceutics, 2012. **438**(1-2): p. 20-32.
5. Leistritz Extrusionstechnik GmbH., *Leistritz NANO 16 - extremely small volume combined with a revolutionary feeder system*. 2014.
6. Thermo Fisher Scientific, *Thermo Fisher Scientific Pharma 16 TSG Twin Screw Granulator*. 2014.
7. G. E. A. Pharma Systems, *ConsiGmaT Tableting Line: our blue sky approach from powder to tablet*. 2014.
8. Gamlen, M.J. and C. Eardley, *Continuous Extrusion Using a Baker Perkins MP50 (Multipurpose) Extruder*. Drug Development and Industrial Pharmacy, 1986. **12**(11-13): p. 1701-1713.
9. Lindberg, N.O., C. Tufvesson, and L. Olbjer, *Extrusion of an Effervescent Granulation with a Twin Screw Extruder, Baker Perkins MPF 50 D*. Drug Development and Industrial Pharmacy, 1987. **13**(9-11): p. 1891-1913.
10. Lindberg, N.O., et al., *Extrusion of An Effervescent Granulation with a Twin Screw Extruder, Baker Perkins MPF 50D. Determination of Mean Residence Time*. Drug Development and Industrial Pharmacy, 1988. **14**(5): p. 649-655.
11. Lindberg, N.O., et al., *Extrusion of an Effervescent Granulation with a Twin Screw Extruder, Baker Perkins MPF 50 D. Influence on Intragranular Porosity and Liquid Saturation*. Drug Development and Industrial Pharmacy, 1988. **14**(13): p. 1791-1798.
12. Ghebre-Sellassie, I., et al., *Continuous production of pharmaceutical granulation*. 2002, Google Patents.
13. Keleb, E.I., et al., *Twin screw granulation as a simple and efficient tool for continuous wet granulation*. International Journal of Pharmaceutics, 2004. **273**(1-2): p. 183-194.
14. Keleb, E.I., et al., *Continuous twin screw extrusion for the wet granulation of lactose*. International Journal of Pharmaceutics, 2002. **239**(1-2): p. 69-80.
15. Cartwright, J.J., et al., *Twin screw wet granulation: Loss in weight feeding of a poorly flowing active pharmaceutical ingredient*. Powder Technology, 2013. **238**: p. 116-121.
16. Van Melkebeke, B., C. Vervaet, and J.P. Remon, *Validation of a continuous granulation process using a twin-screw extruder*. International Journal of Pharmaceutics, 2008. **356**(1-2): p. 224-230.
17. Lakshman, J.P., et al., *Application of melt granulation technology to enhance tableting properties of poorly compactible high-dose drugs*. JOURNAL OF PHARMACEUTICAL SCIENCES, 2011. **100**(4): p. 1553-1565.
18. Mu, B. and M.R. Thompson, *Examining the mechanics of granulation with a hot melt binder in a twin-screw extruder*. Chemical Engineering Science, 2012. **81**: p. 46-56.
19. Van Melkebeke, B., et al., *Melt granulation using a twin-screw extruder: A case study*. International Journal of Pharmaceutics, 2006. **326**(1-2): p. 89-93.
20. Vasanthavada, M., et al., *Application of melt granulation technology using twin-screw extruder in development of high-dose modified-release tablet formulation*. JOURNAL OF PHARMACEUTICAL SCIENCES, 2011. **100**(5): p. 1923-1934.
21. Djuric, D., *Continuous Granulation with a Twin-Screw Extruder*. 2008: Cuvillier.
22. Djuric, D. and P. Kleinebudde, *Impact of screw elements on continuous granulation with a twin-screw extruder*. JOURNAL OF PHARMACEUTICAL SCIENCES, 2008. **97**(11): p. 4934-4942.

23. Thompson, M.R. and J. Sun, *Wet granulation in a twin-screw extruder: Implications of screw design*. JOURNAL OF PHARMACEUTICAL SCIENCES, 2010. **99**(4): p. 2090-2103.
24. Dhenge, R.M., et al., *Twin screw granulation using conveying screws: Effects of viscosity of granulation liquids and flow of powders*. Powder Technology, 2012. **238**: p. 77-90.
25. Barrasso, D., et al., *Multi-dimensional population balance model development and validation for a twin screw granulation process*. Powder Technology, 2015. **270, Part B**(0): p. 612-621.
26. Vercruyssen, J., et al., *Continuous twin screw granulation: Influence of process variables on granule and tablet quality*. EUROPEAN JOURNAL OF PHARMACEUTICS AND BIOPHARMACEUTICS, 2012. **82**(1): p. 205-211.
27. Shah, U., *Use of a modified twin-screw extruder to develop a high-strength tablet dosage form*. Pharmaceutical Technology, 2005. **29**(6): p. 52-66.
28. Gao, Y., F.J. Muzzio, and M.G. Ierapetritou, *A review of the Residence Time Distribution (RTD) applications in solid unit operations*. Powder Technology, 2012. **228**(0): p. 416-423.
29. Kumar, A., et al., *Digital image processing for measurement of residence time distribution in a laboratory extruder*. JOURNAL OF FOOD ENGINEERING, 2006. **75**(2): p. 237-244.
30. Dhenge, R.M., et al., *Twin screw wet granulation: Effect of powder feed rate*. ADVANCED POWDER TECHNOLOGY, 2011. **22**(2): p. 162-166.
31. Dhenge, R.M., et al., *Twin screw wet granulation: Effects of properties of granulation liquid*. Powder Technology, 2012. **229**(0): p. 126-136.
32. Dhenge, R.M., et al., *Twin screw wet granulation: Granule properties*. Chemical Engineering Journal, 2010. **164**(2-3): p. 322-329.
33. El Hagrasy, A.S., et al., *Twin screw wet granulation: Influence of formulation parameters on granule properties and growth behavior*. Powder Technology, 2013. **238**(0): p. 108-115.
34. Kumar, A., et al., *Mixing and transport during pharmaceutical twin-screw wet granulation: Experimental analysis via chemical imaging*. EUROPEAN JOURNAL OF PHARMACEUTICS AND BIOPHARMACEUTICS, 2014. **87**(2): p. 279-289.
35. Lee, K.T., A. Ingram, and N.A. Rowson, *Twin screw wet granulation: The study of a continuous twin screw granulator using Positron Emission Particle Tracking (PEPT) technique*. European Journal of Pharmaceutics and Biopharmaceutics, 2012. **81**(3): p. 666-673.
36. Vercruyssen, J., et al., *Visualization and understanding of the granulation liquid mixing and distribution during continuous twin screw granulation using NIR chemical imaging*. EUROPEAN JOURNAL OF PHARMACEUTICS AND BIOPHARMACEUTICS, 2014. **86**(3): p. 383-392.
37. El Hagrasy, A.S. and J.D. Litster, *Granulation rate processes in the kneading elements of a twin screw granulator*. AIChE Journal, 2013. **59**(11): p. 4100-4115.
38. Keleb, E.I., et al., *Extrusion Granulation and High Shear Granulation of Different Grades of Lactose and Highly Dosed Drugs: A Comparative Study*. Drug Development & Industrial Pharmacy, 2004. **30**(6): p. 679-691.
39. Lee, K.T., A. Ingram, and N.A. Rowson, *Comparison of granule properties produced using Twin Screw Extruder and High Shear Mixer: A step towards understanding the mechanism of twin screw wet granulation*. Powder Technology, 2013. **238**: p. 91-98.
40. Keleb, E.I., et al., *Cold extrusion as a continuous single-step granulation and tableting process*. EUROPEAN JOURNAL OF PHARMACEUTICS AND BIOPHARMACEUTICS, 2001. **52**(3): p. 359-368.
41. Thompson, M.R., B. Mu, and P.J. Sheskey, *Aspects of foam stability influencing foam granulation in a twin screw extruder*. Powder Technology, 2012. **228**(0): p. 339-348.
42. Yu, S., et al., *Granulation of increasingly hydrophobic formulations using a twin screw granulator*. International Journal of Pharmaceutics, 2014. **475**(1-2): p. 82-96.
43. Kumar, A., et al., *Experimental investigation of granule size and shape dynamics in twin-screw granulation*. International Journal of Pharmaceutics, 2014. **475**(1-2): p. 485-495.

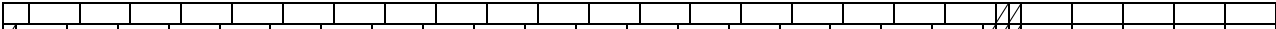
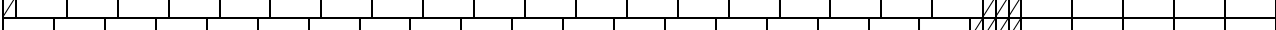
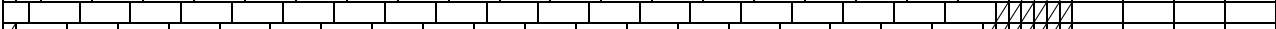
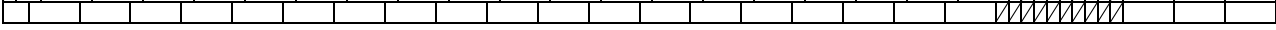
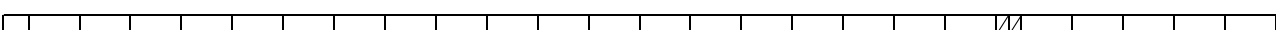
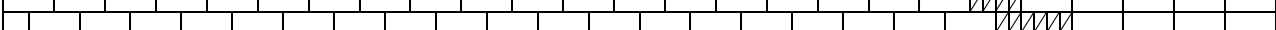
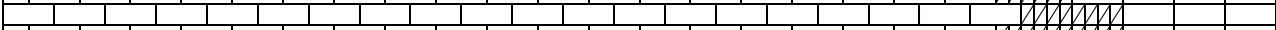
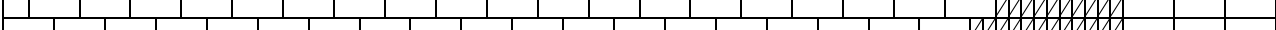
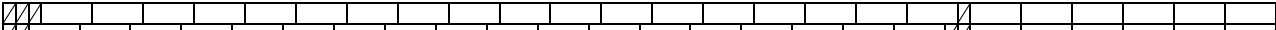
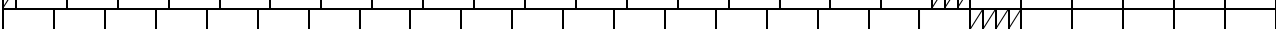
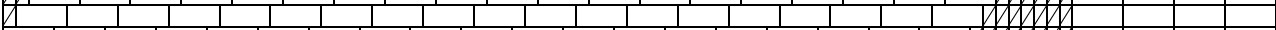
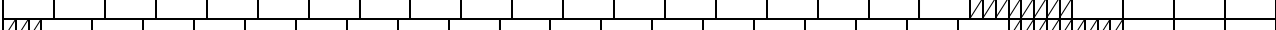
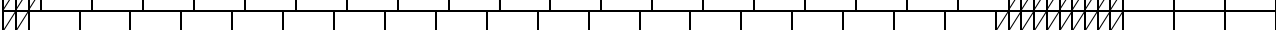
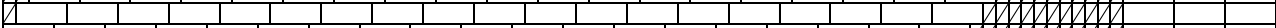
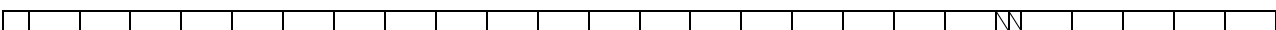
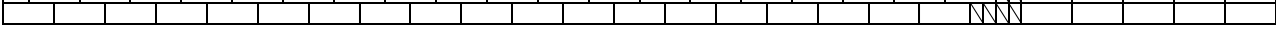
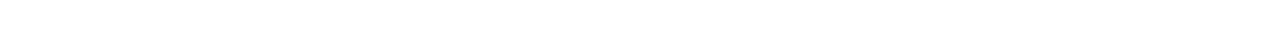
44. Iveson, S.M. and J.D. Litster, *Growth regime map for liquid-bound granules*. AIChE Journal, 1998. **44**(7): p. 1510-1518.
45. Tu, W.D., A. Ingram, and J. Seville, *Regime map development for continuous twin screw granulation*. Chemical Engineering Science, 2013. **87**(0): p. 315-326.
46. Adams, M.J., M.A. Mullier, and J.P.K. Seville, *Agglomerate strength measurement using a uniaxial confined compression test*. Powder Technology, 1994. **78**(1): p. 5-13.
47. Thompson, M.R., et al., *Foam granulation: new developments in pharmaceutical solid oral dosage forms using twin screw extrusion machinery*. Drug Development & Industrial Pharmacy, 2012. **38**(7): p. 771-784.
48. Djuric, D., et al., *Comparison of two twin-screw extruders for continuous granulation*. EUROPEAN JOURNAL OF PHARMACEUTICS AND BIOPHARMACEUTICS, 2009. **71**(1): p. 155-160.
49. Tan, L., et al., *Process optimization for continuous extrusion wet granulation*. Pharmaceutical Development & Technology, 2011. **16**(4): p. 302-315.
50. Djuric, D. and P. Kleinebudde, *Continuous granulation with a twin-screw extruder: Impact of material throughput*. Pharmaceutical Development & Technology, 2010. **15**(5): p. 518-525.
51. Fonteyne, M., et al., *Real-time assessment of critical quality attributes of a continuous granulation process*. Pharmaceutical Development and Technology, 2013, Vol.18(1), p.85-97, 2013. **18**(1): p. 85-97.
52. Barrasso, D., et al., *A multi-scale, mechanistic model of a wet granulation process using a novel bi-directional PBM-DEM coupling algorithm*. Chemical Engineering Science, 2015. **123**(0): p. 500-513.
53. Carotenuto, C. and N. Grizzuti, *Thermoreversible gelation of hydroxypropylcellulose aqueous solutions*. Rheologica Acta, 2006. **45**(4): p. 468-473.
54. Fox, P.F., et al., *Dairy Chemistry and Biochemistry*. 2015: Springer International Publishing.
55. Bakalis, S., P.J. Fryer, and D.J. Parker, *Measuring velocity distributions of viscous fluids using positron emission particle tracking (PEPT)*. AIChE Journal, 2004. **50**(7): p. 1606-1613.
56. Ingram, A., et al., *Axial and radial dispersion in rolling mode rotating drums*. Powder Technology, 2005. **158**(1-3): p. 76-91.
57. Portillo, P.M., et al., *Investigation of the effect of impeller rotation rate, powder flow rate, and cohesion on powder flow behavior in a continuous blender using PEPT*. Chemical Engineering Science, 2010. **65**(21): p. 5658-5668.
58. Parker, D.J., et al., *Positron emission particle tracking - a technique for studying flow within engineering equipment*. Nuclear Instruments and Methods in Physics Research Section A: Accelerators, Spectrometers, Detectors and Associated Equipment, 1993. **326**(3): p. 592-607.
59. Fan, X., D.J. Parker, and M.D. Smith, *Labelling a single particle for positron emission particle tracking using direct activation and ion-exchange techniques*. Nuclear Instruments and Methods in Physics Research Section A: Accelerators, Spectrometers, Detectors and Associated Equipment, 2006. **562**(1): p. 345-350.
60. Fan, X., D.J. Parker, and M.D. Smith, *Enhancing ^{18}F uptake in a single particle for positron emission particle tracking through modification of solid surface chemistry*. Nuclear Instruments and Methods in Physics Research Section A: Accelerators, Spectrometers, Detectors and Associated Equipment, 2006. **558**(2): p. 542-546.
61. Parker, D.J., et al., *Industrial positron-based imaging: Principles and applications*. Nuclear Instruments and Methods in Physics Research Section A: Accelerators, Spectrometers, Detectors and Associated Equipment, 1994. **348**(2): p. 583-592.
62. El Hagrasy, A.S., et al., *Twin screw wet granulation: Influence of formulation parameters on granule properties and growth behavior*. Powder Technology, 2013. **238**: p. 108-115.
63. Dhenge, R.M., et al., *Twin screw granulation using conveying screws: Effects of viscosity of granulation liquids and flow of powders*. Powder Technology, 2013. **238**: p. 77-90.

Appendix 1 – Detailed screw configurations

Key



Haake screw configurations

Description	Screw configuration	
Conveying only	25x1D C	
30°F		
2	1x0.5 D C// 19x1D C// 2x0.25D K 30F// 5x1D C	
3	1x0.25 D K 0// 19x1D C// 3x0.25D K 30F// 5x1D C	
4	19x1D C// 4x0.25D K 30F// 5x1D C	
5	1x0.25D K 0// 1x0.5D C// 19x1D C// 5x0.25D K 30F// 4x1D C	
6	1x0.5D C// 19x1D C// 6x0.25D K 30F// 4x1D C	
7	1x0.25D K 0// 19x1D C// 7x0.25D K 30F// 4x1D C	
8	19x1D C// 8x0.25D K 30F// 4x1D C	
9	1x0.25 D K 0// 1X0.5D C// 19x1D C// 9x0.25D K 30F// 3x1D C	
10	1X0.5D C// 19x1D C// 10x0.25D K 30F// 3x1D C	
60°F		
2	1x0.5 D C// 19x1D C// 2x0.25D K 30F// 5x1D C	
3	1x0.25D K 0// 19x1D C// 3x0.25D K 30F// 5x1D C	
4	19x1D C// 4x0.25D K 30F// 5x1D C	
6	1x0.5D C// 18x1D C// 6x0.25D K 60F// 5x1D C	
8	20x1D C// 8x0.25D K 60F// 3x1D C	
10	1x0.5D C// 19x1D C// 10x0.25D K 60F// 3x1D C	
12	19x1D C// 12x0.25D K 60F// 3x1D C	
90°		
1	3x0.25D K 60F// 18x1D C// 1x0.25D K 90// 6x1D C	
2	2x0.25D K 60F// 19x1D C// 2x0.25D K 90// 5x1D C	
3	1x0.25D K 60F// 19x1D C// 3x0.25D K 90// 5x1D C	
4	19x1D C// 4x0.25D K 90// 5x1D C	
5	3x0.25D K 60F// 19x1D C// 5x0.25D K 90// 4x1D C	
6	2x0.25D K 60F// 19x1D C// 6x0.25D K 90// 4x1D C	
7	1x0.25D K 60F// 19x1D C// 7x0.25D K 90// 4x1D C	
8	19x1D C// 8x0.25D K 90// 4x1D C	
9	3x0.25D K 60F// 19x1D C// 9x0.25D K 90// 3x1D C	
10	2x0.25D K 60F// 19x1D C// 10x0.25D K 90// 3x1D C	
11	1x0.25D K 60F// 19x1D C// 11x0.25D K 90// 3x1D C	
12	19x1D C// 12x0.25D K 90// 3x1D C	
30°R		
2	1x0.5 D C// 19x1D C// 2x0.25D K 30R// 5x1D C	
4	19x1D C// 4x0.25D K 30R// 5x1D C	

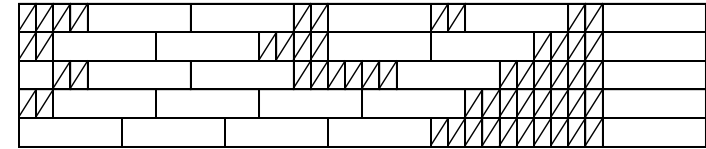
GEA Screw Configurations

Description

Screw Configuration

90°

3x2 KE	4x0.25D K 30F// 2x1.5D C// 2x0.25D K 90// 1x1.5D C// 2x0.25D K 90// 1x1.5D C// 2x0.25D K 90// 1x1.5D C
2x4 KE	2x0.25D K 30F// 2x1.5D C// 4x0.25D K 90// 2x1.5D C// 4x0.25D K 90// 1x1.5D C
2x6 KE	0.5D spacer// 2x0.25D K 30F// 2x1.5D C// 6x0.25D K 90// 1x1.5D C// 6x0.25D K 90// 1x1.5D C
8 KE	2x0.25 D K 30F// 4x1.5D C// 8x0.25D K 90// 1x1.5D C
10 KE	4x1.5D C// 10x0.25D K 90// 1x1.5D C



60°F

2x4KE	2x0.25D K 30F// 2x1.5D C// 4x0.25D K 60F// 2x1.5D C// 4x0.25D K 60F// 1x1.5D C
2x6 KE	0.5D spacer// 2x0.25D K 30F// 2x1.5D C// 6x0.25D K 60F// 1x1.5D C// 6x0.25D K 60F// 1x1.5D C
8 KE	2x0.25D K 30F// 4x1.5D C// 8x0.25D K 60F// 1x.15D C
10 KE	4x1.5D C// 10x0.25D K 60F// 1x1.5D C

